21909

NATIONAL LIBRARY
OTTAWA

CANADA

BIBLIOTHÈQUE NATIONALE
OTTAWA

NAME OF AUTHOR..... MILTON MARTINS DE MATOS

TITLE OF THESIS..... "Stability of Slopes on Residual Soils"

.....

UNIVERSITY..... of Alberta

DEGREE FOR WHICH THESIS WAS PRESENTED..... Master of Science

YEAR THIS DEGREE GRANTED..... 1974

Permission is hereby granted to THE NATIONAL LIBRARY OF CANADA to microfilm this thesis and to lend or sell copies of the film.

The author reserves other publication rights, and neither the thesis nor extensive extracts from it may be printed or otherwise reproduced without the author's written permission.

(Signed)..... [signature]

PERMANENT ADDRESS:

Rua Engº Teixeira Soares, 513
Butantã
05505 São Paulo - SP
BRAZIL

DATED..... November 1st, 1974

NL-91 (10-68)

THE UNIVERSITY OF ALBERTA

STABILITY OF SLOPES IN RESIDUAL SOILS

by

MILTON MARTINS DE MATOS

A THESIS

SUBMITTED TO THE FACULTY OF GRADUATE STUDIES AND RESEARCH

IN PARTIAL FULFILMENT OF THE REQUIREMENTS FOR

THE DEGREE OF MASTER OF SCIENCE

DEPARTMENT OF CIVIL ENGINEERING

EDMONTON, ALBERTA

FALL 1974

THE UNIVERSITY OF ALBERTA

FACULTY OF GRADUATE STUDIES AND RESEARCH

The undersigned certify that they have read, and recommend to the Faculty of Graduate Studies and Research for acceptance, a thesis entitled "STABILITY OF SLOPES IN RESIDUAL SOILS" submitted by Milton Martins de Matos in partial fulfilment of the requirements for the degree of Master of Science in Civil Engineering.

N.R. Morgenstern, Supervisor

Z. Eisenstein

J.B. Nuttall

F. Schwartz

Date 1974

IN MEMORY OF MY MOTHER

ABSTRACT

In areas of hot climate and high humidity, extensive deposits of residual soils develop through weathering processes. The characteristics of these soils together with high rainfall often leads to landslides of catastrophic results causing loss of life and severe property damage.

This thesis is intended to investigate the mechanisms through which slope failure takes place and the factors that must be considered in the analyses of stability of natural and cut slopes in these regions.

It is shown that the dominant mechanism of failure is the infiltration of water through the unsaturated soils with the consequent reduction of the apparent cohesion by elimination of suction that previously existed in the unsaturated soil.

Methods of analyses are presented to study the stability of slopes. It was found that positive pore pressures are not necessarily built up and that a slope can be safely designed in terms of effective stresses by using the shear strength parameters obtained through drained tests carried out on samples saturated before shearing.

Methods of improving slope stability are discussed and a tentative simplified classification of slope failures on the basis of rainfall intensity is also presented.

It is felt that the behaviour of the residual soils with

respect to infiltration of water is dominated by the presence of the relict structure and cracks in the soils that lead to large values of the permeability.

ACKNOWLEDGEMENTS

The investigations reported in this thesis were carried out at the Department of Civil Engineering, University of Alberta, under the supervision of Professor N.R. Morgenstern. The author expresses his sincere gratitude to Professor Morgenstern for his continued guidance, help and support throughout the period of this study.

Financial assistance received from the University of Alberta is gratefully acknowledged.

Stimulating advice came from Mr. R.F. Howells with respect to computing operations.

The author wishes to thank all of his friends who contributed so much to the state of mind required to see the work through, and especially thanks to T.C. Law and W.D. Roggensack for their cooperation and several valuable discussions.

The author also wishes to thank Mrs. Juliet M. Willis for doing a remarkable job of typing.

Finally, the author wishes to acknowledge, with his most sincere gratitude, the continual encouragement, support and understanding rendered by his wife, Vera Lucia, as without her this thesis would not have been possible.

TABLE OF CONTENTS

		Page
Abstract		v
Acknowledgements		vii
Table of Contents		viii
List of Tables		xii
List of Figures		xiii
CHAPTER I	INTRODUCTION	1
CHAPTER II	RESIDUAL SOILS	4
	2.1 Introduction	4
	2.2 Geology of Brazil	4
	2.3 Geology and Climate of Rio de Janeiro	6
	2.4 Geology and Climate of the Area of Anchieta Highway	12
	2.5 Weathering and Weathering Profile	13
	2.6 Properties of Residual Soils	22
	2.6.1 Residual Soils in Rio de Janeiro	23
	2.6.2 Residual Soils in Serra do Mar and Santos	27
CHAPTER III	INFILTRATION OF WATER THROUGH UNSATURATED POROUS MEDIA	41
	3.1 Introduction	41
	3.2 Unsaturated Soils	42
	3.2.1 Suction	42
	3.2.2 Hydraulic Conductivity	45

Page

3.3 Movement of Water through Unsaturated Soils 47

3.3.1 Concept of Total Potential 48

3.3.2 Darcy's Law for Unsaturated Soils 50

3.3.3 General Equation of Soil Water Transfer 51

3.4 Infiltration 54

3.4.1 Physics of Infiltration 54

3.4.2 Infiltration Rate 54

3.4.3 Moisture Profile after Infiltration 58

3.5 Redistribution of Moisture Content 59

CHAPTER IV SOLUTIONS TO THE INFILTRATION EQUATION 71

4.1 Introduction 71

4.2 Boundary and Initial Conditions 73

4.3 Philip's Solution 75

4.3.1 Horizontal Infiltration 75

4.3.2 Vertical Infiltration 77

4.3.3 Cumulative Infiltration 81

4.3.4 Infiltration Rate 83

4.3.5 Results of Philip's Solution 84

4.4 Mein and Larson's Solution 86

4.4.1 General Considerations 86

4.4.2 Solution to the Vertical Infiltration Problem 87

Page

4.4.3 Results of Mein and Larson's Solution 91

4.5 Analysis of Infiltration of Water into Residual Soils 93

4.5.1 Unsaturated Flow Properties of the Residual Soils 94

4.5.2 Results of the Analyses on Residual Soils 95

CHAPTER V DETERMINATION OF THE UNSATURATED FLOW PROPERTIES OF SOILS 133

5.1 Introduction 133

5.2 Capillary Suction 133

5.3 Hydraulic Conductivity and Diffusivity 134

5.4 Comments on Reliability 135

CHAPTER VI MECHANISM OF LANDSLIDES 141

6.1 Introduction 141

6.2 Mechanism of Landslides 144

6.3 Types of Slides 153

6.3.1 Slides 153

6.3.2 Avalanches 154

6.3.3 Other forms of slides 155

6.4 Analysis of Stability 155

6.5 Methods of Treatment and Stabilization of Slopes 159

6.5.1 Flattening of Slope 160

6.5.2 Slope Protection 160

Page

6.5.3 Drainage 161

6.5.3.1 Surface Drainage 161

6.5.3.2 Underdrainage 162

6.5.4 Filling of Cracks and Erosion Cavities 163

6.5.5 Other Methods 163

CHAPTER VII CASE HISTORIES 171

7.1 Introduction 171

7.2 Estrada do Jequiá Slide 171

7.3 Caneleira Slide 175

7.4 Monte Serrate Slides 177

CHAPTER VIII CONCLUDING REMARKS AND SUGGESTIONS FOR FURTHER RESEARCH 185

REFERENCES 190

APPENDIX A - VERTICAL INFILTRATION SOLUTION BY PHILIP'S METHOD 196

APPENDIX B - VERTICAL INFILTRATION SOLUTION BY MEIN AND LARSON'S METHOD 203

APPENDIX C - RESULTS OF MEIN AND LARSON'S SOLUTION FOR RESIDUAL SOILS 211

LIST OF TABLES

Table		Page
2.1	Characteristics of Residual Soils of Different Variety of Gneisses in Rio de Janeiro	29
2.2	Characteristics of the Zones of a Weathering Profile	30
2.3	Properties of Residual Soils from Different Varieties of Gneiss in Rio de Janeiro	31
2.4	Properties of Residual Soils from Rio de Janeiro	32
2.5	Characteristics of Residual Soils of Different Rocks at Serra do Mar	33
2.6	Properties of Residual Soils at Serra do Mar and Santos	34
2.7	Characteristics of Residual Soils at Serra do Mar and Santos	35
4.1	Characteristics of the Soils Referred to in the Study	100
5.1	Methods for the Measurement of the Hydraulic Conductivity and Diffusivity	137
5.2	Determination of the Hydraulic Conductivity by the Instantaneous Profile Methods: Laboratory Measurements	138
5.3	Determination of the Hydraulic Conductivity by the Instantaneous Profile Methods: Field Measurements	139

LIST OF FIGURES

Figure		Page
2.1	Zones of Precambrian Formations in Brazil	36
2.2	Topographic Features of the State of Guanabara	37
2.3	Weathering Profiles at Different Stages	38
2.4	Typical Weathering Profile for Metamorphic and Intrusive Igneous Rocks	39
2.5	Profiles of Weathering on Gneiss in Southern Brazil ..	39
2.6	General Weathering Pattern in a Hill	40
2.7	Typical Profile of Residual Soil of Gneiss	40
3.1	Moisture Characteristic Curve	62
3.2	Hysteresis in Moisture Characteristic Curve	63
3.3	Hydraulic Conductivity Versus Moisture Content	64
3.4	Concept of Total Potential	65
3.5	Diffusivity Versus Moisture Content	66
3.6	Infiltration Rate Versus Time	67
3.7	Stages of Moisture Profile Development	67
3.8	Different Cases of Infiltration Behaviour Under Rainfall	68
3.9	Zones of the Infiltration Profile	68
3.10	Stages in the Development of the Descending Moisture Profile	69
3.11	Redistribution of Moisture Content	69
3.12	Water Redistribution After Infiltration	70
4.1	Hydraulic Conductivity Versus Moisture Content for Several Soils	101

Figure		Page
4.2	Diffusivity Versus Moisture Content for Several Soils	102
4.3	Moisture Characteristic Curves of Different Soils	103
4.4	Descending Moisture Profile for Columbia Sand Loam	104
4.5	Depth of Infiltration Versus Time for Columbia Sand Loam	105
4.6	Infiltration Rates Versus Time for Columbia Sand Loam	106
4.7	Generalized Soil Moisture Profile During Infiltration at the Moment of Surface Saturation	107
4.8	Generalized Soil Moisture Profile During Infiltration After Surface Saturation	107
4.9	Depths of Infiltration for Small Times for Columbia Sand Loam	108
4.10	Depths of Infiltration for Large Times for Columbia Sand Loam	109
4.11	Effect of Rainfall Intensity on the Infiltration Rate for Columbia Sand Loam	110
4.12	Coefficients a and b Versus the I/K_s Ratio for Columbia Sand Loam	111
4.13	Effect of the Initial Degree of Saturation on the Advance of the Wetting Front with Time	112
4.14	Hydraulic Conductivity Curves Adopted for Residual Soils	113
4.15	Assumed Moisture Characteristic Curves for Residual Soils. Void Ratio Equal to 0.75	114
4.16	Assumed Moisture Characteristic Curves for Residual Soils. Void Ratio Equal to 0.89	115
4.17	Assumed Moisture Characteristic Curves for Residual Soils. Void Ratio Equal to 1.00	116

Figure		Page
4.18	Advance of the Wetting Front with Time (S_o = 70%)	117
4.19	Advance of the Wetting Front with Time (S_o = 80%)	118
4.20	Advance of the Wetting Front with Time (S_o = 90%)	119
4.21	Coefficients a and b Versus the I/K_s Ratio for e = 0.75 and $K_s = 8.0 \times 10^{-5}$ cm/sec	120
4.22	Coefficients a and b Versus the I/K_s Ratio for e = 0.75 and $K_s = 2.0 \times 10^{-4}$ cm/sec	121
4.23	Coefficients a and b Versus the I/K_s Ratio for e = 0.75 and $K_s = 5.0 \times 10^{-4}$ cm/sec	122
4.24	Coefficients a and b Versus the I/K_s Ratio for e = 0.89 and $K_s = 8.0 \times 10^{-5}$ cm/sec	123
4.25	Coefficients a and b Versus the I/K_s Ratio for e = 0.89 and $K_s = 2.0 \times 10^{-4}$ cm/sec	124
4.26	Coefficients a and b Versus the I/K_s Ratio for e = 0.89 and $K_s = 5.0 \times 10^{-4}$ cm/sec	125
4.27	Coefficients a and b Versus the I/K_s Ratio for e = 1.00 and $K_s = 8.0 \times 10^{-5}$ cm/sec	126
4.28	Coefficients a and b Versus the I/K_s Ratio for e = 1.00 and $K_s = 2.0 \times 10^{-4}$ cm/sec	127
4.29	Coefficients a and b Versus the I/K_s Ratio for e = 1.00 and $K_s = 5.0 \times 10^{-4}$ cm/sec	128
4.30	Analysis of Sensitivity of Void Ratio and Degree of Saturation on the Coefficients a and b	129
4.31	Analysis of Sensitivity of Hydraulic Conductivity and Degree of Saturation on the coefficients a and b (for a particular rainfall intensity)	130

Figure		Page
4.32	Analysis of Sensitivity of Hydraulic Conductivity and Degree of Saturation on the Coefficients a and b (for a particular value of the I/K_s Ratio) ..	131
4.33	Analysis of Sensitivity of Capillary Suction and Degree of Saturation on the Coefficients a and b	132
5.1	Approximate Range of Techniques for Measuring Suction	140
6.1	Pattern of Water Infiltration into a Slope	166
6.2	Slip Surface Along the Wetting Front Surface	166
6.3	Infiltration of Water Through a Column of Soil	167
6.4	Equilibrium Interface Position and Soil Stability ...	168
6.5	Planar Slide	169
6.6	Analysis of Occurrence of a Landslide for Certain Rainfalls	170
6.7	Analysis of Occurrence of a Landslide for a Particular Rainfall	170
7.1	Estrada do Jequiá Slide. Soil Profile - Scale 1:400	179
7.2	Estrada do Jequiá Slide. Situation After Slide	180
7.3	Analysis of Stability for the Estrada do Jequiá Slide	181
7.4	Caneleira Slide	182
7.5	Monte Serrate Slides	183
7.6	Analysis of Stability for Monte Serrate Slides	184
C.1 to C.9.	Advance of the Wetting Front with Time for the Assumed Residual Soils	

CHAPTER I

INTRODUCTION

Methods of statical analyses of slope stability have been sufficiently developed to such a point that complex analyses through very general procedures are now possible. A major problem still resides in the knowledge of the slope behaviour and in the properties and parameters of the slope-forming materials to be adopted in these analyses. If these factors are known, it is possible to predict whether a slope is stable or otherwise to undertake the necessary measures to prevent the slope from failure by improving its stability.

A general review of the stability of natural and cut slopes has been given by Skempton and Hutchinson (1969) from which the stability of slopes in certain soils under certain conditions can be predicted. However, as they said, with respect to stability of slopes in residual soils they could not draw any general conclusion.

Deere and Patton (1971) in their State of the Art report on Stability of Slopes in Residual Soils have pointed out the important roles of weathering profiles, groundwater and relict structures, and that landslides are more common during periods of heavy rainfall. Although these may be basic conditions relevant to the analyses of such problems, the mechanisms through which slope failure occurs are not understood and the influence of water is not attacked in depth.

Landslides that occur in tropical or sub-tropical regions of high humidity and rainfall, are influenced by the soil characteristic of the region (residual soil) as well as by the action of rainfall. This can be of large intensity and short duration or of moderate intensity and large duration. Extreme cases occur when the rainfall exhibits high intensity and large duration. In this case the result is always catastrophic. Such factors are, however, related to the time of the year.

The purposes of this thesis are to investigate the mechanisms of landslides and the factors that account for the slope failure and to present, on the basis of these, the methods of analysis for natural and cut slopes. Contents of the various chapters of the thesis are summarized below.

Chapter II presents the characteristics of the residual soils in view of the soil-forming process of weathering. Thus, a brief description of geology and climate is introduced and the weathering processes are explained.

Since the residual soils are unsaturated in the natural state, Chapter III deals with the movement of water through unsaturated porous media. The basic physical principles behind this type of flow and the general equation that governs the flow are developed.

In Chapter IV, solutions of the unsaturated flow equation for the particular case of vertical infiltration are presented and discussed.

The methods to determine the required parameters and quantities to analyse the flow through unsaturated soils are treated in Chapter V.

Mechanisms of slope failure are presented in Chapter VI. In this chapter procedures to analyse the stability of natural and cut slopes are discussed. A simplified classification of types of slope failure with respect to rainfall intensity is presented and methods of improving the stability of slopes are discussed.

Chapter VII analyses some case histories in the light of this study and Chapter VIII summarizes the conclusions drawn from this investigation.

CHAPTER II

RESIDUAL SOILS

2.1 Introduction

This chapter presents the characteristics of some residual soils in Brazil, particularly those in the two areas of our study: the City of Rio de Janeiro and the region of the Anchieta Highway, between the cities of São Paulo and Santos at Serra do Mar.

In order to understand residual soils, it is of interest to know how they were formed. For this, an understanding of some geological and climatic features of Brazil are needed.

2.2 Geology of Brazil

In spite of its very large surface (8,511,965 km^2), Brazil is generally of relatively low altitude. Brazilian topography is dominated by an enormous plateau with an average height of 1,000 m. This plateau extends towards the coast on the eastern part of the country, very close to the sea dipping abruptly to form scarps parallel to the coast. Locally they are called "serras" (ridges) but in fact they are "cuestas", a topographic feature exhibiting scarps on only one side, and in our case the eastern side (de Lima and de Meis, 1966; Domingues and Whately, 1966).

Plateaus and ridges of elevation ranging between 200 m and 1200 m occupy about 58.5% of the total area of the country. The low

lands, with altitudes less than 200 m occupy 41% of the country. Only 0.5% of the area of Brazil has altitudes above 1,200 m. Ridges consisting of round mounds and isolated hills in the form of domes due to exfoliation are very common in Brazil.

A summary of Brazilian geology is given by Sant'Anna (1966) and Dantas (1966). We present here some of the important geological features as described by them.

Brazil is predominantly composed of a very old complex of Precambrian formations, firstly deformed by orogenic activities and later, affected by epeirogenic movements.

Overlying this bedrock are sedimentary layers of varying thickness, whose ages range from the Paleozoic to the Recent period, giving rise to sedimentary basins at different altitudes and positions. Figure 2.1 illustrates the Precambrian formations in Brazil and the two sites of our study.

Structurally, the Precambrian formations are mainly distributed in two large rigid blocks: the "Bloco Guianense" and the "Bloco Brasileiro", both partially covered by old and recent sediments and separated by the large geosyncline of Amazonas, shown in Figure 2.1.

The "Bloco Guianense" constitutes a well defined unit but the "Bloco Brasileiro" is divided due to the localization of the Paleozoic and Mesozoic basin, distributed in depressions of different altitudes, the old epicontinental seas.

The principal old Precambrian rocks outcropping in Brazil are: gneisses and granites associated with quartzites, diorites, micaschists and some carbonate rocks such as marble and dolomites. These old terrains are dominant in almost all the "Bloco Guianense" but in the "Bloco Brasileiro" their distribution is more complex. They occur in the northeast, forming the Borborema Plateau, in the southeast, along the coast, forming the Serra do Mar and inward, they occupy large areas of the State of Minas Gerais, like the Mantiqueira Ridge. In central Brazil, they appear in the Goiano and Matogrossense Plateaus, and in southern Brazil they form the ridges of the State of Rio Grande do Sul.

The Precambrian areas are divided as archean, where the granite-gneissic formations are predominant, and as proterozoic.

2.3 Geology and Climate of Rio de Janeiro

The City of Rio de Janeiro occupies the eastern half of the State of Guanabara, and has coordinates: 22°54' (South Latitude) and 43°10' (West Longitude). This State is bordered on the south by the Atlantic Ocean and on the east by Guanabara Bay. Along the northern edge, it is bordered by the State of Rio de Janeiro into which the city extends for many kilometers. West of the city proper are smaller cities and agricultural areas.

Three topographic features can be distinguished in the State of Guanabara: the mountain ranges, the alluvial plains ("Baixadas")

and isolated hills (Barata, 1969; Jones, 1973).

As shown in Figure 2.2, three mountain ranges are aligned in a northeast-southwest direction: the Pedra Branca, the Gericinó, and the Tijuca - Carioca Ranges.

The Pedra Branca Range, in the central part of the State, branches to the southwest and separates the Baixada of Jacarepaguá from the Baixada of Sepetiba. Within the range are the mounts Cabaçu (569 m), Lameirão (482 m), Viegas (205 m), Capim Melado (647 m) and the highest peak, Pedra Branca (1,025 m).

The Gericinó Range, in the northern part of the State has a maximum altitude of 889 m at Mount Gericinó and lies on the border between the States of Guanabara and Rio de Janeiro.

The Tijuca - Carioca Range in the eastern part of the State has a maximum altitude of 1,022 m (Tijuca Peak) and consists of two ridges: the Tijuca and the Carioca. Some famous peaks are in this range: Sugar Loaf (395 m), Corcovado (704 m), Tijuca (1,022 m) and Pedra da Gávea (845 m).

Four alluvial plains, locally called "baixadas" can be distinguished: the Baixada of Guanabara in the northeastern part of the State, the Baixada of Jacarepaguá in the southern part, the Baixada of Sepetiba in the western part and the Urban Baixada which includes the Commercial Center, the South Zone and the Northern Zone of the city of Rio de Janeiro. The Isolated Hills are dispersed through the plains

and are, in general, less than 250 m high.

The hill slopes of the City of Rio de Janeiro are covered by a mantle of soils (mainly residual soils and some colluvium) and fragments of rocks which all originate from decomposition of the underlying rock by weathering.

Geologically the State of Guanabara is composed predominantly of gneisses and granites of Precambrian age. During the geological history as a consequence of rock formation processes at depth, elevation of the land mass and erosion, there was a development of faults, fractures and fissures in the rocks, along which intrusions of granitic and basic rocks occurred forming dikes.

Thus, great masses of granitic rocks were forced into the gneissic rocks during the Ordovician Period. In Cretaceous time, dikes of diabase were formed along faults and in the Tertiary Period, alkaline rocks were emplaced in the same sort of fractures, as observed in the western portion of the State (Jones, 1973).

The most prominent faults in the State of Guanabara originate mainly from land mass elevation and lie in a subparallel system in a northeast-southwest direction.

The most important rocks for our study are the gneisses because they are mainly spread in the eastern half of the State where the City of Rio de Janeiro is concentrated, including the suburbs and Jacarepaguá. They are crossed by minor intrusions of granite and basic

rocks and constitute almost wholly the Tijuca-Carioca Range. Moreover, they represent about 38% of the rocks in the State, followed by the granites that represent up to 20% and dominate in the western half (Barata, 1969).

Two different series of gneisses occur in the eastern half (Jones, 1973; Helmbold, 1967; Barata, 1969). The first and younger one is derived mostly from sedimentary rocks. It is referred to as the paragneisses of geosynclinal facies and includes the gneisses described as:-

1. Biotitic Gneiss. It is the most widely spread gneiss, crossing integrally the State in the northwest-southeast direction. It is the most complex and variable lithologic unit of the paragneisses, being a biotite-plagioclase-quartz-garnet-gneiss, sometimes also having orthoclase. A variety of it, rich in garnet, sillimanite and cordierite is very common and called kinzigite. It is of dark colour due to the high content of biotite.
2. Microcline-Gneiss. It occurs principally in the southeastern part of the City of Rio de Janeiro and is a microcline-quartz-oligoclase-biotite-garnet-gneiss. Several different textures can be found:-
   a) Porphyroid, due to the presence of feldspar crystals of large dimensions. It constitutes the most part of the peaks and abrupt scarps of the Urban Chain: Corcovado, Sugar Loaf, Cabritos Hill. It is locally called "facoidal" gneiss.
   b) Semifacoidal, when presenting poorly developed feldspar crystals. It exists in only a few areas.

c) Laminar. It has a very pronounced lamination and occurs in a very few small areas.

d) Migmatitic gneiss.

3. Leptinites. They are composed of the same minerals as the microcline-gneisses but in different proportions. They are rich in quartz and have a small percentage of mica, thus being hololeucocratic, and they present a very laminated structure. They occupy a relatively small area in comparison with the others.

This younger series includes beds of quartzite and calc-silicate rocks derived from sandstone and limestone, respectively. It includes some intrusive bodies that were metamorphosed together with the metasedimentary series. The textural varieties of the gneiss reflect the varying composition and nature of the original rocks and processes of formation.

The other series, considered an older one, is derived from granitic and mafic rocks. It is composed of gneisses texturally more homogeneous, with a varying mineralogical composition that ranges from granites to quartz-diorites and by migmatites and amphibolites. It is referred to as the inferior series.

Both series are crossed by intrusions of basic and intermediary rocks, partly gneissified and metamorphosed. The paragneisses are the most dominant, occupying the area of the City of Rio de Janeiro and a large part of the suburbs.

In spite of its small territory, the State of Guanabara has a

large variation in climate. Basically the climate of the State is characterized by either a hot or temperate summer, depending on the region, and being, however, always humid. The differences in climate are mainly felt in the winter, which varies from region to region from dry to humid.

The annual average rainfall ranges from 1500 mm to 2500 mm depending on the region, mostly concentrated during the rainy season that occurs in the summer months: December to February or March.

Thus, two main types of climate can be distinguished: "rainy and temperate climate" and "hot and humid tropical climate", types C and A, respectively, according to the criterion of Köppen (Barata, 1969; Fortes, et al, 1966). The "rainy and temperate climate", restricted to the subtype Cfa is distinguished by humidity and moderate temperature. It has hot summers and is typical of the mountainous regions above 500 m, a small area that occupies only about 5% of the State. The "hot and humid tropical climate", the predominant one, presents three varieties:-

a) Sub-type Aw, humid summer and almost dry winter. It occurs over most of the part of the State, mainly on the "Baixadas".

b) Sub-type Am, humid summer and almost humid winter, occurring at the foot of the mountains.

c) Sub-type Af, humid summer and winter, with no dry season. It occurs on the hill slopes of the mountains up to the level 500 m. (Barata, 1969; Fortes, et al, 1966).

2.4 Geology and Climate of the Area of Anchieta Highway

The Anchieta Highway, linking the cities of São Paulo and Santos is located on the hill slopes of the Serra do Mar. Many landslides occur periodically in the area obstructing the highway.

This ridge is really a "cuesta", presenting only one face that dips abruptly toward the ocean, while the opposite face is actually a plateau, dipping very gently toward the Paraná Basin. The Serra do Mar extends along the coastline of Brazil, from the State of Rio de Janeiro to the State of Rio Grande do Sul. It is composed of two branches almost parallel to the coast, an outer one, almost submerged and an inner one, considered as an Atlantic wall with decreasing elevations toward the south, reaching up to 2300 m. In the State of São Paulo the Serra do Mar is concentrated in a narrow zone parallel to the coast.

The accepted idea among geologists is that the Serra do Mar was originated by elevation of land masses along faults, that occurred very slowly during or after the Tertiary Period. Thus, differential movements of rock blocks would have given rise also to the formation of hills on the shoreline and of islands along the coast. Very intense and extended erosion has already modified the surface of the faults.

Geologically the formation of this ridge is very old, of Precambrian age. It is composed of very intensely folded layers of schists and gneisses, with intrusions of granites and limestones.

At upper elevations, large intercalations of micaschist occur close to the gradational contact between gneiss and schist. At these areas the micaschist can be the dominant rock. The gneisses are typically biotitic, with varying content of quartz and banded structure. Both rocks are also crossed by veins of quartz and pegmatites (Teixeira and Kanji, 1970; Fortes, et al, 1966; Vargas, 1967a, 1967b).

The site of the Anchieta Highway at Serra do Mar presents basically the "tropical altitude climate", distributed in two areas: the largest one, with a climate of hot and humid summer (Cwa) and the smaller one with temperate and humid summer (Cwb) (Fortes, et al, 1966).

The average annual rainfall is around 4000 mm or 5000 mm depending on the site but values as high as 6000 mm have been recorded at the foot of the ridge in Cubatão in 1947 (Vargas, 1967a).

2.5 Weathering and Weathering Profile

A considerable percentage of the hill slopes of Rio de Janeiro and Serra do Mar is covered by a thick mantle of soil and fragments of rocks formed by in situ decomposition of the underlying rocks. The processes of decomposition are extremely complex, and several phenomena may act separately or combined to alter the rock. It is well known that the climate is the principal factor that will determine the type of weathering, making some processes to act more intensively (Leinz and do Amaral, 1962).

Obviously, the weathering will also depend on the type of

parent rock and the climatological aspects are associated with other factors such as topography, altitudes, etc.

Basically, the very humid environment makes water available throughout the year from rainfall, mostly distributed during the summer months. This associated with high temperature is the principal agent of the weathering processes.

The temperature is responsible for a certain type of physical weathering, by fracturing the rocks. As a consequence of temperature variations, exfoliation will occur along isothermal lines in the rocks and as a result, the round blocks of rock common in many hill slopes, and the round form of most of the hills in Santos and Rio de Janeiro appear.

Temperature also plays an important role by accelerating the reactions inherent to the chemical processes of weathering.

Another physical process of block fracturing results from the growth of vegetal roots when the rock possesses openings through which the roots can penetrate.

Chemical decomposition occurs by reactions between the minerals forming the rocks and different aqueous solutions. This type of decomposition is more common in humid and hot environments. Several processes of chemical decomposition may occur.

The water from the rainfall contains gases dissolved in it,

such as oxygen and carbon dioxide from the atmosphere. It may also be possible that due to the action of lightning during thunderstorms, atmospheric nitrogen combines with oxygen and water to form nitric and nitrous acid. These diluted acids then have a corrosive action on the rocks when the rain reaches the ground.

When infiltrating into the soil, the water also dissolves and carries several organic and inorganic substances, very often of acid nature which are active in chemical weathering.

Some minerals present in the rocks may decompose in the presence of water due to its ionization. The corresponding reaction is referred to as hydrolysis. As a consequence of hydrolysis the complex silicates typical of igneous and metamorphic rocks are destroyed. As described by Dapples (1959) there is a replacement of large metal ions by H^+ ions. The silicic acid-like molecules formed, being unstable under the presence of water would undergo further hydrolysis with rearrangement of structure and development of clay minerals due to hydroxils entering the lattice. Thus, hydrolysis of orthoclase would undergo the following mechanism:

$$H_2O \rightleftharpoons H^+ + OH^-$$

$$KAlSi_3O_8 + H^+ \rightarrow HAlSi_3O_8 + K^+$$

(orthoclase) (silicic acid-like structure)

$$HAlSi_3O_8 + OH^- \rightarrow (OH)_8Al_4Si_4O_{10} + SiO_2 + H^+$$

(silicic acid-like structure) (rearrangement of lattice) (clay mineral-kaolinite in colloidal form) (ion or colloid form)

The hydrolysis depends on the degree of ionization of the water which in its turn depends on the temperature, increasing considerably with it. Denoting the degree of ionization by I_o for the temperature of 0°C and by I that for a given temperature t°C, the ratio I/I_o increases according to the table below (Vargas, 1971a):

t°C	0	10	18	34
$\frac{I}{I_o}$	1	1.7	2.5	4.5

Carbon dioxide, either from atmosphere or from decomposition of vegetals is mostly dissolved by water. A small part, however, combines with water to form carbonic acid always in the state of dissociation:

$$H_2O + CO_2 \rightleftarrows H_2CO_3$$

$$H_2CO_3 \rightleftarrows H^+ + HCO_3^-$$

$$HCO_3^- \rightleftarrows H^+ + CO_3^{--}$$

In spite of being a weak acid, the carbonic acid is one of the most important agents of the chemical weathering. Its action with feldspars is as follows (e.g., orthoclase):

$$2KAlSi_3O_8 + H_2CO_3 + 2nH_2O \rightarrow K_2CO_3 + Al_2(OH)_2Si_4O_{10} + 2SiO_2$$

(orthoclase) (soluble salt) (clay mineral)

Over the biotite, under oxidant environment it follows:

$$2KMg_2Fe(OH)_2AlSi_3O_8 + \frac{1}{2}O_2 + 10\,H_2CO_3 + nH_2O \rightarrow$$

(biotite)

$$\rightarrow 2KHCO_3 + 4\,Mg(HCO_3)_2 + Fe_2O_3\;H_2O +$$

$$+ Al_2(OH)_2Si_4O_{10} \cdot n\,H_2O + 2\,SiO_2 + 5\,H_2O$$

(clay mineral)

Oxidation is a process that occurs primarily in silicate minerals containing iron. Iron is the substance which primarily undergoes oxidation and its oxidation appears to proceed along with hydrolysis of the silicate structure. The weathering of biotite is as follows:

$$(OH)_2\,K(Mg, Fe)_3\,AlSi_3O_{10} + H^+ - e^- \rightarrow$$

(biotite)

$$\rightarrow H_5AlSi_3O_{10} + Fe^{+++} + Mg^{++} + K^+ + OH^-$$

$$Fe^{+++} + 3OH^{-} \rightleftarrows Fe(OH)_3 \rightleftarrows \frac{1}{2} Fe_2O_3 \cdot nH_2O$$

(limonite)

$$H_5AlSi_3O_{10} + OH^{-} \rightarrow (OH)_8Al_4Si_4O_{10} + SiO_2 + H^{+}$$

(clay mineral)

It is important to note that oxidation develops the Fe^{+++} ion which in hydroxides, hydrates or oxides has a brown to vermilion red colour.

Ferrous ion (Fe^{++}), however, tends to develop compounds of characteristic gray, green or even blue tints.

By virtue of the chemical reactions presented here, kaolinite will be the most dominant clay mineral in the residual soils in these areas of Brazil. In fact, in acid environments, sodium, potassium, calcium, magnesium and iron are completely leached and there is an introduction of hydrogen during the process of clay formation, principally when the ratio silicon-aluminum is low, with a consequent formation of kaolinite (de Mello and Silveira, 1965).

Very few minerals are resistant to chemical attack. Among them the most important is quartz. Most of the minerals are subjected to decomposition with time, being transformed to stable minerals under the conditions at the surface and to soluble substances that are carried by the water.

The non-soluble residue remains in the site and will deposit

to form the clay fraction of the residual soil.

As a consequence of the weathering processes, a mantle of soil will cover the rocks on the hill slopes, composed of clay, silt, sand and even fragments of rocks not totally disaggregated.

The weathering process acts at depth and with time and there is a variation in properties of the materials with depth. First, there is a fracturing of the rock (physical disaggregation) then this is followed by a chemical attack by the acid water that penetrates into the fractures.

A characteristic of this weathering process is that the water tends to wash down some of the constituents of the upper layer, referred to as the zone of eluviation. These constituents will be deposited in lower layers (zone of illuviation). The tendency of this process is, therefore, to give rise to more porous layers in the upper part of the weathering profile.

Depending on the intensity of the chemical attack, small fragments of feldspars and mica, not totally decomposed may occur within the sandy fraction of the soil. As the process proceeds there is a tendency for the formation of more clayey layers. This is illustrated by Haberlehner (1967) in Table 5.1, where the surficial soil is more clayey than the underlying soil. Therefore, we can observe several layers with different properties that range from those corresponding to a soil to those for a sound rock. However, there is a gradual transition between these layers that makes it difficult to establish the boun-

daries in the weathering profile. It should be emphasized, however, that any establishment of different zones within the weathered profile is very arbitrary and qualitative since the soil properties vary continuously with depth.

On the basis of a gradual variation of soil properties with depth, it is obvious that any problem in soil mechanics should recognise this feature.

Vargas (1953) distinguished three different zones in the weathering profile: 1) the mature residual soil zone, resulting from the total action of weathering and composed of a layer of humus and a layer of reddish or yellowish clayey or sandy soil; 2) the young residual soil zone composed of clay or clayey sand and presenting the original structure of the parent rock and 3) the disintegrated rock, just overlying the sound rock.

Figure 2.3 from Vargas (1953) illustrates the three zones for two different sites. One is near the crest of Serra do Mar and the other is near the crest of a lower range of mountains in a deforested zone. This figure shows the tendency towards an increase in the thickness of the mature residual soil and of the total decomposed overburden and towards a decrease in the thickness of the disintegrated rock layer.

Deere and Patton (1971), on the basis of the work of several investigators, give a three fold subdivision for the profiles of rock weathering developed over intrusive igneous rocks and metamorphic rocks as follows:

a) Zone I - residual soil

b) Zone II - weathered rock

c) Zone III - relatively unweathered, fresh bedrock

Each of these zones are also subdivided into layers that exhibit distinct characteristics. We will not describe all of their features but refer to Table 2.2 and Figures 2.4 and 2.5 presented by Deere and Patton. It is important to note that their classification basically corresponds to the one presented by Vargas (1953) with differences shown on Figure 2.5.

Deere and Patton's classification appears to be somewhat general and as they point out, "it is not always easy to apply because of the very irregular and, often, gradational contacts". However, due to the characteristic of their classification and to the enormous variety of names presented by several investigators for the weathering profile, Deere and Patton's classification may be very convenient and useful and we shall adopt it as much as possible, although the classification presented by Vargas may be more specific to our study.

An interesting fact described by Vargas and Pichler (1957) and Pichler (1957) is that, in Santos the slopes are normally very steep and when they reach angles up to 45°, the hill slopes are covered by a mantle of residual soil. However, for angles over 45° they generally exhibit very jointed bare rock, reflecting two systems of joints: one system that in the upper parts of the rocks has the same dip and dip direction and the other consisting of exfoliation joints. Both tend to

separate large blocks of rock due to the ease of weathering along the joints (Figure 2.6). As a consequence, hill slopes of mixed soil and rock boulders are very common. At the top of the hills, the residual soil mantle has a thickness of about 20 m; this thickness being reduced at the slopes to a few meters if the bare rock is not directly exposed.

This same feature can be observed in the City of Rio de Janeiro as described by Barata (1969). There, hill slopes up to 30° are covered by a thick mantle and steeper ones (above 30°) are covered by a shallow mantle. Both are referred to as earthy hill slopes. Steep hill slopes of 60° and over exhibit no mantle and are referred to as scarps.

In areas of constantly humid climate the depth of zone IC can be as large as 80 m (Vargas, 1971a).

Teixeira and Kanji (1970) describe the features of a landslide on Anchieta Highway at elevation 500 m. There, the zone of partly weathered rock (zone IIA) occurs at depths over 50 or 60 m. An unusual depth of 75 m, however, has been reported by them for the residual soil zone (zone I) at the same site.

2.6 Properties of the Residual Soils

Figure 2.7 illustrates the profile of weathering that has occurred over gneiss under constantly hot and humid climate, at Serra do Mar (Vargas, 1971a).

A very thin layer of organic material overlies a layer of clay or clayey sand, 3.0 to 10.0 m thick, zones IA and IB. The predominant clay mineral in these zones is kaolinite. Underlying this zone there is a layer that exhibits relict structures from the gneiss and has 10 to 80 m of thickness, zone IC. It is underlain by a zone of weathered gneiss that has corestones and boulders surrounded by soil not totally decomposed.

It can be observed that the percentage of clay decreases with depth, thus, with a tendency for the material to be coarser, as already discussed. It is also seen that the porosity has a value of about 50% throughout the profile reflecting the relatively large voids of these soils.

The same type of profile can be observed in Rio de Janeiro with coarse soil, sandy silt or silty sand, and a small percentage of clay, higher at the upper layer.

2.6.1 Residual Soils in Rio de Janeiro

As we noted before, gneiss is the predominant rock in the City of Rio de Janeiro. All the varieties of gneiss will lead to residual soils of slightly different properties. Table 2.1 illustrates some properties of the residual soils, corresponding to each variety of gneiss.

It can be seen from this table that the residual soil derived from microcline gneiss (porphyroid), "facoidal gneiss", is the most

plastic. The kinzigite, richest in iron minerals, also has as a result, a higher unit weight of solid particles.

The differences between these soils can be better illustrated through Table 2.3 which shows average values of the shear strength parameters for these soils.

A description of the characteristics of some residual soils of Rio de Janeiro has been presented by Sandroni (1973). Although he does not mention it, they are likely derived from microcline-gneiss, as we can see from the location of the sites from where the samples were obtained. His samples, however, have a very small void ratio when compared to other, as shown for example by Ferreira (1967) and presented in our Table 2.3.

The average value of the void ratios described by Sandroni is about 0.58, ranging however from about 0.12 to 1.1. However, as he points out, the samples were obtained from zones of young residual soil, and perhaps these soils would exhibit these smaller void ratios, keeping in mind that the tendency of the weathering process is to develop a porous structure characterized by large voids as has been pointed out by Vargas (1971a, 1973).

These soils mainly consist of silty sand, with the percentage of clay mainly falling in the range from about 7 to 22% although a few values have appeared out of this range. The soils in question have low to medium plasticity:

Liquid Limit	(w_L)	=	20 to 40%
Plastic Limit	(w_p)	=	12 to 32%
Plasticity Index	(I_p)	=	5 to 15%

and some were non-plastic.

Although Sandroni's results do not show a good correlation with the void ratio, it is possible, however, to identify some trends:

a) The percentage of fine materials (< # 200) increases with the void ratio. This trend can be explained since the more porous soils correspond to a more advanced stage of evolution, thus, with the tendency of having a larger percentage of fines.

b) The natural moisture content increases with the void ratio.

Other results have been presented in a report by Geotecnica (1967) concerning a landslide that took place at Governador Island in Rio de Janeiro, referred to as the Estrada do Jequiá slide, and that we shall be analysing in detail in Chapter VII. There, the soils were predominantly sandy-silt of low plasticity, having the characteristics below:

Clay (< 2μ)	14 to 40%
Silt (2μ - 0.06 mm)	36 to 50%
Sand (0.06 - 2 mm)	24 to 45%
Liquid limit	26 to 49%
Plastic limit	19 to 27%
Void ratio	0.48 to 1.09

In Table 2.3, we have included the values of void ratio and dry unit weight calculated from Tables 2.1 and 2.3 for the residual

round grains instead of angular ones.

Other data shown in Table 2.4, have been obtained by Geotecnica (1967) with respect to the Estrada do Jequiá slide in Governador Island. They also illustrate the same reduction of cohesion after saturation, as described.

Also shown in Table 2.4 are the results presented by Sandroni (1973) from drained direct shear tests on samples saturated before shearing. Due to his large number of tests, Sandroni presents the strength parameters as a function of void ratio, obtained by regression analysis. We see from his data that both, cohesion and angle of internal friction decrease as void ratio increases.

Since his results show that the percentage of fines (< # 200) increases with void ratio, we see that a larger cohesion occurs for a smaller percentage of fine grains and he found that fracturing of grains was occurring during the tests. Note that his void ratios are small, with an average value of about 0.6, consequently giving large values for the cohesion and the angle of internal friction.

2.6.2 Residual Soils at Serra do Mar and Santos

In this area, the residual soils of gneiss, granite-gneiss and micaschist can be distinguished. Table 2.5 illustrates the characteristics of the residual soils of the mature and young soils horizons in this region, as presented by Hessing (1969).

Table 2.6 and 2.7 illustrates the properties of the soils at different locations where landslides occurred. It is interesting to note that the results shown in Table 2.6 presented by Vargas and Pichler (1957) and Vargas (1967a) show an important reduction of the angle of internal friction and only a slight reduction of cohesion. Also, an interesting fact is that the soils of Serra do Mar and Santos presented by Vargas have larger void ratios than those from Rio de Janeiro but exhibit a much larger apparent cohesion after saturation of the samples.

According to Vargas (1974), however, his tests are very old and were not well conducted and associated with the difficulty of ensuring a good saturation of the samples in the laboratory. These tests were also carried out long after the landslides had occurred and after some possible drying of the samples. Recent tests (Vargas, 1971a, 1974) show that, upon saturation, the apparent cohesion of these soils is very low and even zero and the angle of shearing resistance ranges between 28 and 33°.

Parent Rock	Location	Liquidity Limit (%)	Plasticity Limit (%)	Plasticity Index (%)	Particles Density	Grain Size (%)		Colour
						< # 200	< 2 μ	
Kinzigite Gneiss	Surficial* Soil	37.2-63.5	19.1-30.2	18.1-33.3	2.65-2.74	40.3-61.0	16.7-31.0	Yellow to red
	Residual Soil	0.0-65.7	0.0-37.9	0.0-37.8	2.68-2.77	16.3-44.3	0.0-18.0	Light yellow to dark grey
Leptinitic Gneiss	Surficial Soil	38.0-69.1	19.1-28.3	23.9-40.8	2.60-2.64	44.9-57.0	23.5-37.6	Light yellow to light grey
	Residual Soil	0.0-50.8	0.0-26.0	0.0-25.3	2.61-2.64	12.7-50.0	0.0-20.7	White to light grey
Porphyroid Gneiss (facoidal)	Surficial Soil	41.7-75.0	20.0-35.0	21.0-40.0	2.57-2.69	42.4-73.2	17.5-45.8	Yellow, brown red
	Residual Soil	32.0-72.5	20.5-36.3	11.5-33.8	2.64-2.71	18.0-66.8	0.0-43.0	Light yellow to red

* The surficial soil may have been subject to some transport by water (erosion) or creep.

TABLE 2.1 CHARACTERISTICS OF RESIDUAL SOILS OF DIFFERENT VARIETY OF GNEISSES IN RIO DE JANEIRO (After Haberlehner, 1967)

ZONE		DESCRIPTION	RQD* (% Core, pressed)	PERCENT CORE RECOVERY* (% Core)	RELATIVE PERMEABILITY	RELATIVE STRENGTH
I RESIDUAL SOIL	IA--A HORIZON	-top soil, roots, organic material -zone of leaching and elluviation may be present	———	0	medium to high	low to medium
	IB--B HORIZON	-illuvial/eluvially clay-enriched -clay accumulations of Fe, Al and Si, -lower may be unleached -no relict structures present	———	0	LOW	moderately LOW High if unleached
	IC--C HORIZON (Saprolite)	-relict rock structures retained -very grading to sandy mantle -less than 10% core stones -often micaceous	0 or non significant	generally 0--10%	medium	low to medium Relict structures very significant
II WEATHERED ROCK	IIA--TRANSITION (Zone residual soil or saprolite to partly weathered rock)	-highly variable, and may be rock like -zone commonly five to eleven feet thick -10 to 90% core stones -spheroidal weathering common	variable, generally 0--50	variable, generally 10--90%	MOD/ Lower Zones dominant	medium to low where rock structures and relict structures are present
	IIB--PARTLY WEATHERED ROCK	-rock like, soft to hard rock -joints stained to altered -minor alteration of feldspars and micas	generally 50--75%	generally >90%	medium to high	medium to high**
III UNWEATHERED ROCK		-no iron stains in rock along joints -no weathering of feldspars and micas	> 75% Generally >90%	generally 100%	low to medium	very high **

* Note: The descriptions provide the only reliable means of distinguishing the zones

** Considering only relict rock masses with no adversely oriented geologic structure.

TABLE 2.2 DESCRIPTION OF A WEATHERING PROFILE FOR IGNEOUS AND METAMORPHIC ROCKS (After Deere and Patton, 1971)

Parent rock	Unit Weight (g/cm^3)		Apparent Cohesion*** (kg/cm^2)		Angle of Shearing Resistance***		Void Ratio*	Dry Unit Weight* (g/cm^3)
	Natural State	Saturated**	Natural State	Saturated	Natural State	Saturated		
Leptinitic Gneiss	1.566	1.787	0.214	0.092	34.3	25.0	1.06	1.28
Porphyroid Gneiss (facoidal)	1.709	1.863	0.304	0.108	35.8	31.6	0.95	1.38
Kinzigite Gneiss	1.698	1.848	0.254	0.104	32.9	28.1	1.02	1.35

* Back-calculated values.

** Samples saturated before shearing.

*** Results from consolidated undrained direct shear test.

TABLE 2.3 PROPERTIES OF RESIDUAL SOILS FROM DIFFERENT VARIETIES OF GNEISS IN RIO DE JANEIRO (After Ferreira, 1967)

Type of Soil	Parent Rock	% < 2μ	Liquidity Limit (%)	Plasticity Limit (%)	Void Ratio	Type of Test	Apparent Cohesion (kg/cm^2)		Angle of Shearing Resistance		Reference
Sandy-silt (Governador Island - Rio de Janeiro		19-40	20-49	19-27	0.48-1.09	DDST	0.45	0.15	30	30	Geotécnica (1967)
						DDST (residual strength)		0		30	
						CDT	0.45	0.1	32.4°	32°	
						CUT	0.45		32.4°		
	Microcline Gneiss		20-40	12-32	0.4	DDST	0.35		43°10'		Sandroni (1973)
					0.5		0.28		39°30'		
					0.6		0.23		36°30'		
					0.7		0.19		34°30'		
					0.8		0.17		33°40'		

DDST - Drained Direct Shear Test.

CDT - Consolidated Drained Triaxial Test.

CUT - Consolidated Undrained Triaxial Test.

TABLE 2.4 PROPERTIES OF RESIDUAL SOILS FROM RIO DE JANEIRO

Parent Rock	Characteristics of the Residual Soils	
	Mature Soil	Young Soil
Gneiss	Sandy-clay or clayey-sand with small grains of quartz concretions of limonites	Silty-sand or sandy-silt Small amount of clay Blocks of partly weathered feldspar, mica Grains of quartz Structure of gneiss Not very plastic
Granite-gneiss	Similar as above	Angular fragments of quartz Large amount of mica and partly weathered feldspars Structure of granite
Micaschist	Homogeneous clayey-sand very easy disaggregation	Sandy-silt or silty sand with fine sand Original structure of the rock and intrusions of different nature Very heterogeneous

TABLE 2.5 CHARACTERISTICS OF RESIDUAL SOILS OF DIFFERENT ROCKS AT SERRA DO MAR (After Hessing, 1969)

Type of Soil	% < 2μ	w_L (%)	w_P (%)	e	γ_{dry} (g/cm^3)	w (%)	S_{in} (%)	Test	c (kg/cm^2)		φ		Reference
									nat	sat	nat	sat	
Sandy clay (Monte Serrate Slide - Santos)	5	20-40	2-13	0.87-1.02	1.35	20-25	63	DDST	0.4	0.3	42	31	Vargas and Pichler (1957) and Vargas (1967a)
"	7	18			1.50	19	70	DDST	0.4		40		
							70	UUT	0.7		20		
							85	UUT	0.7		18		
Clayey sand Caneleira Slide - Santos)		20-48	0-18	0.73-1.07		19-27		DDST	0.4	0.4	40°	30°	Vargas (1967a)
(Anchieta Highway) Elev 500)						12-40		CUT		0		37	Teixeira and Kanji (1970)
								CUT		0		29	

TABLE 2.6 PROPERTIES OF RESIDUAL SOILS AT SERRA DO MAR AND SANTOS

Parent Rock	Horizon	Composition	Liquid Limit	Plastic Limit	% < # 200
Gneiss	Mature Residual Soil	Sandy-clay or Clayey sand	42.2	15.6	47.2
	Young Residual Soil	Silty-sand or Sandy-silt	31.5	10.9	41.7
Micaschist	Mature Residual Soil	Clayey sand	32.7	11.5	56.0
	Young Residual Soil	Sandy-silt or Silty-sand	40.0	14.8	82.2

TABLE 2.7 CHARACTERISTICS OF RESIDUAL SOILS AT SERRA DO MAR AND SANTOS (After Hessing, 1969)

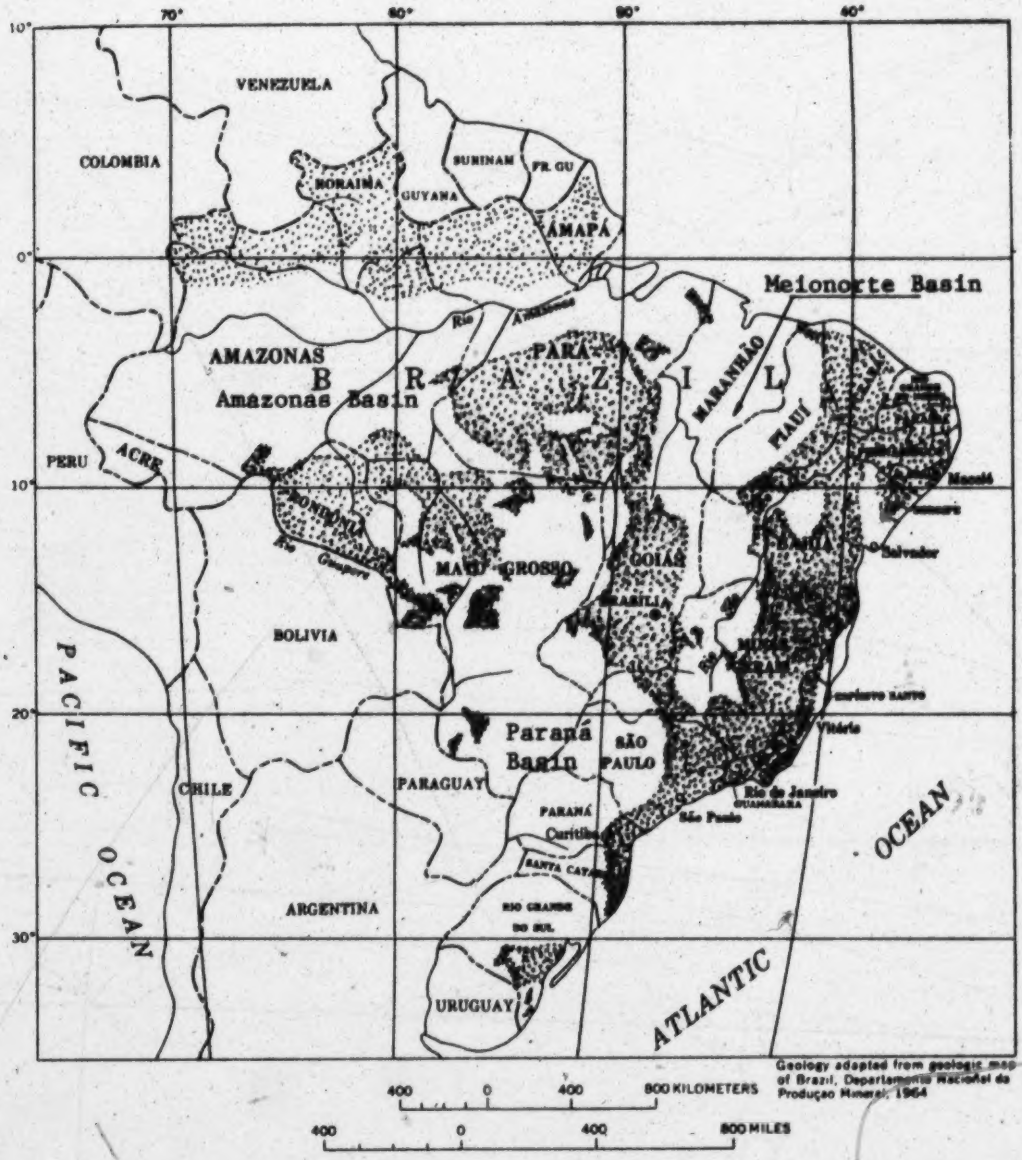

FIGURE 2.1 ZONES OF PRECAMBRIAN FORMATIONS IN BRAZIL (SHADED AREAS). (After Jones, 1973)

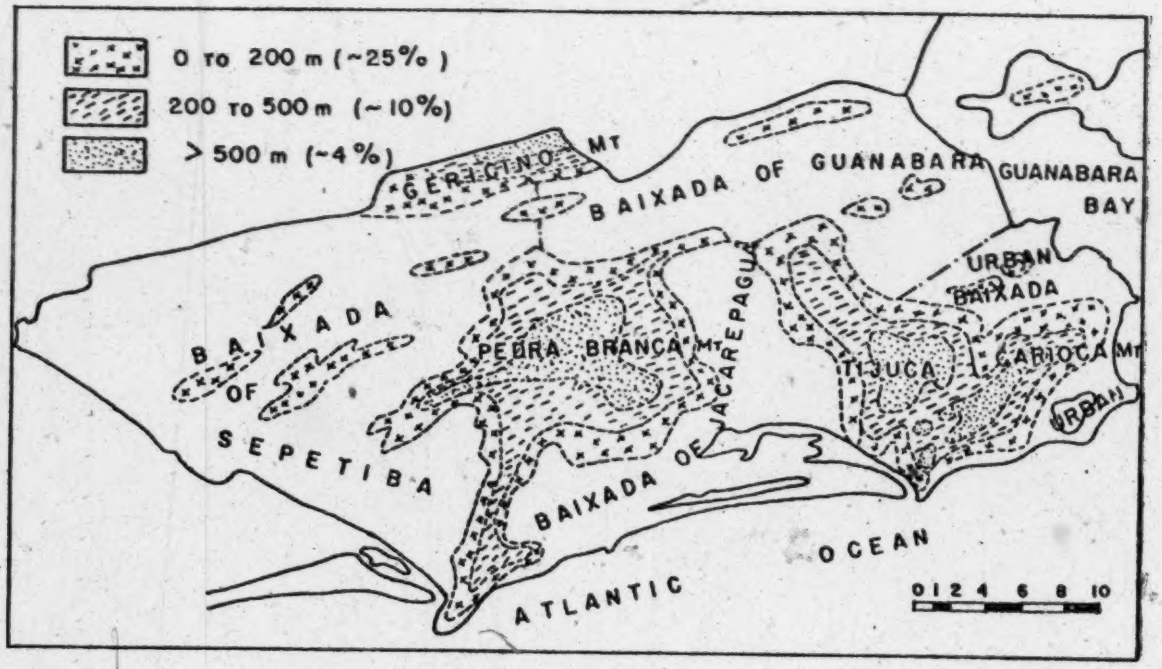

FIGURE 2.2 TOPOGRAPHIC FEATURES OF THE STATE OF GUANABARA
(After Barata, 1969)

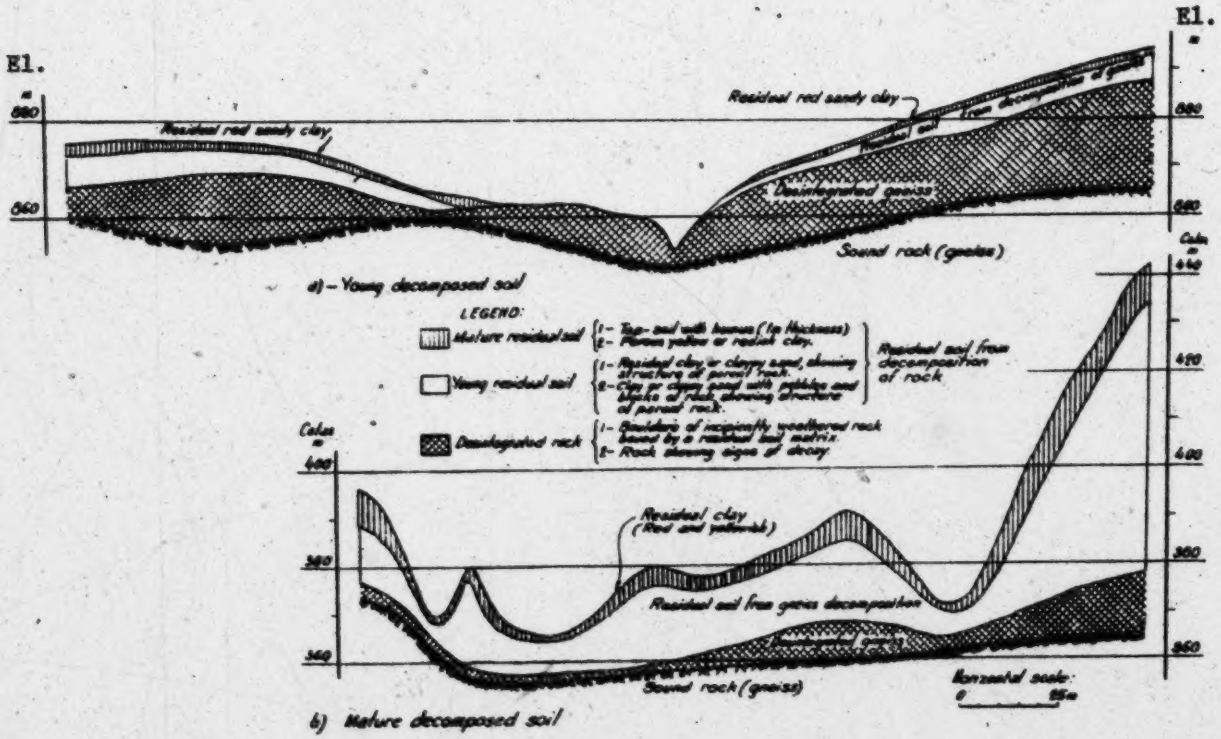

FIGURE 2.3 WEATHERING PROFILES AT DIFFERENT STAGES
(After Vargas, 1953)

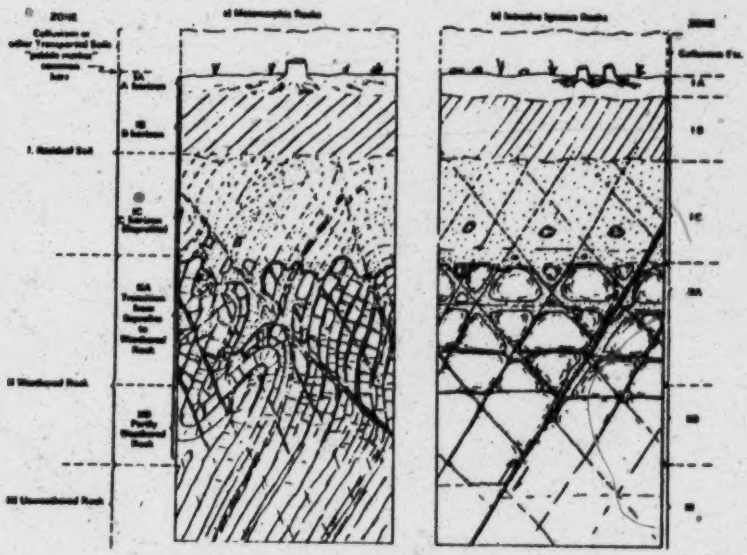

FIGURE 2.4 TYPICAL WEATHERING PROFILE FOR METAMORPHIC AND INTRUSIVE IGNEOUS ROCKS
(After Deere and Patton, 1971)

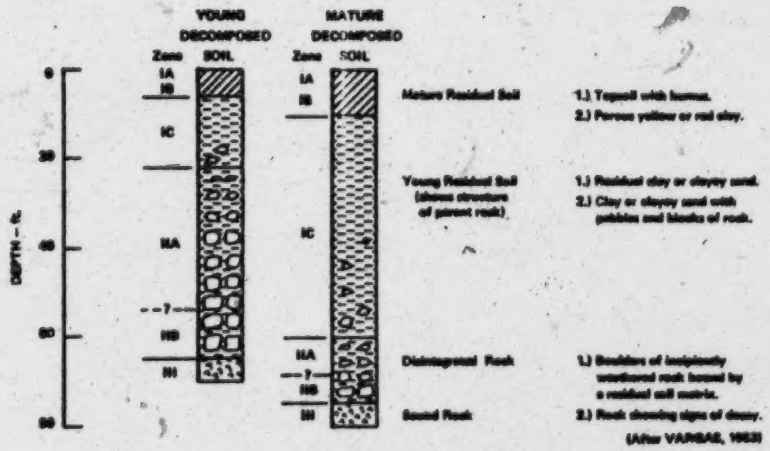

FIGURE 2.5 PROFILES OF WEATHERIN ON GNEISS IN SOUTHERN BRAZIL
(After Deere and Patton, 1971)

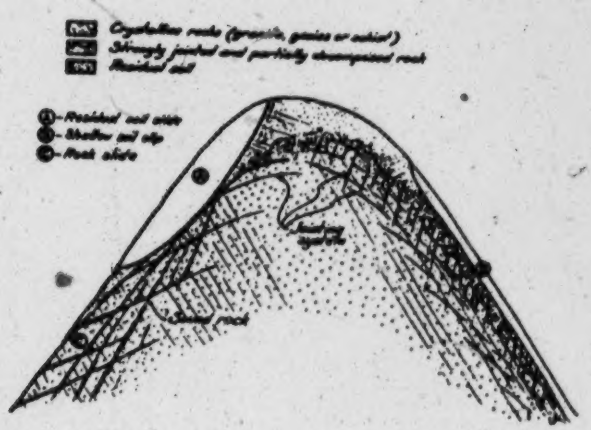

FIGURE 2.6 GENERAL WEATHERING PATTERN IN A HILL
(After Vargas and Pichler, 1957)

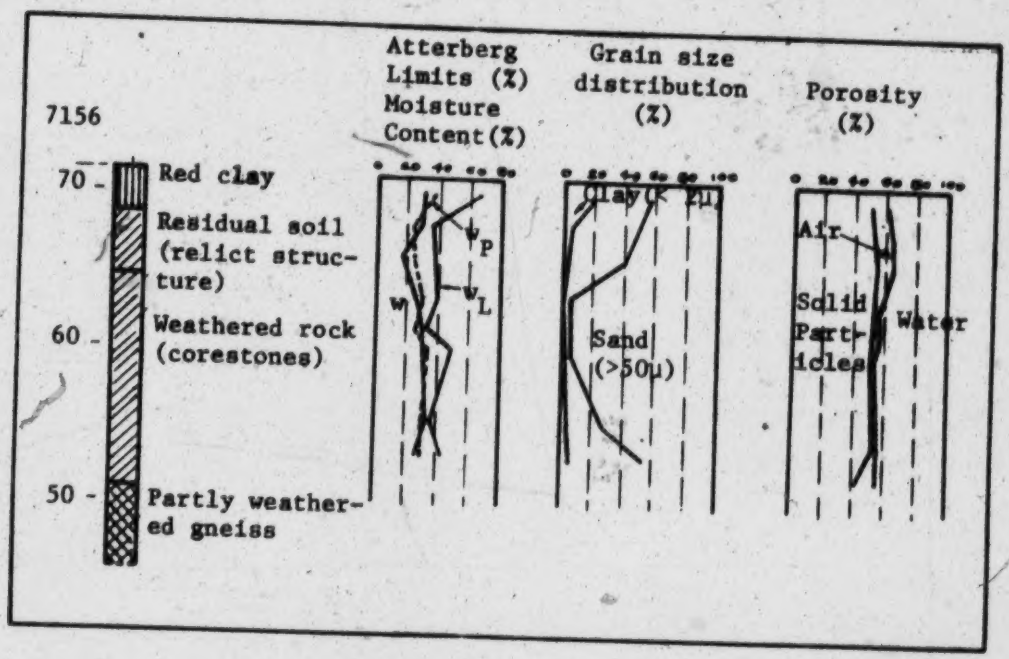

FIGURE 2.7 TYPICAL PROFILE OF RESIDUAL SOIL OF GNEISS : UNDER CONSTANTLY HOT AND HUMID ENVIRONMENT
SERRA DO MAR
(After Vargas, 1971a)

CHAPTER III

INFILTRATION OF WATER THROUGH UNSATURATED POROUS MEDIA

3.1 Introduction

Any soil normally has variations of its properties with respect to depth. Even a homogeneous soil may have variations of its moisture content with respect to depth, due to seasonal variations of rainfall. Such variations of moisture content in a homogeneous soil lead to variations in other properties. Thus, the permeability which is considered an intrinsic parameter of a soil for a given void ratio, varies instead with the degree of saturation or moisture content of the soil.

As noted in Chapter II, for a constant void ratio, the shear strength parameters vary with moisture content. Another property, the suction in unsaturated soils also varies with moisture content.

A very large fraction of the water falling as rain on the land surface of the earth imposes a certain rate of percolation at the soil surface and moves through unsaturated soils during the subsequent processes of infiltration, drainage, evaporation, and the absorption of the soil water by plant roots. This alters not only the moisture profile with time but also all the other soil properties associated with the moisture content.

The great majority of the soils covering the earth surface

are in an unsaturated state, in particular the residual soils in Brazil which are of our main concern in this study. Thus, in this chapter, we shall present the theory of infiltration of water through unsaturated porous media which will constitute the basis of our study.

3.2 Unsaturated Soils

As we have seen in Chapter II, the Brazilian residual soils are normally in an unsaturated state. Saturation of these soils occurs only at, or close to, the end of the rainy season when instability of the slopes in residual soils may occur.

Infiltration of water from rainfall through these soils, leading to their saturation, has great implications for landslides.

3.2.1 Suction

The pore water in unsaturated soils is under a negative pressure or suction, whose magnitude depends on the moisture content of the soil. Let us consider the model presented by Childs (1967) in which a body of water external to a soil is put in contact with it. Under a suitable suction applied to the external body, there will be moisture equilibrium in such a way that the external body neither gains water from the soil nor looses water to it. Increasing suction progressively decreases the soil water content, while relaxation of the suction permits the re-entry of water.

The above fact shows the dependence of the pore water content

on the prevailing hydrostatic pressure, in this case a negative pressure or suction.

Figure 3.1 illustrates this experimentally. The suction decreases (algebraically) rapidly as the moisture content decreases. When the moisture content is so small that water is retained only in the smallest pores, or in the absorbed films, the forces holding it are very great indeed (Philip, 1969). Such a curve is referred to as the moisture characteristic curve, implying an equilibrium between the suction exerted in the pore water phase and the existing soil moisture content.

It must be pointed out that although the curvature of the air-water interface is the principal determinant of suction in inert soils, it is not so for soils of high colloidal content and those very dry soils, out of our scope. Phenomena related to these colloidal soils are discussed for example in Childs (1969), but even they exhibit a moisture characteristic curve of the type shown in Figure 3.1.

The moisture characteristic curve, however, is not unique. Differences exist when the soil is under an increasing suction, thus being progressively dried and when this suction is decreasing and thus the soil is being wetted. Such differences occur due to the irregularity of shape of the pore space as explained by Childs (1969). He also explains why during the drying process of the soil, the suction must be larger (in numerical value) than during wetting of the same soil. Therefore, depending on the direction of the changes in moisture

content, the moisture characteristic curves would not be reversible. The greater the disparity between the size of the large and of the small pores, the more marked is the difference between the suction of wetting and drying. This difference is referred to as the hysteresis of the moisture characteristic curve.

Analyses of problems of infiltration or absorption of water into a homogeneous soil would require the moisture characteristic curve corresponding to wetting. Conversely, a drying curve should be used in the analysis of suitably uniform processes of removal of soil water, such as evaporation, etc.

As we shall see, however, problems such as redistribution of moisture content and drainage after infiltration ceases, wherein wetting and drying occur simultaneously, would require knowledge of all the moisture characteristic curves corresponding to the previous history of the soil (Childs, 1969).

Experimental evidence of the hysteresis as discussed has been shown in the past by Haines (1930) and is given in Figure 3.2.

In Figures 3.1 and 3.2 and in those that follow in the subsequent analysis, the moisture content will be referred to as the volumetric moisture content, defined as the ratio between the volume of water present in the soil and the total volume of soil. This will be convenient since in our analysis we will be dealing with variations of volume of water present in an incompressible soil. Accordingly, the symbol θ will be reserved for the volumetric moisture content while

the symbol w will be reserved for the conventional gravity moisture content. Some useful relations between these two moisture contents are as follow:

$$\theta = \frac{G}{1 + e} w \tag{3.1}$$

or:

$$\theta = \frac{\gamma_{dry}}{\gamma_w} w \tag{3.2}$$

or:

$$\theta = nS \tag{3.3}$$

where the symbols denote:

θ	volumetric moisture content
w	gravimetric moisture content
G	density of soil particles
e	void ratio
γ_{dry}	dry unit weight of the soil
γ_w	unit weight of water
n	porosity
S	degree of saturation

3.2.2 Hydraulic Conductivity

Movement of water in unsaturated soils can take place through water films or through those pores full of water at the particular suction corresponding to the existing moisture content.

Liquid flow taking place through thin films is slow, as com-

pared with the flow through pores when full of water.

Air-filled pores would be ineffective in conducting water through them and they would be filled by water first, prior to conduction. Thus an empty pore would contribute only negligibly to the total movement of water through the soil.

Therefore it is expected that the permeability, considered an intrinsic parameter of a soil of a definite void ratio for saturated flow, decreases with a reduction in saturation and it will be referred to as hydraulic conductivity here.

It is also expected that for a soil with a certain void ratio, the hydraulic conductivity is larger for a larger moisture content and that the maximum hydraulic conductivity occurs for the saturated soil.

If the moisture content of a soil is progressively reduced by a progressive increase of suction, the larger pores are emptied first and since they are the more effective conductors when full of water, the early stage of unsaturation represents a more effective stage in reducing the conductivity. Besides, as a pore is emptied, it also becomes an obstacle to the passage of water, and forces the flow to be carried through much smaller and considerably more tortuous channels.

A typical variation of the hydraulic conductivity with moisture content, as determined experimentally, is shown in Figure 3.3. It is worth noting that for unsaturated soils, a certain value of the

moisture content may signify different distributions of the water in the pore spaces. Thus, different hydraulic conductivities may occur as a consequence of variations in tortuosity by virtue of different water distribution.

This variation of hydraulic conductivity is also characterized by a minor hysteresis effect (Childs, 1969). The existence of a small hysteresis loop has been confirmed by Poulovassilis (1969).

The hydraulic conductivity depends on the moisture content or degree of saturation and since the moisture content is related to the prevailing suction, the hydraulic conductivity will also depend upon the suction.

According to Miller and Klute (1967), the relation hydraulic conductivity-suction for soils is highly hysteretic, though the relation conductivity-moisture content is only slightly hysteretic.

3.3 Movement of Water through Unsaturated Soils

Movement of water in unsaturated soils may occur in the liquid phase as well as in the water vapour present. In the presence of temperature gradients, for example, there is transport of water by diffusion in the vapour phase. According to Philip (1957a), however, during infiltration, liquid phase movement is of much greater magnitude than movement in the other phase. Even differences of vapour pressure due to differences of hydrostatic pressure produce vapour movements that could also be included in a general statement of laws of water movement, but this

type of flow would achieve dominance only when soils become quite dry and in the presence of large temperature gradients (Miller and Klute, 1967). Therefore, in our analysis, attention will be paid only to the movement of water in the liquid phase.

3.3.1 Concept of Total Potential

Flow takes place under the combined influence of gravitational and capillary forces. The former tends to move the element of water to a lower level while the forces due to differences of hydrostatic pressure (capillary forces) at different points in the soil, tend to move the element of water from a zone of higher to one of lower pressure; in the case of unsaturated soils, from a zone of lower suction (wetter soil) to a zone of larger suction (dryer soil) since the suction is negative.

Therefore, the combined influence of both gravity and capillarity will control the movement of water and, as in the case of saturated flow, the total potential Φ can be defined as the sum of the gravitational potential and the pressure potential.

The gravitational potential of a point in the soil is associated with a height z of this point with respect to an arbitrary datum. The pressure potential of the same point is associated with the hydrostatic pressure p that acts at the point and is also referred to an arbitrary datum, in our case the atmospheric pressure. Thus, this hydrostatic pressure is negative.

Since this hydrostatic pressure can be associated with a manometric height h_c such that:

$$p = \gamma_w h_c \tag{3.4}$$

we can write the equation for the total potential:

$$\Phi = \frac{p}{\gamma_w} + z \tag{3.5}$$

or:

$$\Phi = h_c + z \tag{3.6}$$

We have adopted the symbol h_c for the manometric height that indicates the hydraulic pressure because of the capillarity effects associated with this hydraulic pressure (suction). It is also called by the name pressure head.

Now, on a basis of this definition for the total potential, flow of water takes place from a point of larger potential to a point of lower one, or in other words, exactly opposite to the direction of the gradient of total potential. Figure 3.4 is explanatory of how movement of water takes place on a basis of the above concept of total potential.

Examining points A and B we see that both have the same suction ($h_{cA} = h_{cB}$) and, therefore, the moisture content is of equal dryness at A and B. However, movement of water takes place from B to A since the total potential Φ_B is greater than the total potential Φ_A. The soil at point C is at a dryer state than point B, since $h_{cC} > h_{cB}$ but since both of the total potentials are the same

($\Phi_C = \Phi_B$) movement of water does not occur between these two points. Finally, moisture must move upward from point C to point D since Φ_C is larger than Φ_D, but point D must be at a considerably higher suction than point C to cause the upward movement.

3.3.2 Darcy's Law for Unsaturated Soils

It is well known that flow of water through saturated porous media obeys Darcy's law that can be written generalized for a three-dimensional canal as:

$$\vec{U} = -K_s \nabla \Phi \qquad (3.7)$$

where $\vec{U}$ is the vector flow velocity, Φ is the total potential and K_s is the permeability or saturated hydraulic conductivity.

Questions arise as to whether this same law would apply for unsaturated soils in a modified form, where K, the hydraulic conductivity as a function of moisture content would be substituted for the permeability K_s.

Although Richards (1931) has assumed Darcy's law to be valid for unsaturated soils under the assumption that the hydraulic conductivity as well as moisture content could be treated as (nonhysteretic) functions of the pressure head (suction) and Miller and Klute (1967) have reported the use of the modified equation of Darcy's law to be widely accepted as a practical success, experimental evidence is needed to test its validity.

Experimental work has been carried out by Childs and Collis-George (1950) keeping moisture content and suction uniform down a long column of porous media. In this way the potential gradient was due only to the gravitational component and variations in it were achieved by inclining the column to several angles with respect to the vertical. They found that the rate of flow for a given degree of saturation was proportional to the potential gradient, as in the case of saturated materials.

Thus, Darcy's law for the flow of water in unsaturated porous media can be written in the modified form:

$$\vec{U} = - K(\theta)\nabla\Phi \qquad (3.8)$$

where $K(\theta)$, the hydraulic conductivity of the medium, is a function of moisture content, for a given soil with a particular void ratio. The other symbols are as defined previously in Equation 3.7.

3.3.3 General Equation of Soil Water Transfer

The generalized Darcy's law relates flow velocity to driving forces. Since the soil is not saturated, movement of water would change the moisture of a certain volume element, and the condition of conservation of matter or the requirement of continuity should be applied. If the rate of change of moisture content θ with time t is expressed by $\partial\theta/\partial t$, then the later requirement can be written as:

$$\frac{\partial\theta}{\partial t} = - \nabla \cdot \vec{U} \qquad (3.9)$$

Combining Equation 3.9 with Darcy's law (Equation 3.8) we obtain:

$$\frac{\partial \theta}{\partial t} = \nabla \cdot [K(\theta) \nabla \Phi] \tag{3.10}$$

If now we substitute Equation 3.6 in Equation 3.10, we then have:

$$\frac{\partial \theta}{\partial t} = \nabla \cdot [K(\theta) \nabla h_c] + \frac{\partial K(\theta)}{\partial z} \tag{3.11}$$

This last equation is the general equation that governs the flow of water through unsaturated soils. We have seen in its derivation that use was made only of the definition of total potential, Darcy's law and of the requirement of continuity. In this way, Equation 3.11 is quite general as well as Equation 3.10, and they apply equally well to both homogeneous and heterogeneous soils, and there is no requirement that the functions $K(\theta)$, h_c and θ should not be hysteretic (Philip, 1969).

If we assume now that our problem is one of only wetting or only drying, then hysteretic effects could be avoided and in this case the functions $K(\theta)$ and h_c would be single-valued functions of θ. We can then define another quantity, D, also a single-valued function of θ (Figure 3.5), such that:

$$D = K(\theta) \frac{dh_c}{d\theta} \tag{3.12}$$

Substituting Equation 3.12 in Darcy's law (Equation 3.8), we obtain a new expression for Darcy's law as:

$$\vec{U} = - (D \nabla \theta + K \vec{k}) \tag{3.13}$$

whose components of velocity are:

$$v_x = - D \frac{\partial \theta}{\partial x} \tag{3.14}$$

$$v_y = - D \frac{\partial \theta}{\partial y} \tag{3.15}$$

$$v_z = - D \frac{\partial \theta}{\partial z} - K \tag{3.16}$$

The velocity of flow is proportional to the moisture gradient, the parameter D expressing this proportionality.

Equation 3.14, for example, has been pointed out by Childs and Collis-George (1950) to be of the form of Fick's law of molecular diffusion and by analogy D is referred to as the diffusivity, although this does not imply that water moves through the pore space of a porous media by molecular diffusion.

The general equation of movement can now be written as:

$$\frac{\partial \theta}{\partial t} = \nabla \cdot (D \nabla \theta) + \frac{\partial K(\theta)}{\partial z} \tag{3.17}$$

This is a more tractable form (Philip, 1969). Many problems can be solved by using either Equation 3.11 or Equation 3.17 in the one-dimensional form, written respectively as:

$$\frac{\partial \theta}{\partial t} = \frac{\partial}{\partial z} \left[K(\theta) \frac{\partial h_c}{\partial z} \right] + \frac{\partial K(\theta)}{\partial z} \tag{3.18}$$

and:

$$\frac{\partial \theta}{\partial t} = \frac{\partial}{\partial z} \left(D \frac{\partial \theta}{\partial z} \right) + \frac{\partial K(\theta)}{\partial z} \tag{3.19}$$

Thus problems like evaporation, drainage, vertical infiltration, redistribution of water could be solved by use of the appropriate boundary conditions and of the appropriate functions $K(\theta)$, $h_c(\theta)$ and $D(\theta)$.

3.4 Infiltration

3.4.1 Physics of Infiltration

When available at the surface of an unsaturated soil, water will enter into it due to the combined effects of gravity and capillary forces, both effects acting in a vertical direction to cause percolation downward. This process of entry of water into the soil is referred to as infiltration. Capillary forces may also act to divert water laterally from larger pores to capillary pore spaces, although when water is available in large quantity and over a large area, as well as on a horizontal soil surface, lateral absorption would not be relevant to the general flow, and thus infiltration would take place in a one-dimensional pattern.

3.4.2 Infiltration Rate

The infiltration of water is characterized by a rate that depends on the initial degree of saturation of the soil, on its porosity, on the hydraulic conductivity and on the prevailing suction.

The maximum rate at which a given soil under a given condition can absorb water is referred to as the infiltration capacity.

When water is made available at the soil surface, from rain-

fall, as we shall see, the rate of infiltration will also depend on the rainfall intensity.

Let us consider initially a dry soil that is suddenly flooded at its surface. Darcy's law for the vertical infiltration can be written as:

$$v_z = - D \frac{\partial \theta}{\partial z} - K \tag{3.20}$$

and immediately after flooding D and K are suddenly given their maximum values D_{sat} and K_{sat} corresponding to saturation, thus:

$$v_z = - D_{sat} \frac{\partial \theta}{\partial z} - K_{sat} \tag{3.21}$$

However, just below the saturated surface, the moisture content is not affected instantaneously. Thus, the moisture gradient is initially positive and infinitely steep and the rate of infiltration v_z is initially very great.

Since below the saturated surface the conductivity and diffusivity have their initial min mum values corresponding to the initial moisture content and the moisture gradient is very small if not zero, the velocity of flow should be accordingly very small, and therefore the large infiltration rate at the surface would be responsible for an increase of moisture content of this subsurface soil. Thus the process is characterized by an advance of a saturating front or, as it will be referred to, a wetting front.

As the wetting front advances to greater depths, D and K remain at their saturated values but the moisture gradient decreases and consequently there is a reduction of the infiltration rate with time. With penetration of the wetting front, the moisture gradient is still reducing and becomes vanishingly small. As a consequence the rate of infiltration tends asymptotically to its value K_{sat}. Figure 3.6 illustrates the variation of the rate of infiltration with time.

Let us consider now the case of a homogeneous soil with an uniform initial moisture content θ_i and let the soil surface be under a rainfall of constant intensity i. Say this soil has also a saturated hydraulic conductivity K_{sat}. The rainfall intensity as compared to the saturated hydraulic conductivity will determine not only the infiltration rate but also the final moisture content of the soil. Thus, a rainfall intensity I lower than the saturated hydraulic conductivity will determine a final moisture content θ_u such that satisfies the equation (Braester, 1973; Childs, 1969):

$$I = K(\theta) \qquad (3.22)$$

In other words, the final moisture content would be that value corresponding to which the hydraulic conductivity equals the rainfall intensity.

Conversely, if I is larger than or equal to K_{sat} then saturation of the soil surface would be achieved and $\theta_u = \theta_{sat}$.

It should be noted, however, that the final moisture content

θ_u will not be achieved instantaneously or immediately after rainfall starts. As pointed out by Braester (1973), three typical stages can be distinguished during the infiltration process, according to Figure 3.7. First, when infiltration is dominated by capillary forces, the moisture content at the surface increases gradually. This is represented by curve a in Figure 3.7. In the second stage the moisture content at the soil surface reaches its final value θ_u (curve b) and finally the moisture content profile reaches a fixed shape and moves downward.

With respect to the infiltration rate, three distinct cases exist according to Mein and Larson (1973), as illustrated in Figure 3.8. Here, depending on the rainfall intensity relative to the infiltration rate, water may be entirely absorbed by the soil or may accumulate and flow from the area as surface runoff.

When I is less than K_{sat}, all the rainfall infiltrates with a constant infiltration rate represented by curve A in Figure 3.8, and thus runoff does not occur. The moisture content is increased from its initial value θ_{in} to its final value determined by Equation 3.22.

If the rainfall intensity I is larger than the saturated hydraulic conductivity K_{sat} but less than the infiltration capacity, saturation of the soil surface will occur for a period of time referred to as the time of saturation of the soil surface. During this time, all the rainfall infiltrates into the soil and the capacity of the soil to absorb water decreases until it becomes less than the rainfall in-

tensity. At this point, water begins to accumulate on the soil surface and runoff can begin. In Figure 3.8, this event is represented by line B, followed by curve C.

Finally, when the rainfall intensity is larger than the saturated hydraulic conductivity and than the infiltration capacity, this stage could be represented by the previous one for a very large rainfall intensity in such a way that the time of surface saturation would be negligibly small. Then, the infiltration rate is at capacity and decreasing while runoff is being generated. This case is represented by curve D in Figure 3.8.

3.4.3 Moisture Profile After Infiltration

As noted previously, infiltration of water through an unsaturated soil takes place characterized by the advance of the moisture profile. One may, however, distinguish several zones in the advancing moisture profile.

Bodman and Coleman (1944) measured the water content distribution in a vertical soil column during infiltration from a ponded surface and delineated four zones in the moisture profile as indicated in Figure 3.9.

1. Zone of saturation, of a small depth at the soil surface.
2. Zone of transition, where the moisture content would present a reduction.
3. Transmission zone, an ever-lengthening unsaturated zone of fairly uniform moisture content.

4. Wetting zone, where the moisture content increases as infiltration proceeds.

The presence of the transition zone has been explained to be due to alterations of soil structure or of packing near the surface (Miller and Klute, 1967). Philip (1957a), however, suggests that in this region the relation between water content and pressure is dependent on the depth because of air bubbles entrapped below the saturation zone. This fact would lead us to conclude that for coarse soils this transition zone would not be very pronounced and, in fact, for random granular materials, curves by Youngs (1957) do not show the transition zones and the moisture profile seems to be really sharper for coarser materials, as illustrated in Figure 3.10.

3.5 Redistribution of Moisture Content

We have seen in the previous section that rainfall will give rise to infiltration of water into the soil characterized by the advance of a wetting front with time. During the rainfall the advance of wetting front proceeds always at greater depths.

A rainfall, however, is not characterized only by an intensity but also by a certain duration so that after rainfall ceases, changes will occur in the moisture profile as determined by the infiltration.

Let us suppose that at the instant that rainfall ceased, the wetting front had achieved a certain depth and that the corresponding moisture profile is represented by curve 1 of Figure 3.11. One may

distinguish with respect to this curve, two zones in the moisture profile: an upper one, conventionally saturated and a lower zone, below the wetting front where the moisture content is still the initial one, or say, the moisture content previous to infiltration.

At the time rainfall ceases, according to Childs (1969) there is not an instantaneous change of the moisture profile and the potential gradient must, for a brief time, be altered so that the water movement and the penetration of the moisture profile must continue.

In order that this movement of moisture continues to deeper soil, since there is no longer infiltration, there will be a withdrawal of water from the saturated upper zone which must, from this time on, decrease in moisture content while the moisture content of the lower zone still increases. Therefore, cessation of rainfall is characterized by a redistribution of the moisture content in the soil as is observed in Figure 3.11, where the other curves 2, 3, etc., represent subsequent stages of redistribution.

It is thus possible to note that during redistribution, the moisture content decreases in the upper zone, increasing in the lower one. For a large time after redistribution started, the moisture profile will be approximately uniform. This uniform moisture content, however, is less than that corresponding to saturation but larger than the initial one prior to infiltration. The curves illustrated in Figure 3.9 have been obtained experimentally by Childs who used columns of sand.

Other features of the redistribution process can be observed by analyzing the experimental curves obtained by Young (1958) and illustrated in Figures 3.12. From this we see that the greater the initial depth of infiltration, the greater the moisture content after redistribution for the same material.

Analysis of problems of redistribution of moisture can be made through Equation 3.18 written in one-dimensional form, but it is worth noting that in this type of problem, the functions $h_c(\theta)$ and $K(\theta)$ are hysteretic.

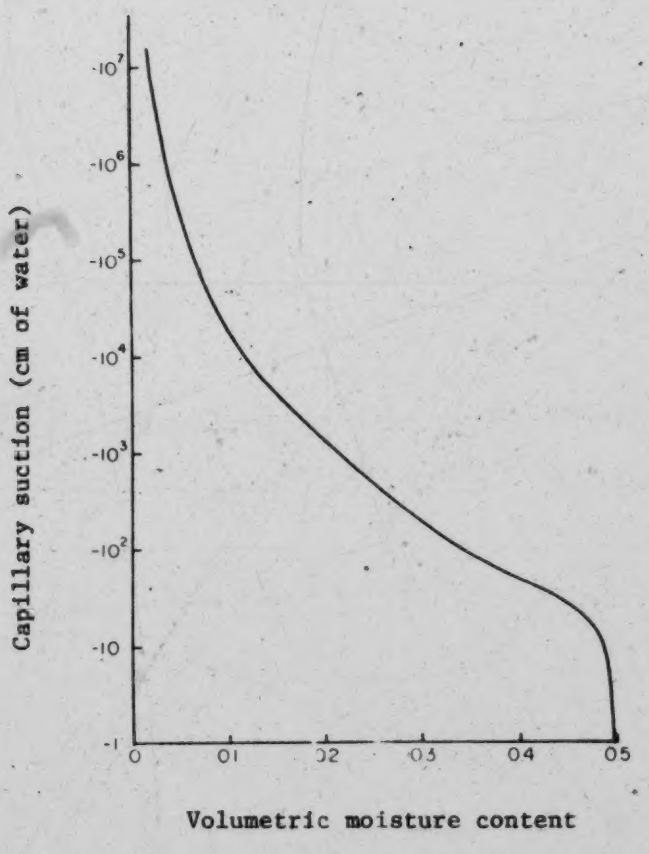

FIGURE 3.1 MOISTURE CHARACTERISTIC CURVE
(After Philip, 1969)

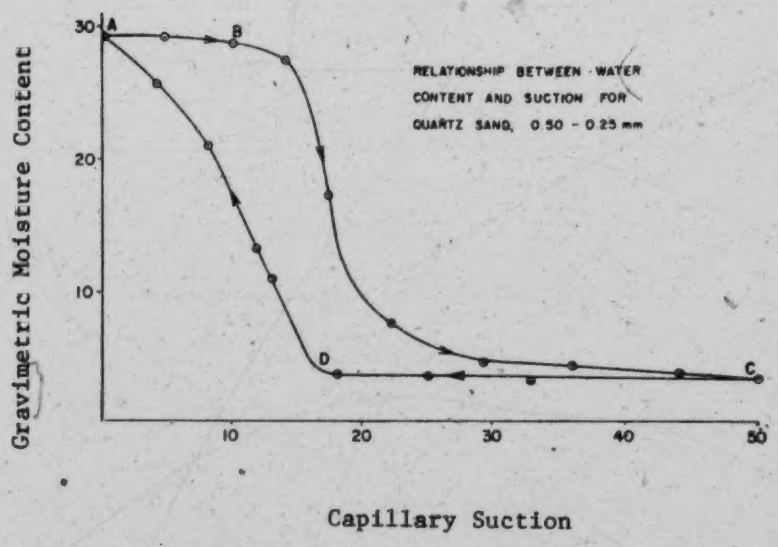

FIGURE 3.2 HYSTERESIS IN MOISTURE CHARACTERISTIC CURVE

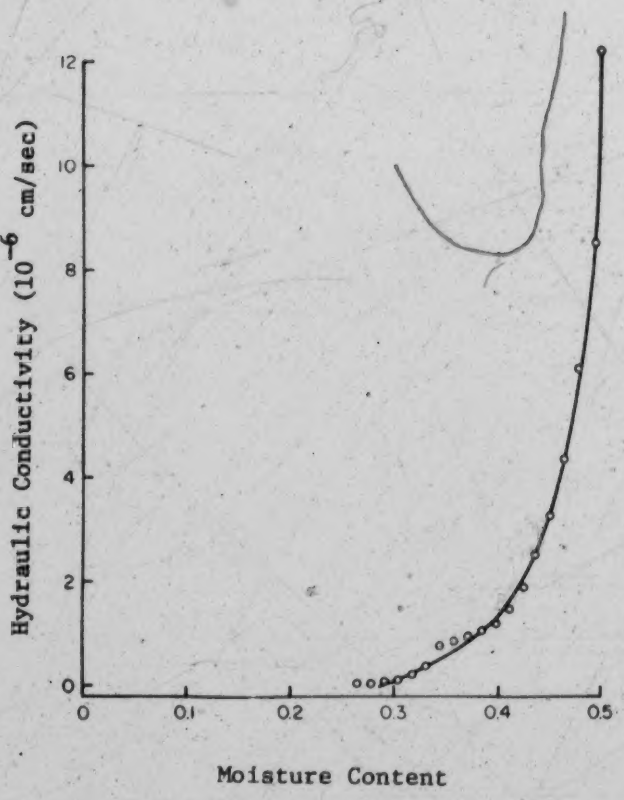

FIGURE 3.3 HYDRAULIC CONDUCTIVITY VERSUS MOISTURE CONTENT
(After Philip, 1969)

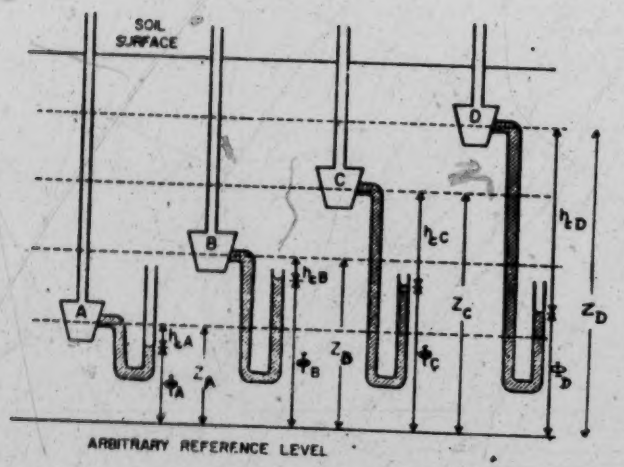

FIGURE 3.4 CONCEPT OF TOTAL POTENTIAL
(After Kirkham and Powers, 1972)

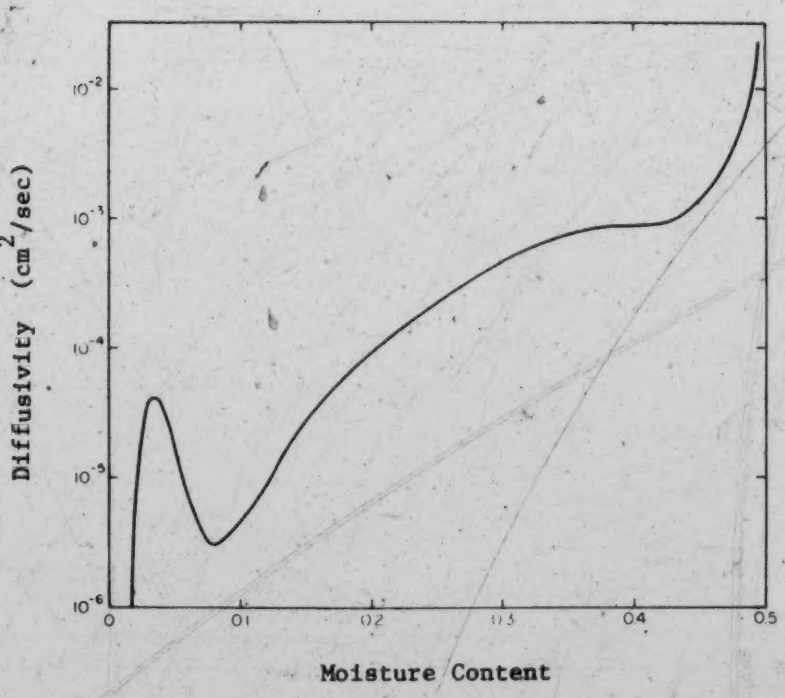

FIGURE 3.5 DIFFUSIVITY VERSUS MOISTURE CONTENT
(After Philip, 1969)

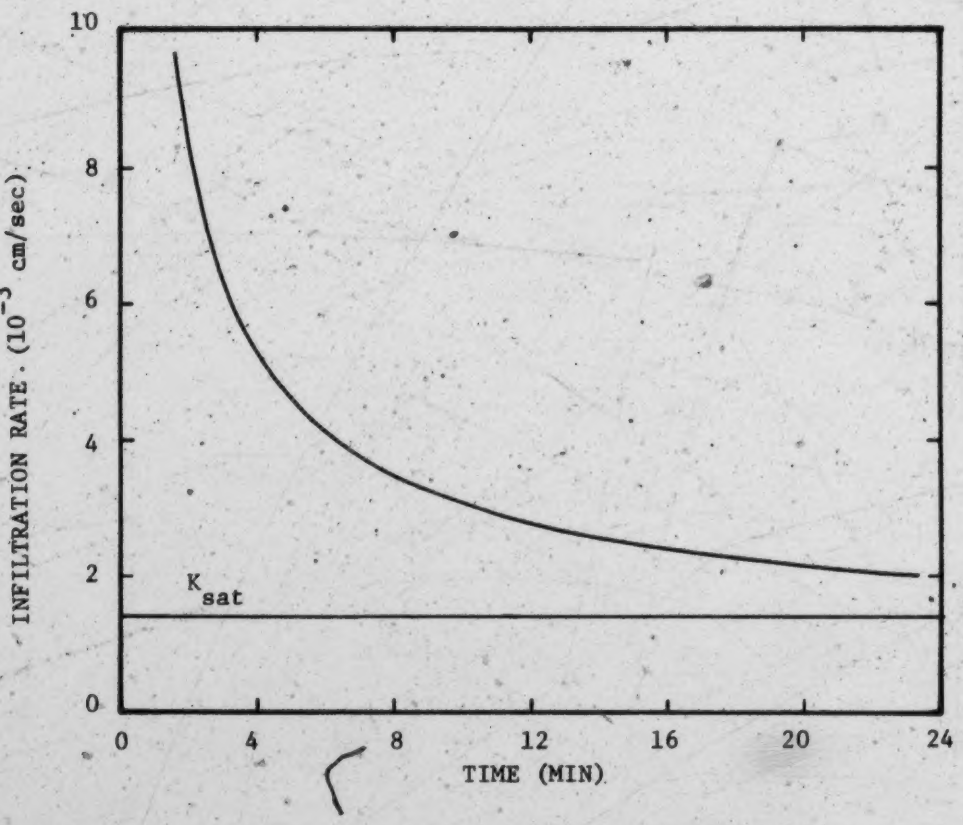

FIGURE 3.6 INFILTRATION RATE VERSUS TIME

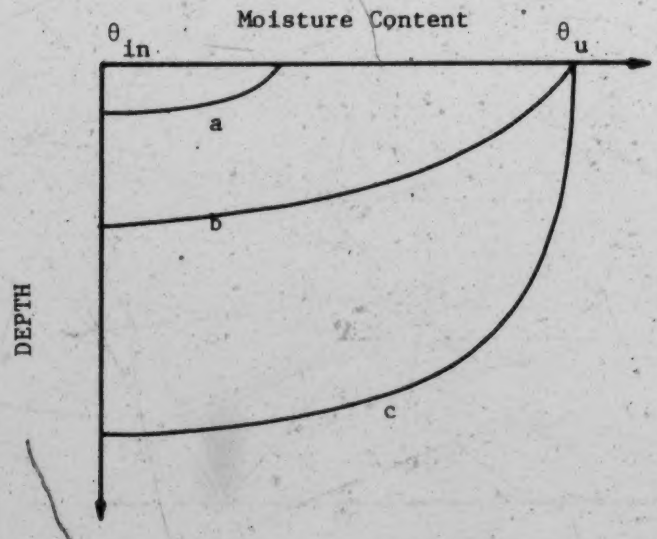

FIGURE 3.7 STAGES OF MOISTURE PROFILE DEVELOPMENT
(After Braester, 1973)

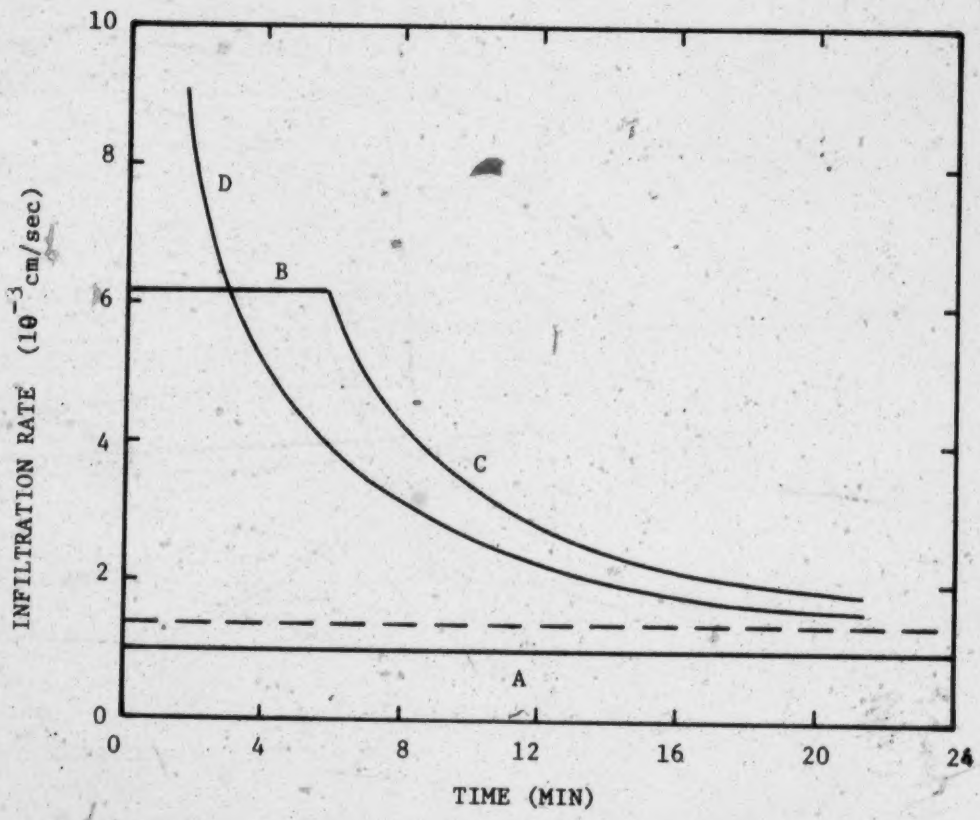

FIGURE 3.8 DIFFERENT CASES OF INFILTRATION BEHAVIOUR UNDER RAINFALL

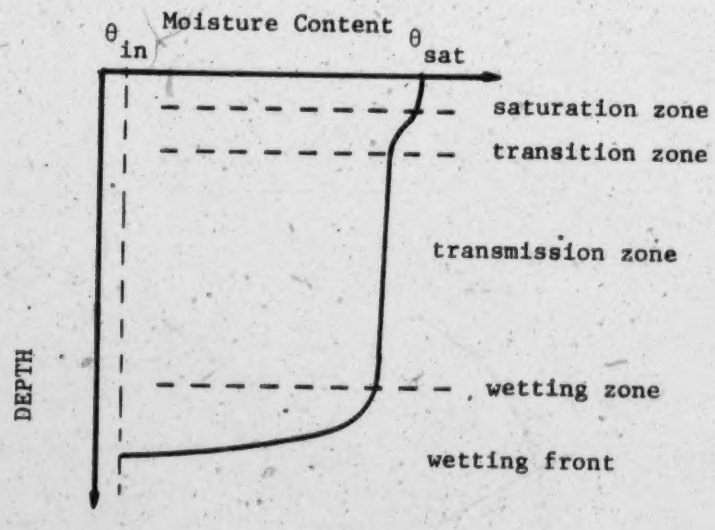

FIGURE 3.9 ZONES OF THE INFILTRATION PROFILE
(After Bodman and Coleman, 1944)

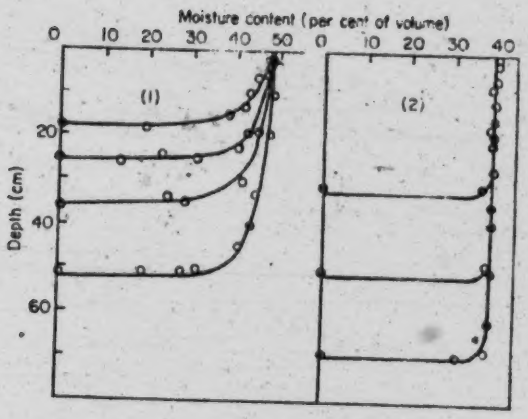

FIGURE 3.10 STAGES IN THE DEVELOPMENT OF THE DESCENDING MOISTURE PROFILE
(After Youngs, 1957)

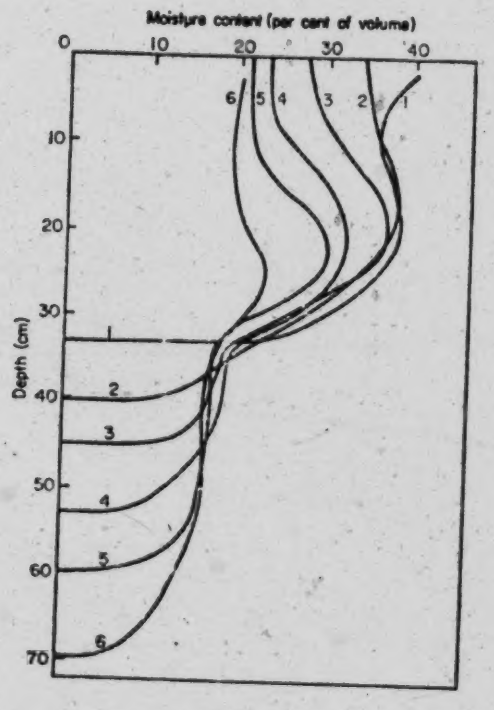

FIGURE 3.11 REDISTRIBUTION OF MOISTURE CONTENT
(After Childs, 1969)

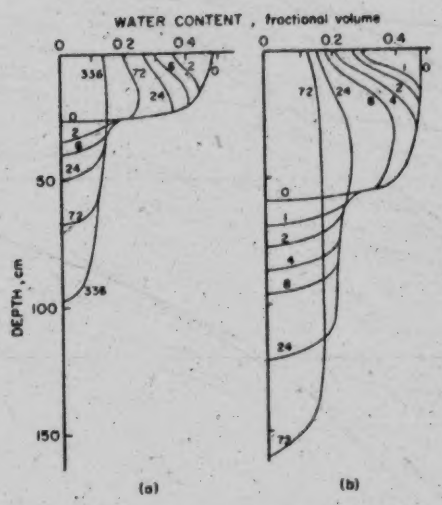

Fig. 131–17. Experimental water content profiles during the redistribution of water after infiltration in slate dust. The numbers near the curves are the time in hours after cessation of infiltration. Depth of initial wetting, (*a*) 27 cm, (*b*) 59 cm.

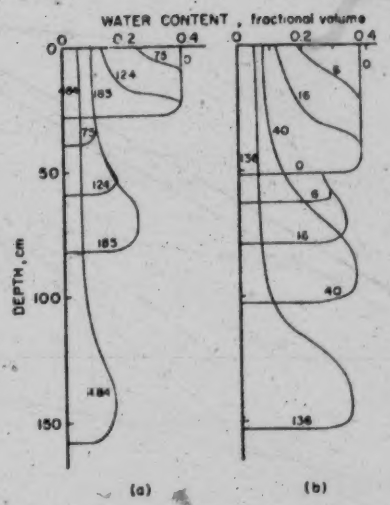

Fig. 131–18. Experimental water content profiles during the redistribution of water after infiltration in "Ballotini" grade 15. Depth of initial wetting, (*a*) 27.5 cm, (*b*) 51.5 cm. The numbers near the curves are the time in hours after cessation of infiltration.

FIGURE 3.12 WATER REDISTRIBUTION AFTER INFILTRATION
(After Youngs, 1958)

CHAPTER IV

SOLUTIONS TO THE INFILTRATION EQUATION

4.1 Introduction

In the previous chapter we saw how movement of water takes place through the unsaturated soils in a general way and also particularly in the case of one-dimensional vertical infiltration. The general equation of the movement of water was derived and it was pointed out that any kind of flow problem could be solved, in the first instance, numerically, by use of Equations 3.11 or 3.17 in the general form or by use of Equations 3.18 or 3.19 in the particular case of one-dimensional flow, by defining the appropriate boundary and initial conditions relevant to the type of problem concerned.

Here we will be concerned with the solutions of the one-dimensional vertical infiltration problem which can be expressed by Equation 3.19, written here for convenience as:

$$\frac{\partial \theta}{\partial t} = \frac{\partial}{\partial z}\left(D \frac{\partial \theta}{\partial z}\right) - \frac{\partial K}{\partial z} \qquad (4.1)$$

where z is the vertical distance, taken positive downward. An analytical solution obtained directly from Equation 4.1 and expressed as the variation of moisture content as a function of the distance z and time t :

$$\theta = \theta(z, t) \qquad (4.2)$$

or a variation from it, such as:

$$z = z(\theta, t) \tag{4.3}$$

would be highly desirable for the type of problem we are concerned with since it would facilitate computation of moisture profile as a function of time and so, prediction of the advance of the wetting front with time.

Such solutions have not been obtained yet for the general condition where the parameters D, K and h_c are functions of θ. Analytical solutions exist for particular cases such as the solution for the absorption problem with constant diffusivity. The problem of absorption is expressed by a particular form of Equation 4.1, where the term $\partial K/\partial z$ does not appear. Thus, this equation written as:

$$\frac{\partial \theta}{\partial t} = \frac{\partial}{\partial z}\left(D \frac{\partial \theta}{\partial z}\right) \tag{4.4}$$

would be applied only to horizontal flows or to vertical flows through fine-textured soils in which the influence of the moisture gradient is much more important than that of gravity, this latter being then neglected.

In the case of constant diffusivity, Equation 4.4 above is the same as that for heat flow diffusion and has been solved analytically by Carslaw and Jaeger (1959).

Philip (1955, 1957a, 1957b, 1969) has obtained what he calls "quasi-analytical" solutions for Equation 4.1. According to him, these

are solutions where the basic form of the solution is established by the methods of mathematical analysis although the coefficients that appear in that solution are determined by numerical methods. Because of the advantage of these solutions over the numerical solutions, in the way that they provide a better understanding of the phenomenon of infiltration and also in providing an easier manner to treat the solutions, we shall deal with them.

It must be pointed out that since we will pay attention only to the vertical infiltration problem and thus, wetting of the soil, hysteresis effects in h_c, D and K will not be considered here.

As we shall see, Philip's solution to the vertical infiltration problem makes use of the solution of the simple form of the absorption problem.

Finally, a solution that takes into account the rainfall intensity and presented by Mein and Larson (1973) will also be discussed here.

In all these solutions, it will be assumed that the initial moisture content of the soil profile prior to infiltration has a constant value and influence of different initial values on the solutions will be analysed.

4.2 Boundary and Initial Conditions

We will be concerned exclusively with infiltration into a

semi-infinite soil mass at uniform initial moisture content θ_{in}. The semi-infinite medium can be either a horizontal (in the case of the absorption problem) or a vertical soil column of semi-infinite length, with one boundary of the flow medium being $z = 0$.

Therefore, the first condition of initial moisture content can be expressed as:

$$\theta = \theta_{in} \quad , \quad t = 0 \quad , \quad z > 0 \qquad (4.5)$$

We need to know the boundary condition at $z = 0$. This can be either a moisture content at the soil surface or a hydrostatic pressure or a constant flux imposed by a rainfall.

Let us follow initially Philip's development that assumes the soil surface to be suddenly flooded, consequently at a moisture content corresponding to saturation.

As noted before, water from rainfall does not saturate the soil surface instantaneously but there is a certain period of time, referred to as the time of saturation of the soil surface, for which saturation of the soil surface is achieved. For a very intense rainfall, the time of saturation of the soil surface would be small and Philip's solution would apply, although it makes no reference to the rainfall intensity.

Mein and Larson's solution accounts for this time of saturation, dependent not only on the rainfall intensity but also on the

initial moisture content and on the unsaturated properties of the soil such as the suction and the hydraulic conductivity.

For a soil surface suddenly flooded, the initial condition can be expressed as:

$$\theta = \theta_{sat} \quad , \quad z = 0 \quad , \quad t \geq 0 \tag{4.6}$$

Just to illustrate how a change of boundary conditions would describe different problems, if in conditions 4.5, θ_{in} is replaced by θ_{sat} and in conditions 4.6, θ_{sat} is replaced by a moisture content $\theta < \theta_{sat}$, then Equation 4.4 and the modified boundary conditions describe the removal of water by the application of a constant suction at the soil surface.

4.3 Philip's Solution

As mentioned before, Philip's solution for the vertical infiltration equation makes use of the solution for the absorption problem or horizontal infiltration.

4.3.1 Horizontal Infiltration

This is the simplest special case of Equation 3.17 that can be written, since gravity is not considered:

$$\frac{\partial \theta}{\partial t} = \frac{\partial}{\partial x} \left(D \frac{\partial \theta}{\partial x} \right) \tag{4.7}$$

where x is the horizontal distance. It will be solved subject to the

following conditions:

$$\theta = \theta_{in} \quad , \quad t = 0 \quad , \quad x > 0$$
$$\theta = \theta_{sat} \quad , \quad x = 0 \quad , \quad t \geq 0 \tag{4.8}$$

as described by Philip (1957a) and in detail by Philip (1955).

Basically his method consists of using the Boltzmann transformation:

$$\psi = xt^{-1/2} \tag{4.9}$$

thus reducing Equation 4.7 to the ordinary differential equation:

$$-\frac{\psi}{2}\frac{d\theta}{d\psi} = \frac{d}{d\psi}\left(D\frac{d\theta}{d\psi}\right) \tag{4.10}$$

If both sides of Equation 4.10 are multiplied by $d\psi/d\theta$, we obtain the following equation in which θ is the independent variable:

$$-\frac{\psi}{2} = \frac{d}{d\theta}\left(D\frac{d\theta}{d\psi}\right) \tag{4.11}$$

Integration leads to:

$$\int_{\theta_{in}}^{\theta} \psi d\theta = -2D\frac{d\theta}{d\psi} \tag{4.12}$$

subject to conditions:

$$\theta = \theta_{sat} \quad , \quad \psi = 0 \tag{4.13}$$

Philip (1955) then solves Equation 4.12 subject to conditions 4.13 by means of forward integration with one initial condition determined by

trial and improved by iterations, giving:

$$\psi = \psi(\theta) \tag{4.14}$$

which enables us to calculate the horizontal moisture profile from:

$$x = \psi(\theta) t^{1/2} \tag{4.15}$$

where the distance x is expressed as a function of moisture content θ for each time t specified.

4.3.2 Vertical Infiltration

The vertical infiltration equation is our Equation 4.1, written as:

$$\frac{\partial \theta}{\partial t} = \frac{\partial}{\partial z}\left(D \frac{\partial \theta}{\partial z}\right) - \frac{\partial K}{\partial z} \tag{4.16}$$

where z is the vertical ordinate, positive downward. The governing conditions are:

$$\begin{aligned} &\theta = \theta_{in} \quad , \quad t = 0 \quad , \quad z > 0 \\ &\theta = \theta_{sat} \quad , \quad z = 0 \quad , \quad t \geq 0 \end{aligned} \tag{4.17}$$

Philip (1957b) developed a numerical approach to solve Equation 4.16 subject to conditions 4.17. First, he introduces the equation:

$$\frac{\partial \theta}{\partial t} = \frac{\partial}{\partial x'}\left(D \frac{\partial \theta}{\partial x'}\right) \tag{4.18}$$

subject to conditions:

$$\theta = \theta_{in} \quad , \quad t = 0 \quad , \quad x' > 0$$
$$\theta = \theta_{sat} \quad , \quad x' = 0 \quad , \quad t \geq 0 \tag{4.19}$$

The solution $x' = x'(\theta, t)$ is of the form:

$$x' = \psi(\theta) t^{1/2} \tag{4.20}$$

and is readily evaluated by the previous method and described by Philip (1955), giving a first estimate of z. Philip first transforms Equations 4.16 and 4.18 to the forms that make θ the independent variable, giving respectively:

$$-\frac{\partial z}{\partial t} = \frac{\partial}{\partial \theta}\left(D \frac{\partial \theta}{\partial z}\right) - \frac{\partial K}{\partial \theta} \tag{4.21}$$

$$-\frac{\partial x'}{\partial t} = \frac{\partial}{\partial \theta}\left(D \frac{\partial \theta}{\partial x'}\right) \tag{4.22}$$

With x' from 4.20, he expresses the exact solution z of Equation 4.16 as:

$$z = x' + y \tag{4.23}$$

where y is the error in x' made by considering x', of horizontal flow, the solution z for vertical flow.

To evaluate mathematically the error y, he subtracts 4.21 from 4.22 obtaining:

$$\frac{\partial y}{\partial t} = \frac{\partial}{\partial \theta}\left(D \frac{\partial \theta}{\partial x'} \frac{\partial y}{\partial z}\right) + \frac{\partial K}{\partial \theta} \tag{4.24}$$

where y, from Equation 4.23 is:

$$y = z - x' \tag{4.25}$$

Unable to solve easily Equation 4.24 for y, Philip finds an approximate solution y' to an equation that he derives from Equation 4.24 by assuming that:

$$\frac{\partial y}{\partial z} = \frac{\partial y}{\partial x'} \tag{4.26}$$

Applying this to Equation 4.24 leads to the following equation:

$$\frac{\partial y'}{\partial t} = \frac{\partial}{\partial \theta}\left[D\left(\frac{\partial \theta}{\partial x'}\right)^2 \frac{\partial y'}{\partial \theta} + \frac{\partial K}{\partial \theta}\right] \tag{4.27}$$

where y' is written for y, since the use of approximation 4.26 implies that Equation 4.27 cannot give y exactly.

By making use of the transformation:

$$\chi = y' t^{-1} \tag{4.28}$$

Equation 4.27 is reduced to the ordinary equation:

$$\chi = \frac{d}{d\theta}\left(P \frac{d\theta}{d\psi}\right) + \frac{dK}{d\theta} \tag{4.29}$$

in which:

$$P(\theta) = D\left(\frac{d\theta}{d\psi}\right)^2 . \tag{4.30}$$

and:

$$\psi(\theta) = x' t^{-1/2} \tag{4.31}$$

Integration of Equation 4.29 gives:

$$\int_{\theta_{in}}^{\theta} \chi d\theta = P \frac{d\chi}{d\theta} + (K - K_{in}) \qquad (4.32)$$

subject to condition:

$$\theta = \theta_{sat} \quad , \quad \chi = 0 \qquad (4.33)$$

where K_{in} is written for the value of k at $\theta = \theta_{in}$.

Equation 4.32 subject to 4.33 is simply solved numerically. The new residual error:

$$s = y - y' \qquad (4.34)$$

is then introduced. The solution z to Equation 4.16 now becomes, on placing 4.34 in 4.23:

$$z = x' + y' + s \qquad (4.35)$$

The error s in using y' in place of y may be formulated from Equation 4.34 and Philip derives a differential equation in s given by:

$$\frac{\partial s}{\partial t} = \frac{\partial}{\partial \theta}\left[D \frac{\partial \theta}{\partial x'} \left(\frac{\partial s}{\partial z} - \frac{\partial y'}{\partial x'} \frac{\partial y}{\partial z}\right)\right] \qquad (4.36)$$

Again Philip does not solve Equation 4.36. Instead he solves a similar equation where s' approximates and replaces s in such a way that:

$$s = s' + w \qquad (4.37)$$

where w is the error made in using s' as a solution to 4.36. Thus, placing Equation 4.37 in Equation 4.35, we see that our solution z to Equation 4.16 becomes:

$$z = x' + y' + s' + w \tag{4.38}$$

The procedure above may be repeated with new residuals as often as required to give the necessary accuracy. The solution is then found as a power series in $t^{1/2}$:

$$z = \psi t^{1/2} + \chi t + \phi t^{3/2} + \omega t^{2} + \ldots + f_m(\theta) t^{m/2} + \ldots \tag{4.39}$$

in which the coefficients $\psi, \chi, \phi, \omega, \ldots, f_m(\theta)$ are functions of θ which are the solutions of a series of ordinary equations that can be solved by numerical methods.

In general, $f_m(\theta)$ is solved by:

$$\frac{m}{2} \int_{\theta_{in}}^{\theta} f_m d\theta = P \frac{df_m}{d\theta} - R_m \tag{4.40}$$

subject to condition;

$$\theta = \theta_{sat} \quad , \quad f_m = 0 \tag{4.41}$$

In Equation 4.40, R_m is a function of θ which may be determined from K_{in}, K_{sat}, D, ψ, χ, ϕ, ω, ..., $f_m - 1$.

4.3.3 Cumulative Infiltration

Water that infiltrates into the soil will cause an increase

of moisture content of the soil profile.

The cumulative infiltration q_o is defined as the time integral of the flow velocity at the soil surface, and is equal to the change of moisture content in the profile plus any water that passes out of the bottom of the profile, i.e., q_∞.

We have seen that Darcy's Law for the vertical movement of water can be expressed as:

$$v = D\frac{\partial\theta}{\partial z} + K \tag{4.42}$$

At infinity, since the moisture content is uniform at its value θ_{in}, the moisture gradient is zero and K assumes the corresponding value K_{in}. Thus:

$$v_\infty = K_{in} \tag{4.43}$$

and:

$$q_\infty = K_{in}t \tag{4.44}$$

If we write the moisture change after a time t as the integral:

$$\text{moisture change} = \int_{z=o}^{\infty} (\theta - \theta_{in})dz \tag{4.45}$$

that is the area of the moisture profile over the depth z, we can express the relation:

$$q_o - K_{in}t = \int_{z=}^{\infty} (\theta - \theta_{in})dz \tag{4.46}$$

but the moisture change can also be expressed as:

$$\text{moisture change} = \int_{z=o}^{\infty} (\theta - \theta_{in})dz = \int_{\theta_{in}}^{\theta_{sat}} z d\theta \qquad (4.47)$$

Therefore, we can write for q_o:

$$q_o = \int_{\theta_{in}}^{\theta_{sat}} z d\theta + K_{in} t \qquad (4.48)$$

By substituting Equation 4.39 in Equation 4.48 we get:

$$q_o = A_1 t^{1/2} + (A_2 + K_{in})t + A_3 t^{3/2} + A_4 t^2 + \ldots \qquad (4.49)$$

where A_1 is called sorptivity by Philip and:

$$A_m = \int_{\theta_{in}}^{\theta_{sat}} f_m d\theta \qquad (4.50)$$

4.3.4 Infiltration Rate

The infiltration rate is the flow velocity at the soil surface, i.e., at $z = 0$. It can be obtained by differentiating Equation 4.49 with respect to the time t. Thus:

$$f(t) = \frac{\partial q_o}{\partial t} \qquad (4.51)$$

Substitution of Equation 4.49 in Equation 4.51 yields:

$$f(t) = \frac{1}{2} A_1 t^{-1/2} + (A_2 + K_{in}) + \frac{3}{2} A_3 t^{1/2} + 2A_4 t + \ldots \quad (4.52)$$

4.3.5 Results of Philip's Solution

Philip's solution needs the parameters $K(\theta)$ and $D(\theta)$ defined a priori for each moisture content. The hydraulic conductivity $K(\theta)$ is determined from laboratory tests and the diffusivity can be either determined directly in the laboratory or from the Equation 3.12 that defines it, provided that the suction is also determined through laboratory tests. Here we present the results of Philip's solution as applied to Columbia Sand Loam, the properties of which are shown in Table 4.1 and Figures 4.1, 4.2 and 4.3.

His results have led to the conclusion that the depth of the wetting front could be expressed as:

$$z = at^{1/2} + bt \quad (4.53)$$

In fact, this equation applies very well, at least for small times. As the time increases, other terms must be added, since due to the power of time, the subsequent coefficients of the equation start influencing the values of the depth z. However, as the time t becomes large, depending on the soil, Philip's solution fails as we can see from the curve of the infiltration rate with time shown in Figure 4.6. As time increases, the infiltration rate decreases to its smallest value equal to the saturated hydraulic conductivity and for large times Philip's

solution for the infiltration rate departs from this general behaviour.

In fact, Philip (1969) shows that a suitable criterion for practical convergence of his series, as determined by him empirically, would be:

$$t \leq \left(\frac{S}{K_{sat} - K_{in}}\right)^2 \tag{4.54}$$

where S, called sorptivity, is equal to:

$$S = A_1 = \int_{\theta_{in}}^{\theta_{sat}} \psi d\theta \tag{4.55}$$

Thus, for values of t smaller than those given by Equation 4.54, convergence should occur.

Equation 4.52 for the infiltration rate could be written, accordingly, with two terms only and since its value should converge to the saturated hydraulic conductivity, Miller and Klute (1967) have proposed the expression below:

$$f = \frac{1}{2} A_1 t^{-1/2} + K_{sat} \tag{4.56}$$

The corresponding curve is also illustrated in Figure 4.6.

Philip (1969) develops another procedure for large times but from Equation 4.54 these values appear to be beyond our concern. In Appendix A we present the program to compute the moisture profile as well as the infiltration rate with time following Philip's solution.

Figure 4.4 illustrates how the moisture profile advances with time. We see that Philip's analysis predicts all the zones of Bodman and Coleman (1944) except the transition zone since the diffusivity is not a unique function of moisture content in this zone because of fewer entrapped air bubbles near the surface, as explained by Philip (1957a).

To show the advance of the wetting front with time as illustrated in Figure 4.5, we have taken the moisture content at the wetting front θ_{wf} as the average between the initial and the final moisture content, as expressed by Equation 4.57 below:

$$\theta_{wf} = \frac{1}{2} (\theta_{in} + \theta_{fin}) \tag{4.57}$$

The results show that for small times, Philip's theory gives very high values for the infiltration rate (Figure 4.6) decreasing, however, very rapidly with time to the saturated value of the hydraulic conductivity. This leads to a very large rate of advancing of the wetting front in the beginning of the process but as the time increases, this rate also decreases tending to a constant value, as shown by Philip (1969) to be given by:

$$u = \frac{K_{sat} - K_{in}}{\theta_{sat} - \theta_{in}} \tag{4.58}$$

4.4 Mein and Larson's Solution

4.4.1 General Considerations

We have seen in Chapter III that water from rainfall does not

saturate the soil surface instantaneously as assumed in Philip's solution. As the moisture content at the soil surface increases, there is also a corresponding infiltration to a shallow depth at the same time, as described in Chapter III, and saturation of the soil occurs for a certain period of time and at a certain depth. The time of saturation as well as the corresponding depth depend on the initial moisture content of the soil profile, on the rainfall intensity and on the porosity and hydraulic characteristics of the medium, related to the hydraulic conductivity and suction of the soil.

To account for these effects, Mein and Larson (1973) have proposed a different solution, without departing from the infiltration equation. Although they discuss the existence of three distinct cases of infiltration, depending on the relative magnitudes of rainfall intensity, saturated hydraulic conductivity K_{sat} and the infiltration capacity, the case of interest here is the most frequent case of rainfall intensity larger than K_{sat}. In this case, during saturation of the soil surface, all the rainfall water infiltrates and the moisture content at the surface increases until surface saturation is reached. After this time, the infiltration rate decreases and surface runoff is generated.

4.4.2 Solution to the Vertical Infiltration Problem

Assuming the moisture profile at the moment of surface saturation to be approximately as shown in Figure 4.7, the area above the new moisture profile is the amount of infiltration F_s up to surface saturation.

Let us consider the shaded area in Figure 4.7 to be equal to the above mentioned area where the depth Z_s is chosen to be the depth of this saturated zone. Defining the moisture deficit M_d as:

$$M_d = \theta_{sat} - \theta_{in} \tag{4.59}$$

we can express the amount of water infiltrated as:

$$F_s = M_d Z_s \tag{4.60}$$

Let us write Darcy's law for this condition as:

$$v = - K(\theta) \frac{\partial \phi}{\partial z} \tag{4.61}$$

where v is the flow rate

$K(\theta)$ is the hydraulic conductivity

ϕ is the total potential

z is the depth below the soil surface

Adopting the subscripts 1 and 2 referring to the surface and the wetting front respectively, and assuming the hydraulic conductivity to be equal to the saturated value K_{sat}, we can write from Equation 4.61:

$$v = - K_{sat} \frac{\phi_2 - \phi_1}{z_2 \quad z_1} \tag{4.62}$$

Taking the potential at the surface ϕ_1 as 0:

$$\phi_2 = - (Z_s + h_{av}) \tag{4.63}$$

where h_{av} is the average capillary suction at the wetting front.

At the moment of surface saturation, the infiltration rate is still equal to the rainfall intensity I, so that:

$$I = K_{sat} \frac{h_{av} + Z_s}{Z_s} \tag{4.64}$$

which, combined with Equation 4.60 gives:

$$F_s = \frac{h_{av} M_d}{\frac{I}{K_{sat}} - 1} \tag{4.65}$$

This predicts the amount of infiltration prior to runoff and the time to the beginning of runoff is:

$$t_s = \frac{F_s}{I} \tag{4.66}$$

After saturation of the surface, runoff begins and the infiltration rate starts decreasing. Assuming that some time after the surface has become saturated, the moisture profile can be represented by Figure 4.8 and applying Darcy's law again, we have:

$$f = K_{sat} \frac{h_{av} + z}{z} \tag{4.67}$$

where f is the infiltration rate

z is the depth of the wetting front

In Figure 4.8, F is the cumulative infiltration at any time and is related to the depth z of the wetting front through:

$$F = M_d z \tag{4.68}$$

Thus:

$$z = \frac{F}{M_d} \tag{4.69}$$

and substituting Equation 4.67 in Equation 4.69, we get:

$$f = K_{sat}\left[1 + \frac{h_{av} M_d}{F}\right] \tag{4.70}$$

Since the infiltration rate is the flow velocity at the soil surface, it can be obtained by differentiating the cumulative infiltration with respect to time. Thus:

$$f = \frac{dF}{dt} \tag{4.71}$$

and substituting Equation 4.71 in Equation 4.70, we obtain:

$$\frac{dF}{dt} = k_{sat} + \frac{A}{F} \tag{4.72}$$

where:
$$A = K_{sat}\, h_{av}\, M_d = \text{constant} \tag{4.73}$$

Integration of Equation 4.72 with the lower limits F_s and t_s yields:

$$F - \frac{A}{K_{sat}} \log \frac{K_{sat} F + A}{K_{sat} F_s + A} = F_s + K_{sat}(t - t_s) \tag{4.74}$$

Equation 4.74 can be solved for a particular time, by iteration, giving the cumulative infiltration F, and with this value, the depth of the wetting front z is computed through Equation 4.69.

It is worthy of mention that Mein and Larson's theory does not predict the entire moisture profile but they assume the soil to be saturated above the depth of the wetting front and, therefore, predict the advance of the wetting front. Another point of their theory is that the

average capillary suction h_{av} can be obtained from the moisture characteristic curve, by integrating across the wetting front over the range of moisture content $\theta_{in} - \theta_{sat}$. They, however, prefer to integrate from the relationship of suction versus hydraulic conductivity, over the full range of moisture content. Thus, if the relative hydraulic conductivity k_r is defined as:

$$k_r = \frac{K - K_{in}}{K_{sat} - K_{in}} \tag{4.75}$$

the average capillary suction will be simply the area under the curve suction versus the relative hydraulic conductivity between $k_r = 0$ and $k_r = 1$ or:

$$h_{av} = \int_0^1 h_c \, dk_r \tag{4.76}$$

4.4.3 Results of Mein and Larson's Solution

The analysis with Mein and Larson's solution have been obtained for the case of Columbia Sand Loam. The data for this soil are shown in Table 4.1 and Figures 4.1, 4.2 and 4.3.

Appendix B presents the program to compute the depth of wetting front with time for a certain rainfall intensity and an initial degree of saturation. Figures 4.9 and 4.10 illustrate how the wetting front advances with time for several rainfall intensities and for a certain initial degree of saturation.

One can note that as the rainfall intensity increases, the depth of infiltration does not increase in the same proportion. In fact, for any rainfall intensity I , the rate of infiltration decreases very rapidly with time (Figure 4.11) approaching values approximately equal since for large times the final value of the infiltration rate is the saturated hydraulic conductivity. In fact, for any rainfall intensity the soil can take water only at the infiltration rate corresponding to the time considered. A large rainfall intensity, thus, would only lead to a runoff of larger rate.

As seen before, Philip's solution showed that the depth of the wetting front could be expressed as a power series of time. Figure 4.9, obtained with Mein and Larson's solution, shows that for small times, when the depth of the wetting front is dominated by the capillary forces, only the first term of Equation 4.39 would be needed. As the time increases, the slope of the curve: depth of wetting front versus time becomes constant, as shown in Figure 4.10, also from Mein and Larson's solution. Hence this function can be expressed analytically as:

$$Z = at^{1/2} + bt \qquad (4.77)$$

The slope of this curve decreases as the time increases and tends to its constant value b.

Regression analyses using the series of Equation 4.39, has shown that the first two terms only would represent the best fitting curve for the results of Mein and Larson's solution and, thus, it is reasonable to adopt Equation 4.77. In this equation, the coefficients

a and b are functions of the soil properties, the initial degree of saturation and of the rainfall intensity. Figure 4.12 illustrates the variation of these coefficients with the rainfall intensity and for a certain initial degree of saturation.

As expected, for large values of the rainfall intensity, the coefficients a and b become approximately constant and in this case, rainfall intensities larger than 2 times the saturated hydraulic conductivity would not produce deeper infiltration of the wetting front for the same time considered. Surface runoff, however, is larger since the infiltration rates of Figure 4.11 are approximately the same for large times.

An important aspect is that for larger degrees of saturation prior to rainfall, the advance of the wetting front is faster, as illustrated in Figure 4.13. This was also expected since less water would be needed to saturate the soil and a certain amount of water would lead to a deeper penetration of the moisture profile for a larger initial degree of saturation. Therefore, it is concluded that the degree of saturation is more dominant than the rainfall intensity in leading to faster and deeper advance of the wetting front.

4.5 Analysis of Infiltration of Water into Residual Soils

Mein and Larson's method has been applied to the analysis of infiltration of water into residual soils because of its simplicity and because we are mainly concerned with the advance of the wetting front.

Because of lack of data of unsaturated flow properties of the residual soils, a parametric study was made by assuming certain ranges for these properties.

4.5.1 Unsaturated Flow Properties of the Residual Soils

In Chapter II we have seen that average values of some physical indexes for the residual soils are:

- density of soil particles : 2.65
- void ratio : 0.9
- dry unit weight : 1.3 to 1.4 g/cm^3

It was also seen that the natural degree of saturation of the residual soils ranges from about 60 to 70% and thus, these will be the starting values for our analysis.

Saturation of these soils occurs for a moisture content (gravimetric) between 30 to 40% and thus an average value of about 35% is a fair representation, corresponding to a volumetric moisture content of about 47%. Since this value is numerically equal to the porosity of the soil and corresponds to a void ratio of 0.89, these data are compatible.

Although these values are reasonable, because of the natural variation of the soil properties, three values of void ratio were considered in our analysis: 0.75, 0.89 and 1.00, corresponding to porosities equal to 43, 47 and 50%, respectively.

Three values of the saturated hydraulic conductivity were also considered: 8.0×10^{-5}, 2.0×10^{-4} and 5×10^{-4} cm/sec, which,

combined with the three values of the void ratio give us 9 soils to be analysed.

The curves for the hydraulic conductivity were estimated on the basis of known curves for other soils found in the literature. Therefore, the corresponding curves for clays and sand gave us, to a certain extent, the lower and upper limits of the curves for residual soils. Curves for sandy-clays, sandy-silts and clayey-sands provided the means to establish the general pattern of the curves for the residual soils.

The range of curves adopted for this study is indicated in Figure 4.1 and the curves adopted for the analyses and indicated in Figure 4.14.

Observing Figure 4.3, we see that more sandy soils (coarse soils) present a moisture characteristic curve characterized by a large flat portion while the curves for clayey soils (fine soils) do not. Thus, several curves were adopted for the residual soils, starting at the volumetric moisture content at saturation, numerically equal to the porosity of the soil, at which the suction is zero. Thus, the limits were established by taking the residual soil to be comparable to either a sand or a clay and an average curve was also established. Such curves are shown in Figures 4.15 to 4.17, and the range of moisture characteristic curves adopted is shown in Figure 4.3.

4.5.2 Results of the Analyses on Residual Soils

Figures 4.18 to 4.20 show the variation of the depth of wet-

ting front with time for a soil with average values of saturated hydraulic conductivity and void ratio, respectively 2.0×10^{-4} cm/sec and 0.89 (porosity equal to 47%), assuming the initial degree of saturation equal to 70, 80 and 90%. Since these curves are susceptible of analysis by means of Equation 4.77, the influence of all factors over the unsaturated flow is analysed in terms of the coefficients a and b. Variation of these coefficients with rainfall intensity for the 9 soils considered are shown in Figures 4.21 to 4.29.

Analysis of these figures show that the coefficient a increases with the rainfall intensity, while b decreases. As a consequence, the curves depth versus time have more pronounced curvature for small times, as the rainfall intensity increases, as shown in Figures 4.18 to 4.20. The slope of these curves also decreases as the rainfall intensity increases.

Comparing the curves of a and b for the same void ratio but for different initial degrees of saturation S_o, we see that for larger S_o, a and b also increase, thus, leading to a faster advance of the wetting front, as noted before.

Finally, it must be noted that both a and b tend to constant values as the rainfall intensity increases. This fact has also been pointed out before and we see that in all cases for I/K_s ratio over 4 the depth of the wetting front is not governed by the rainfall intensity. In what follows, analyses will be carried out for the average values of saturated hydraulic conductivity and void ratio, and

for an I/K_s ratio equal to 4.

Figure 4.30 illustrates the variation of a and b with the void ratio and the initial degree of saturation. It is seen that a and b increase for smaller values of the void ratio, however, the effect of the initial degree of saturation is appreciably more pronounced than the influence of the void ratio.

Figures 4.31 and 4.32 show the influence of the saturated hydraulic conductivity K_s on the coefficients a and b, as compared with the initial degree of saturation S_o. For any given value of S_o, a and b increase appreciably with K_s although the effect upon b is more relevant.

It must be noted that the coefficient b is closely related to the saturated hydraulic conductivity K_s, since for large times, the infiltration rate is constant and equal to K_s, and the rate of advance of the wetting front is also constant and equal to the coefficient b. Philip (1969) showed that the rate of advance of the wetting front is for large times given by Equation 4.58, thus we could write:

$$b = \frac{K_s - K_{in}}{\theta_{sat} - \theta_{in}} \qquad (4.78)$$

although our results show that this equation is, in our case, valid only for small values of the initial degree of saturation.

Finally, to study the influence of the suction for each void ratio, 3 curves were considered as shown in Figures 4.15 to 4.17.

Figure 4.33 shows the variation of the coefficients a and b with the average suction at the wetting front. This was obtained simply by taking the suction at the average moisture content θ_{av} defined as:

$$\theta_{av} = \frac{1}{2}(\theta_{in} + \theta_{sat}) \tag{4.79}$$

The analyses, however, have been performed by calculating the average suction as indicated in Section 4.4.2, and both values appeared to be approximately the same. Figure 4.33 shows, however, that small variations in the suction considered do not lead to significant error. In fact, the coefficient b is independent of the suction as illustrated, for any initial degree of saturation, although the coefficient a varies appreciably over the range of suction considered.

The curves of the depth of wetting front with time for the 9 soils we have analysed are shown in Appendix C. Only the curves corresponding to an initial degree of saturation of 90% are considered since this value represents a critical situation, leading to a fast advance of the wetting front.

The depths of infiltration are closely related to the rainfall duration since the time during which the source of water would be maintained is obviously relevant. We see, however, that depths of infiltration of practical engineering interest are obtained for saturated hydraulic conductivity larger than 2.0×10^{-4} cm/sec, for the range of void ratio considered. Significant depth is also obtained for a lower value of the saturated hydraulic conductivity provided that the void

ratio is correspondingly small. Conversely, a larger void ratio would require a larger value for the saturated hydraulic conductivity.

In Chapter VII, we will see that a value of 5.0×10^{-4} cm/sec is required for the saturated hydraulic conductivity in connection with the depths of the Estrada do Jequiá slide and it is felt that water would possibly infiltrate through cracks and relict structures present in the soil.

Soil	Porosity (%)	Saturated Hydraulic Conductivity (cm/sec)	References
Columbia Silt Loam	34.0	3.17×10^{-4}	Kirkham and Powers 1972
Columbia Sand Loam	51.8	1.39×10^{-3}	Mein and Larson 1973
Ballotini Grande 15	38.0	6.0×10^{-6}	Youngs, 1957
Webster Soil	48.0	3.4×10^{-4}	Kunze and Kirkham 1962
Ida Soil	53.5	2.6×10^{-4}	Kunze and Kirkham 1962
Yolo Light Clay	49.5	1.23×10^{-5}	Philip, 1957a
Plainfield Sand	47.7	3.44×10^{-3}	Mein and Larson 1973
Guelph Loam	52.3	3.67×10^{-4}	Mein and Larson 1973

TABLE 4.1 CHARACTERISTICS OF THE SOILS REFERRED TO IN THE STUDY

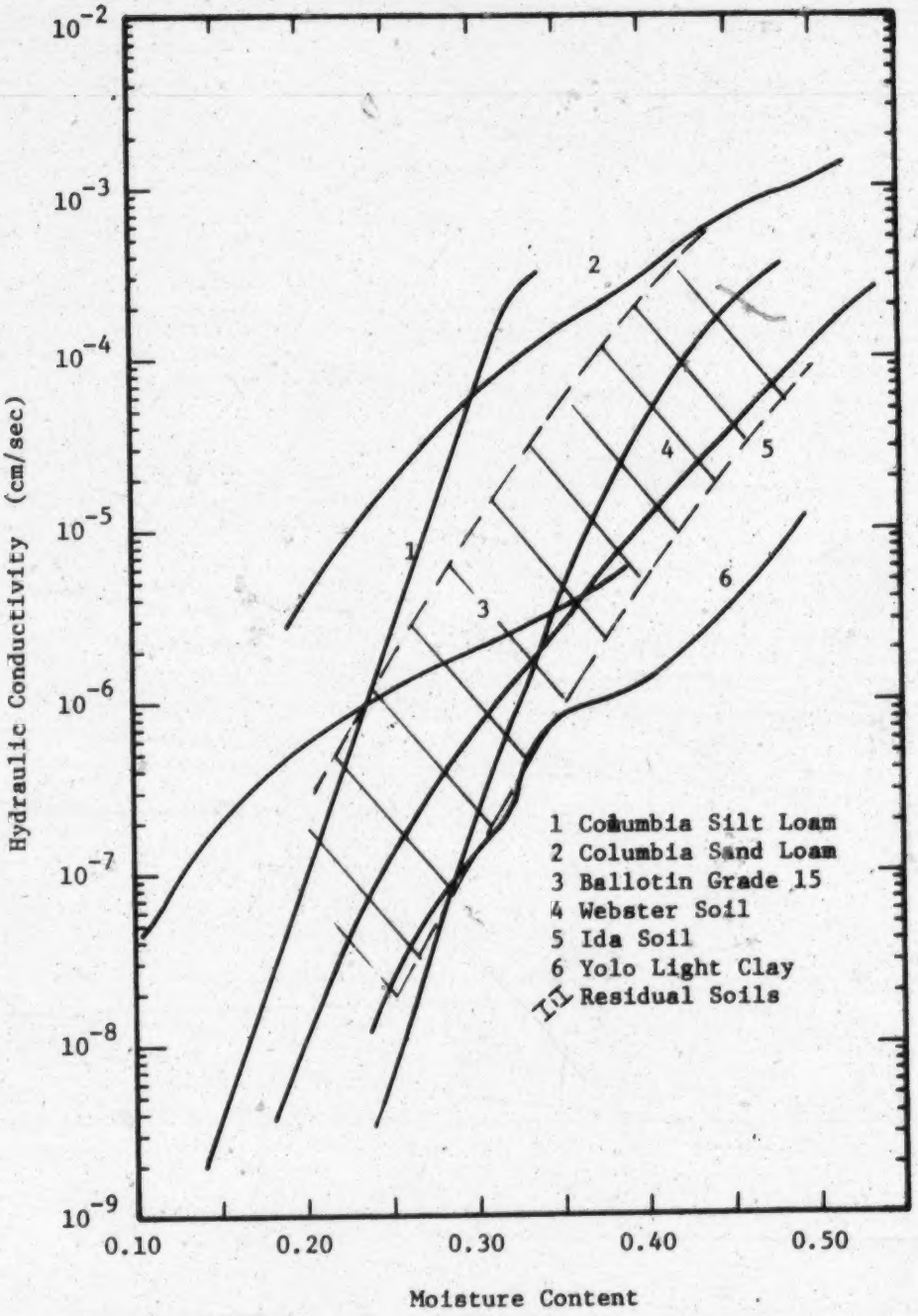

FIGURE 4.1 HYDRAULIC CONDUCTIVITY VERSUS MOISTURE CONTENT FOR VARIOUS SOILS

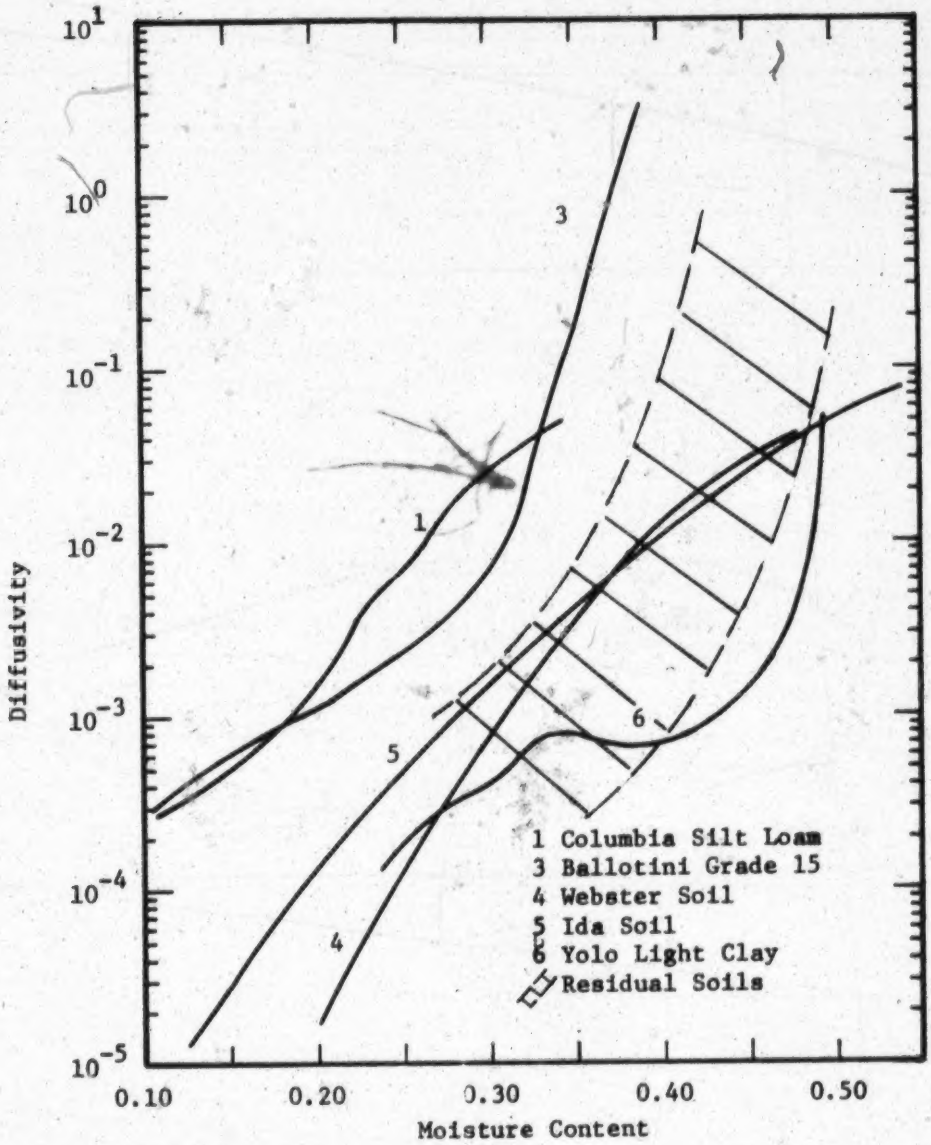

FIGURE 4.2 DIFFUSIVITY VERSUS MOISTURE CONTENT FOR VARIOUS SOILS

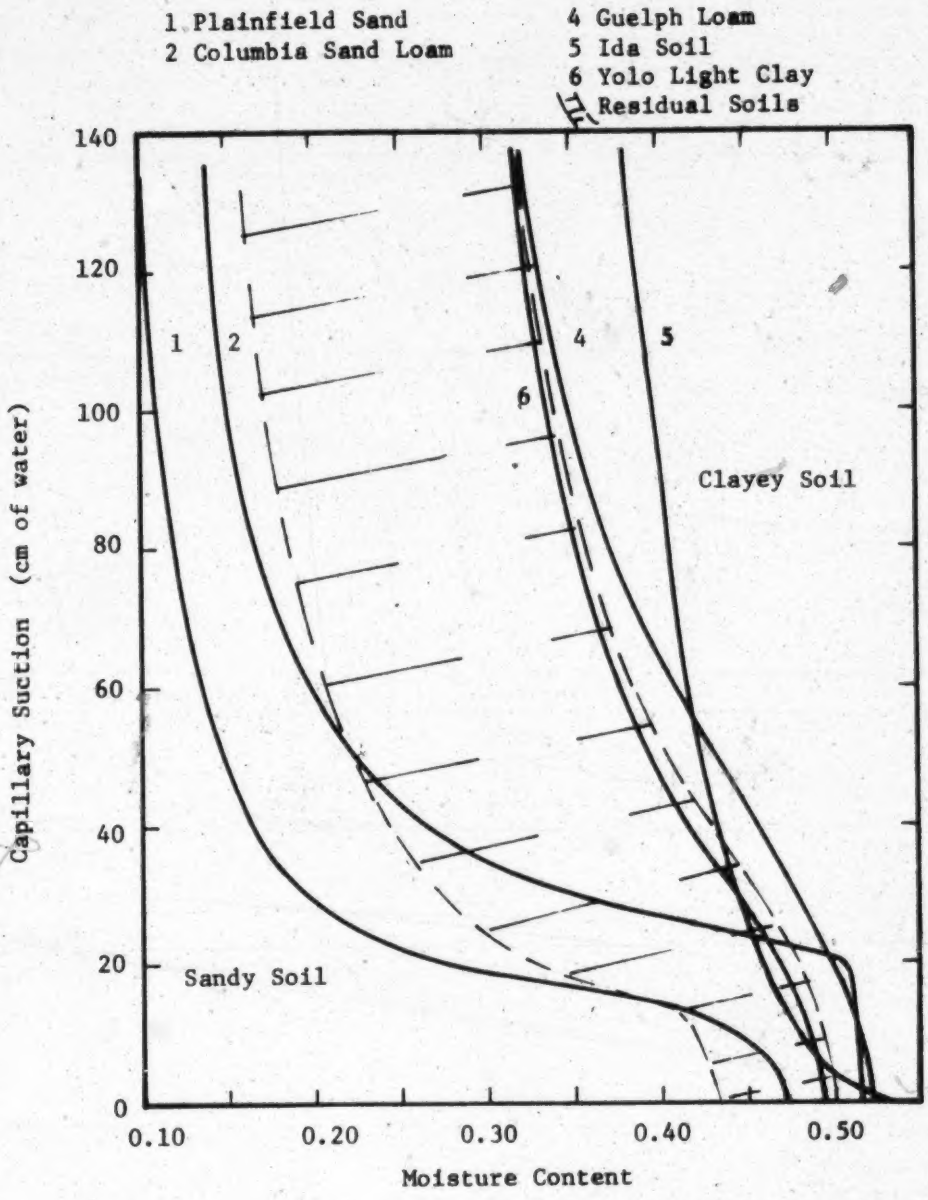

FIGURE 4.3 CHARACTERISTIC CURVES FOR VARIOUS SOILS

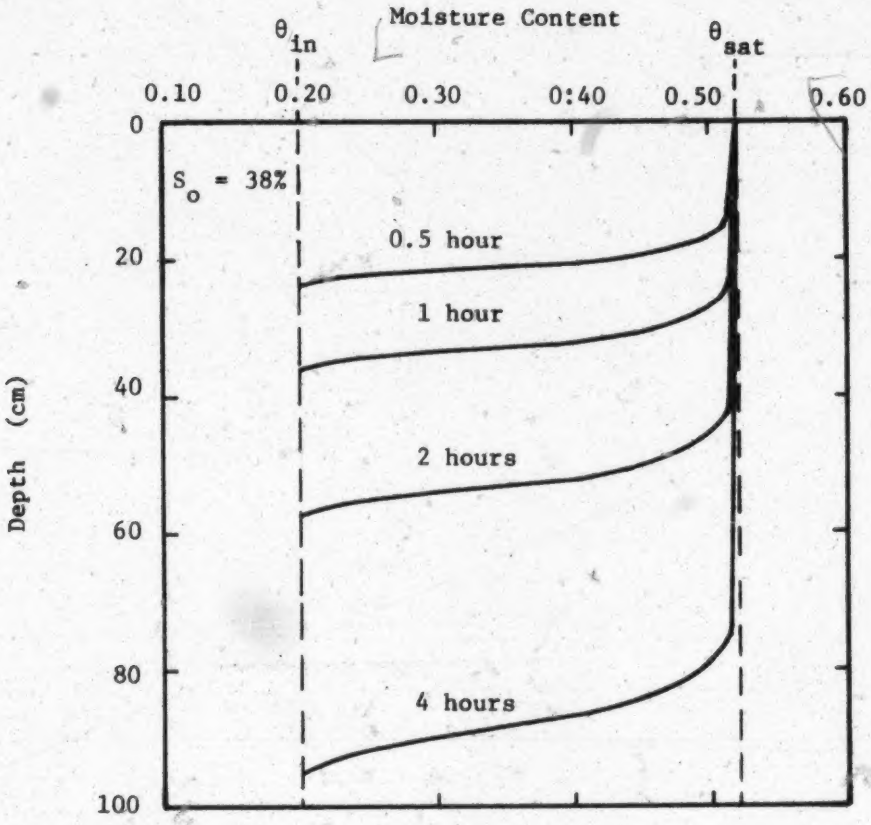

FIGURE 4.4 DESCENDING MOISTURE PROFILE FOR COLUMBIA SAND LOAM

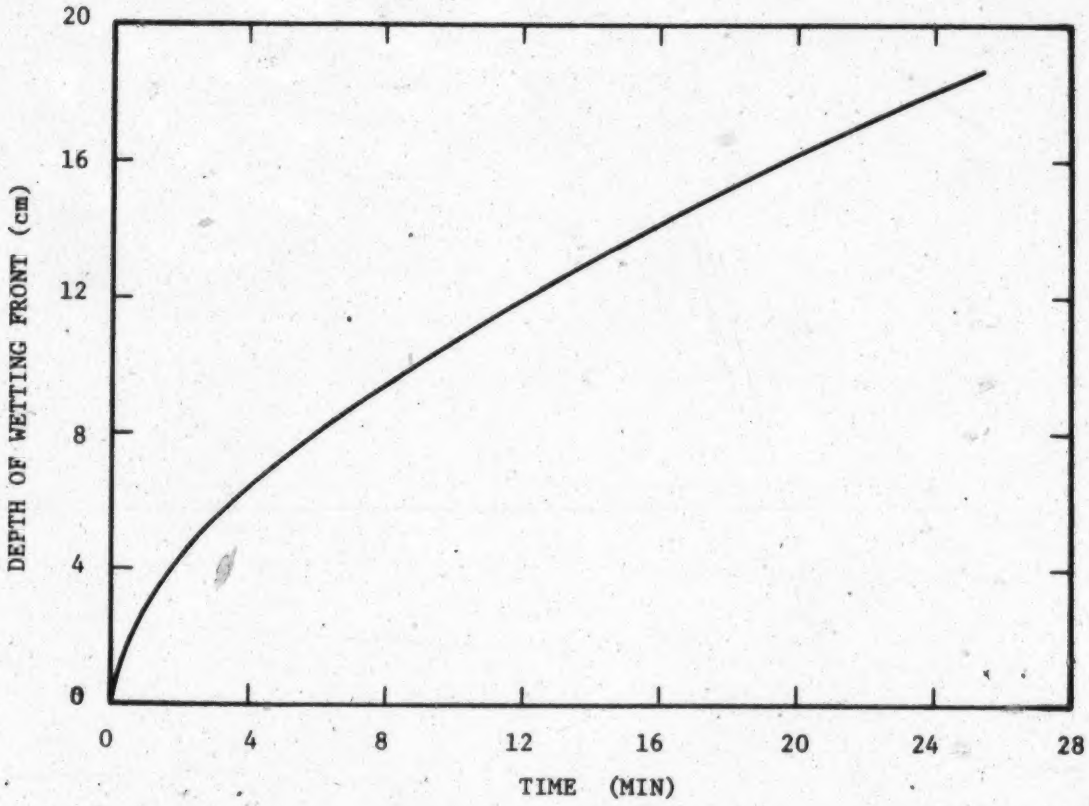

FIGURE 4.5 DEPTH OF INFILTRATION VERSUS TIME FOR COLUMBIA SAND LOAM

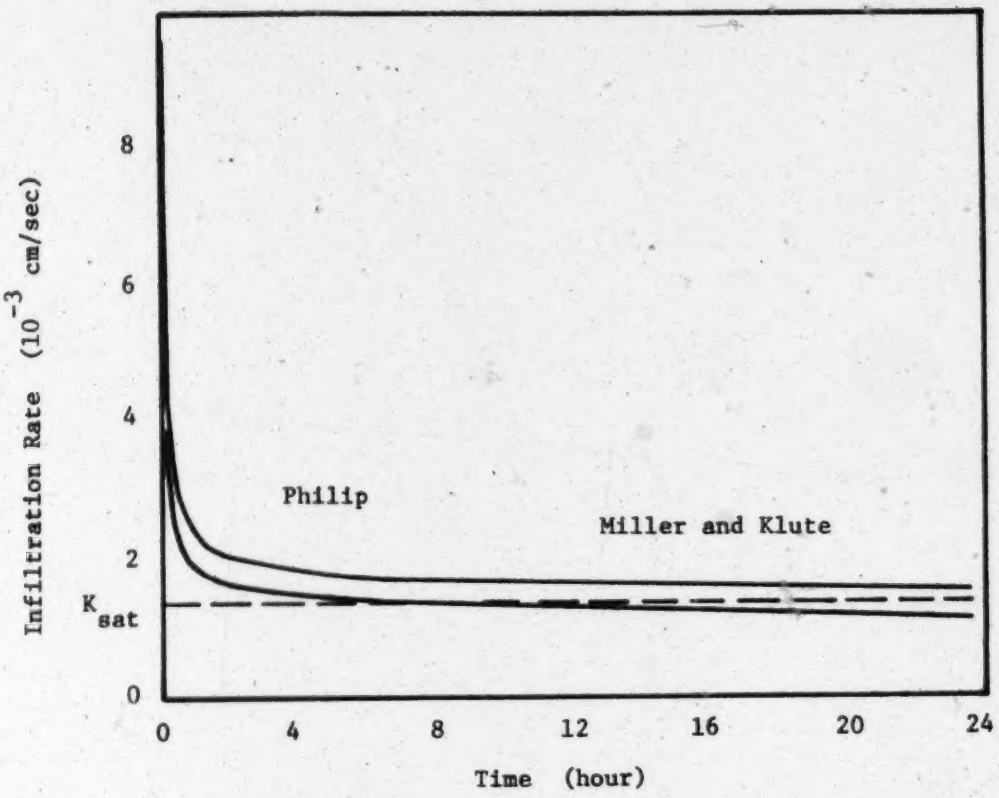

FIGURE 4.6 INFILTRATION RATES VERSUS TIME FOR COLUMBIA SAND LOAM

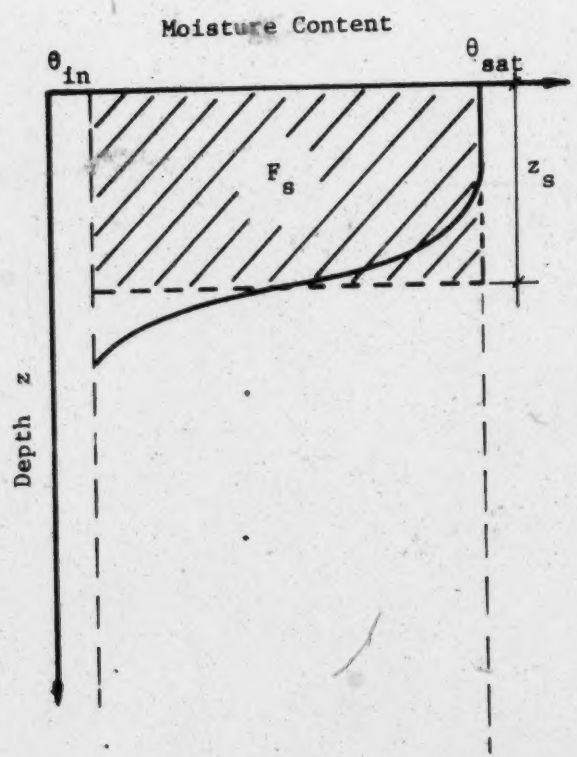

FIGURE 4.7 GENERALIZED SOIL MOISTURE PROFILE DURING INFILTRATION AT THE MOMENT OF SURFACE SATURATION
(After Mein and Larson, 1973)

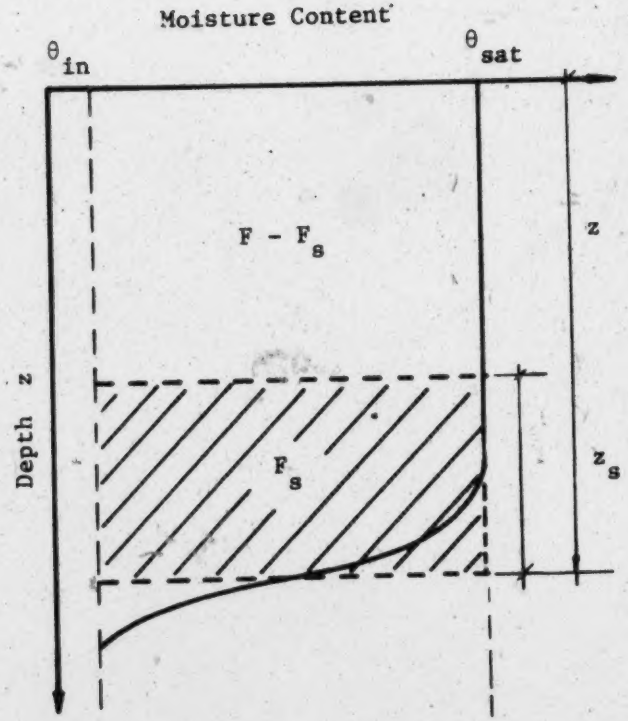

FIGURE 4.8 GENERALIZED SOIL MOISTURE PROFILE DURING INFILTRATION AFTER SURFACE SATURATION
(After Mein and Larson, 1973)

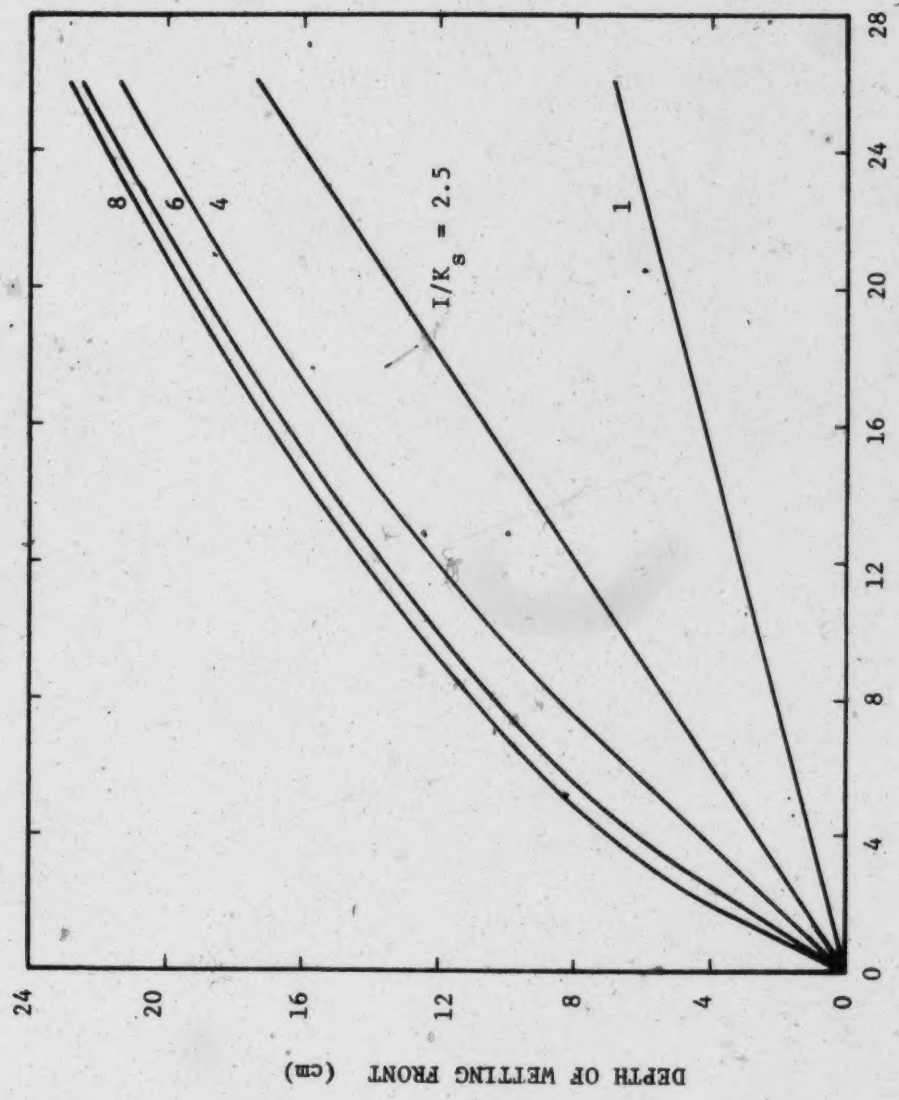

FIGURE 4.9 DEPTHS OF INFILTRATION FOR SMALL TIMES FOR COLUMBIA SAND LOAM

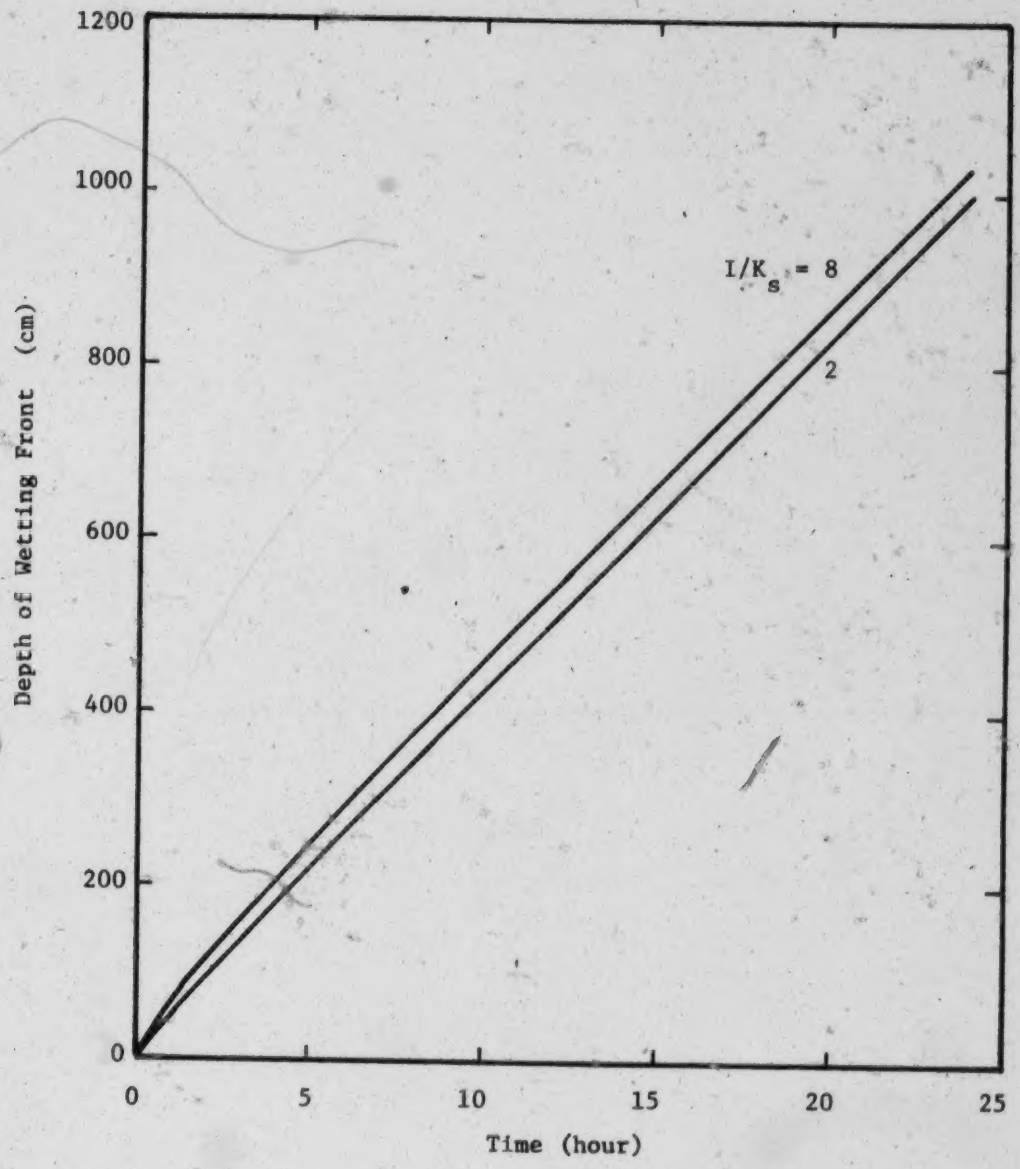

FIGURE 4.10 DEPTHS OF INFILTRATION FOR LARGE TIMES FOR COLUMBIA SAND LOAM

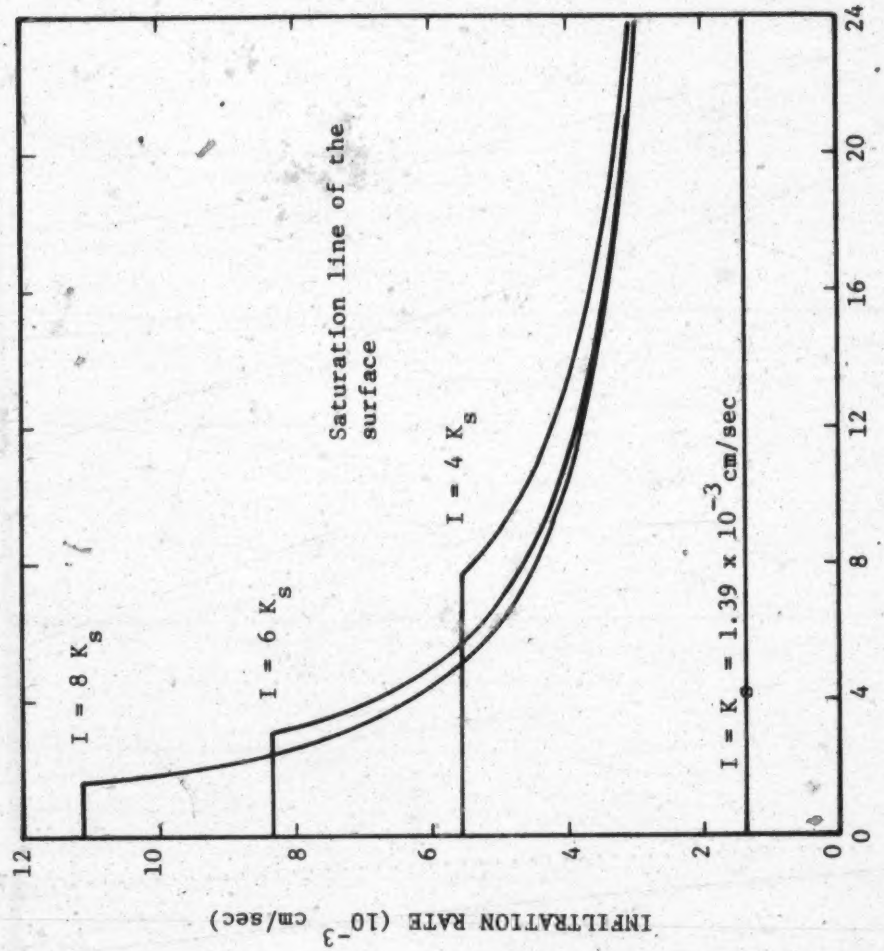

FIGURE 4.11 EFFECT OF RAINFALL INTENSITY ON THE INFILTRATION RATE FOR COLUMBIA SAND LOAM

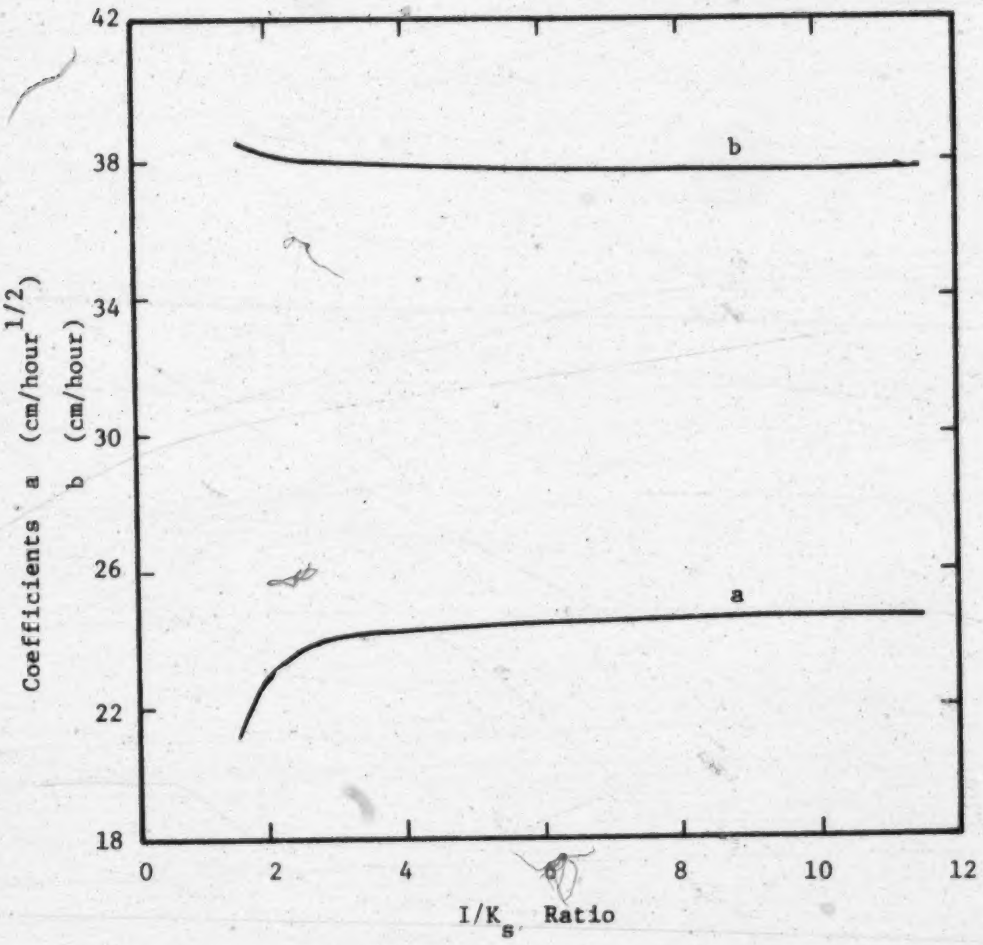

FIGURE 4.12 COEFFICIENTS a AND b VERSUS THE I/K_s RATIO FOR COLUMBIA SAND LOAM

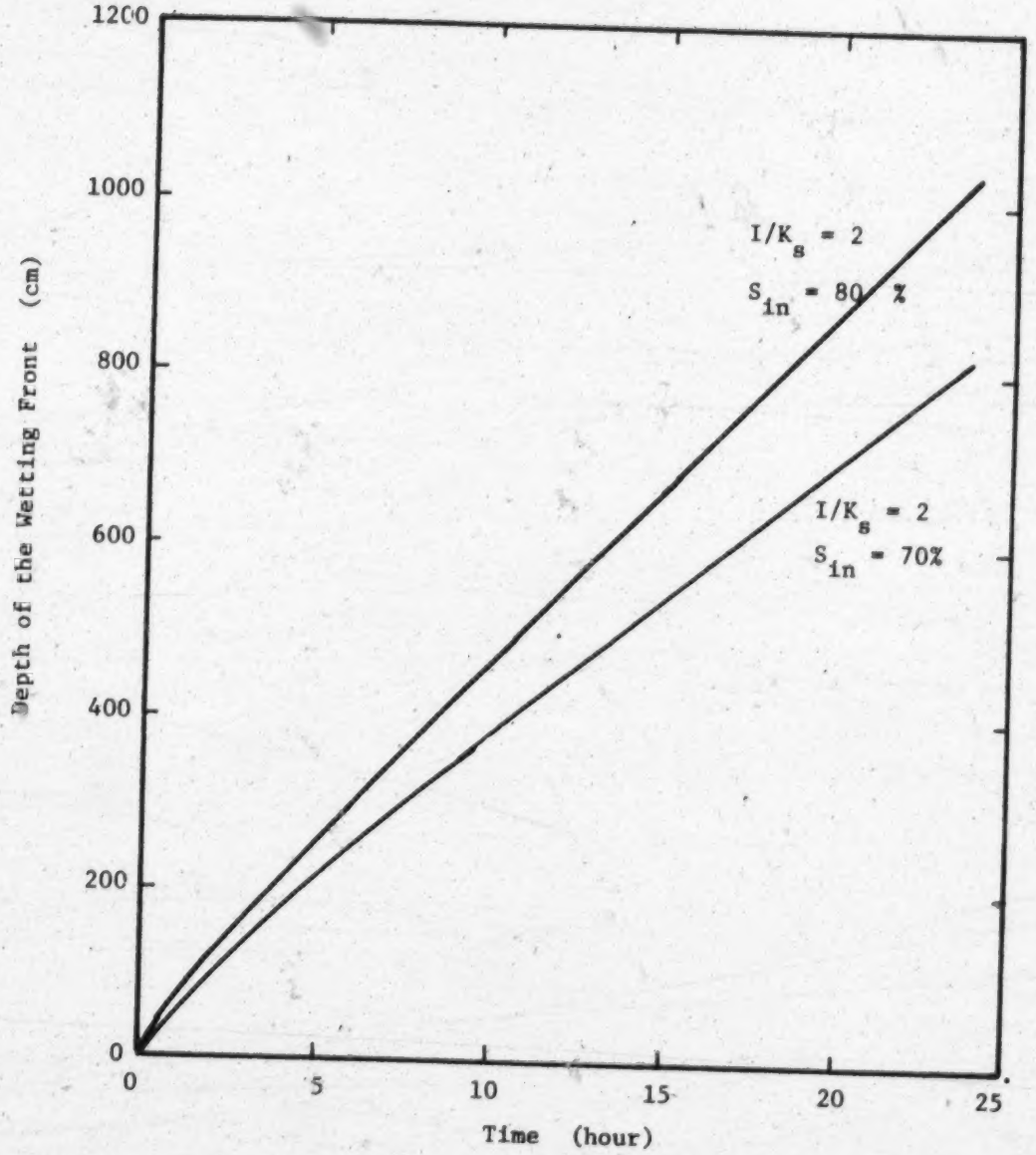

FIGURE 4.13 EFFECT OF THE INITIAL DEGREE OF SATURATION ON THE ADVANCE OF THE WETTING FRONT WITH TIME

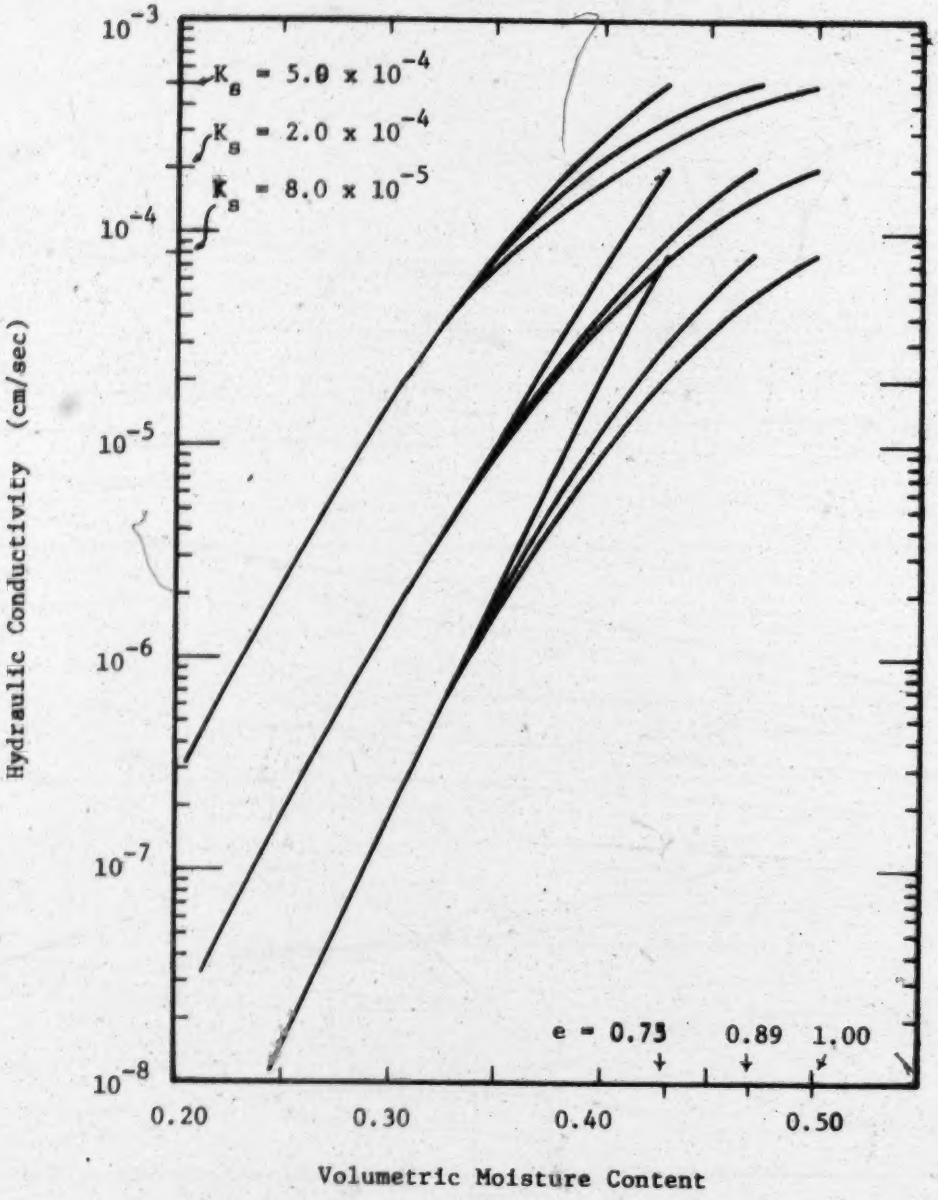

FIGURE 4.14 HYDRAULIC CONDUCTIVITY CURVES ADOPTED FOR RESIDUAL SOILS

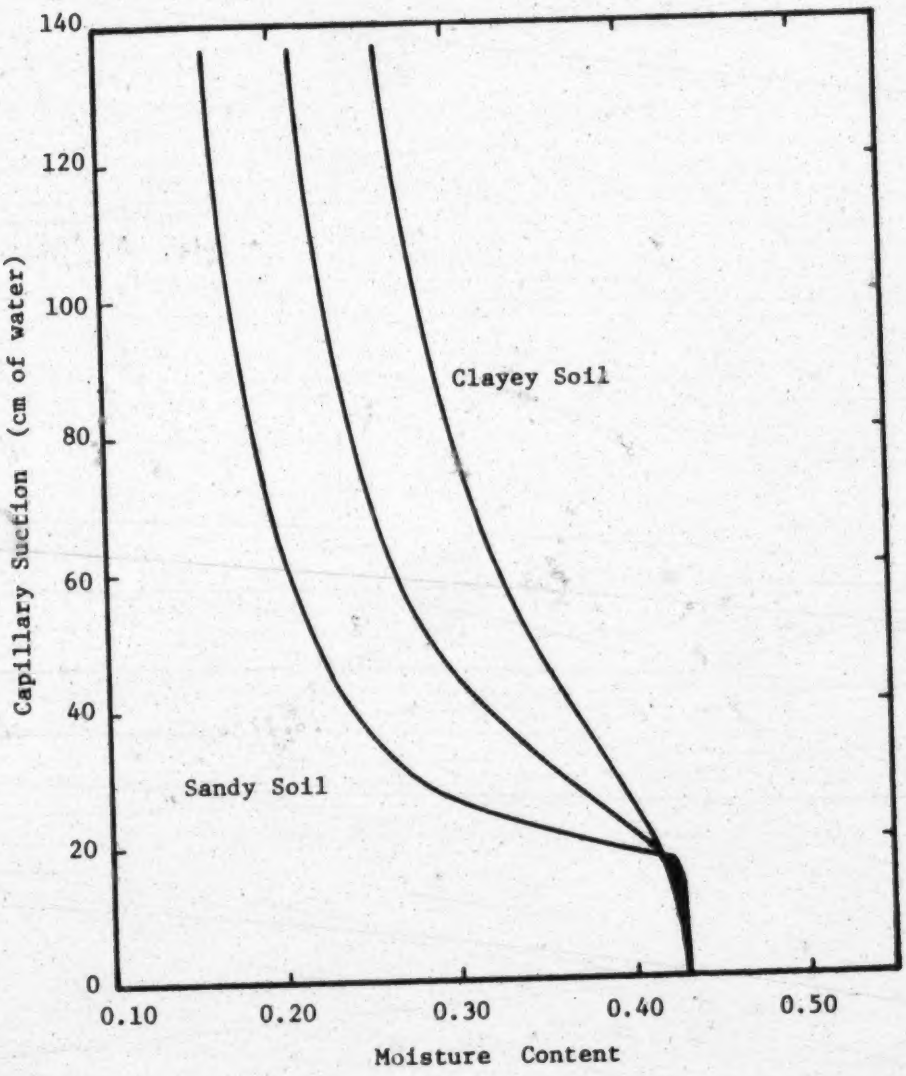

FIGURE 4.13 ASSUMED MOISTURE CHARACTERISTIC CURVES FOR RESIDUAL SOILS. VOID RATIO EQUAL TO 0.75

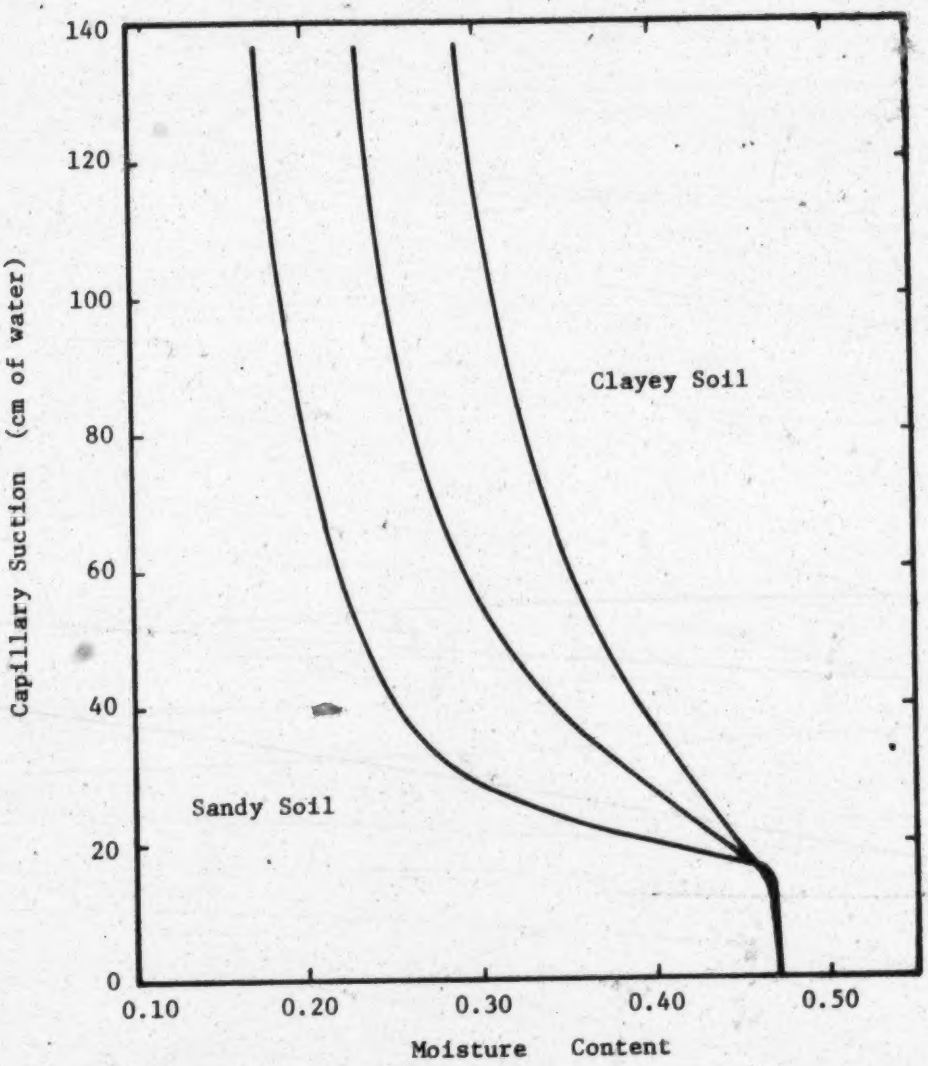

FIGURE 4.16 ASSUMED MOISTURE CHARACTERISTIC CURVES FOR RESIDUAL SOILS. VOID RATIO EQUAL TO 0.89

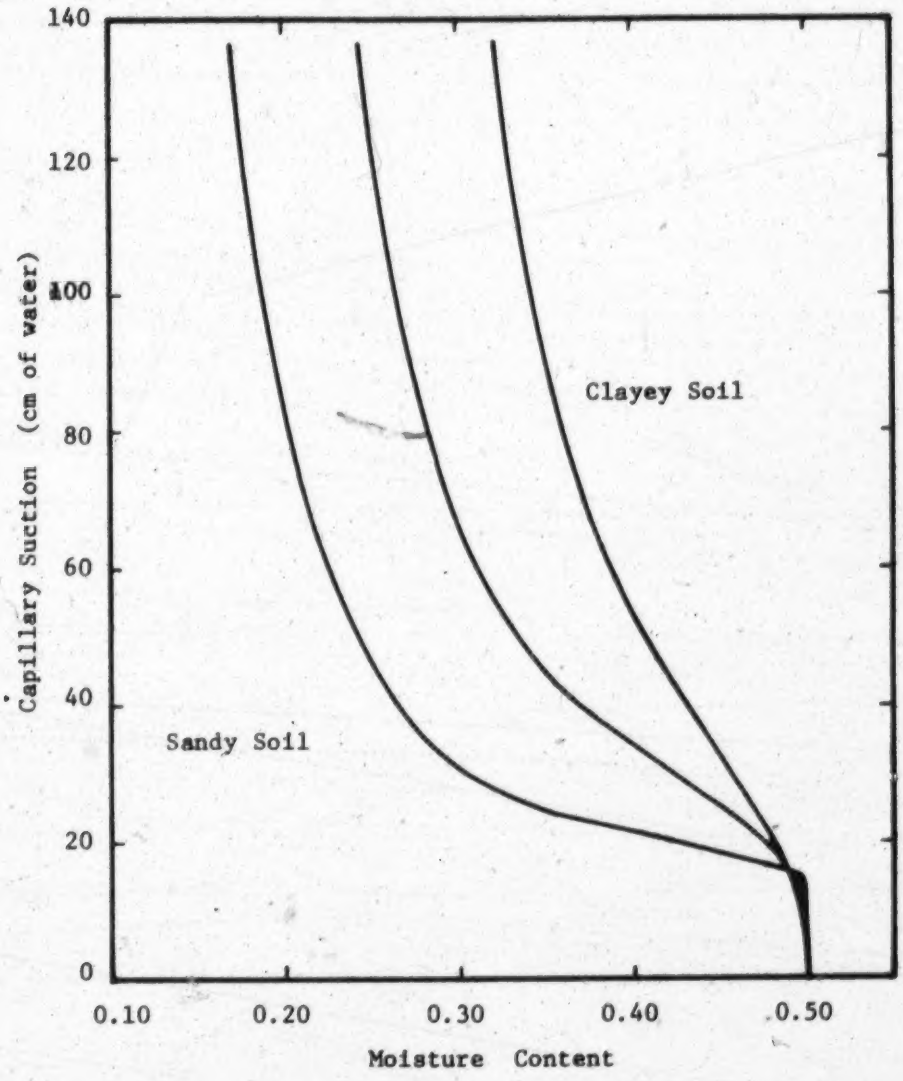

FIGURE 4.17 ASSUMED MOISTURE CHARACTERISTIC CURVES FOR RESIDUAL SOILS. VOID RATIO EQUAL TO 1.00

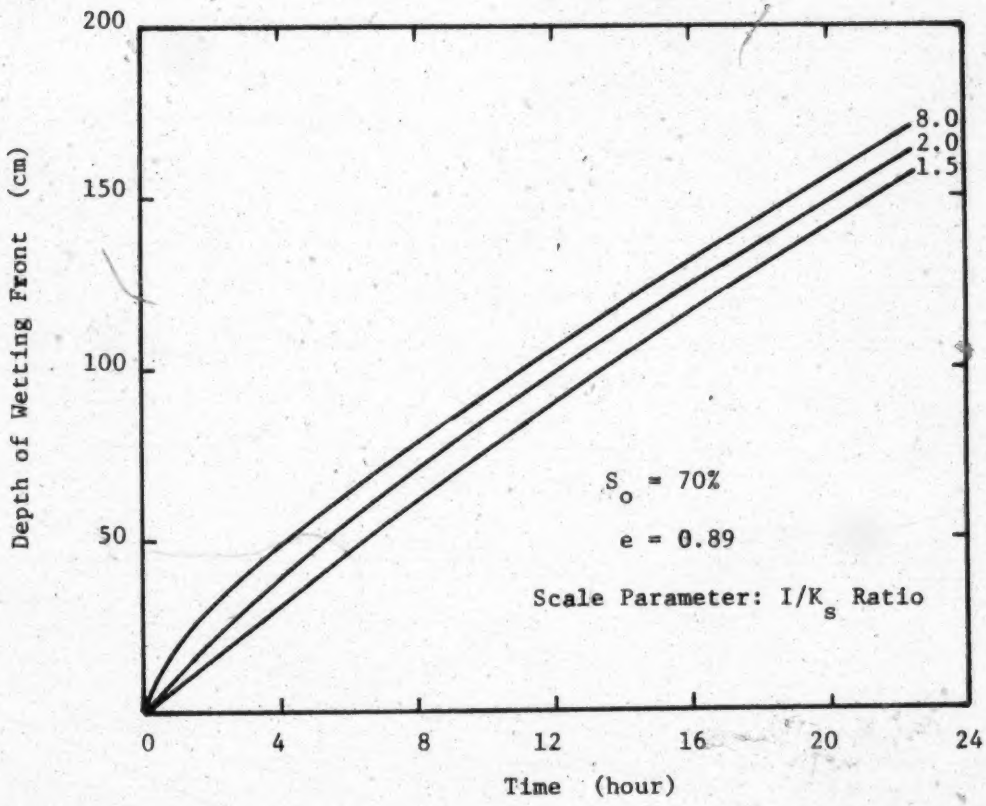

FIGURE 4.18 ADVANCE OF THE WETTING FRONT WITH TIME (S_o = 70%)

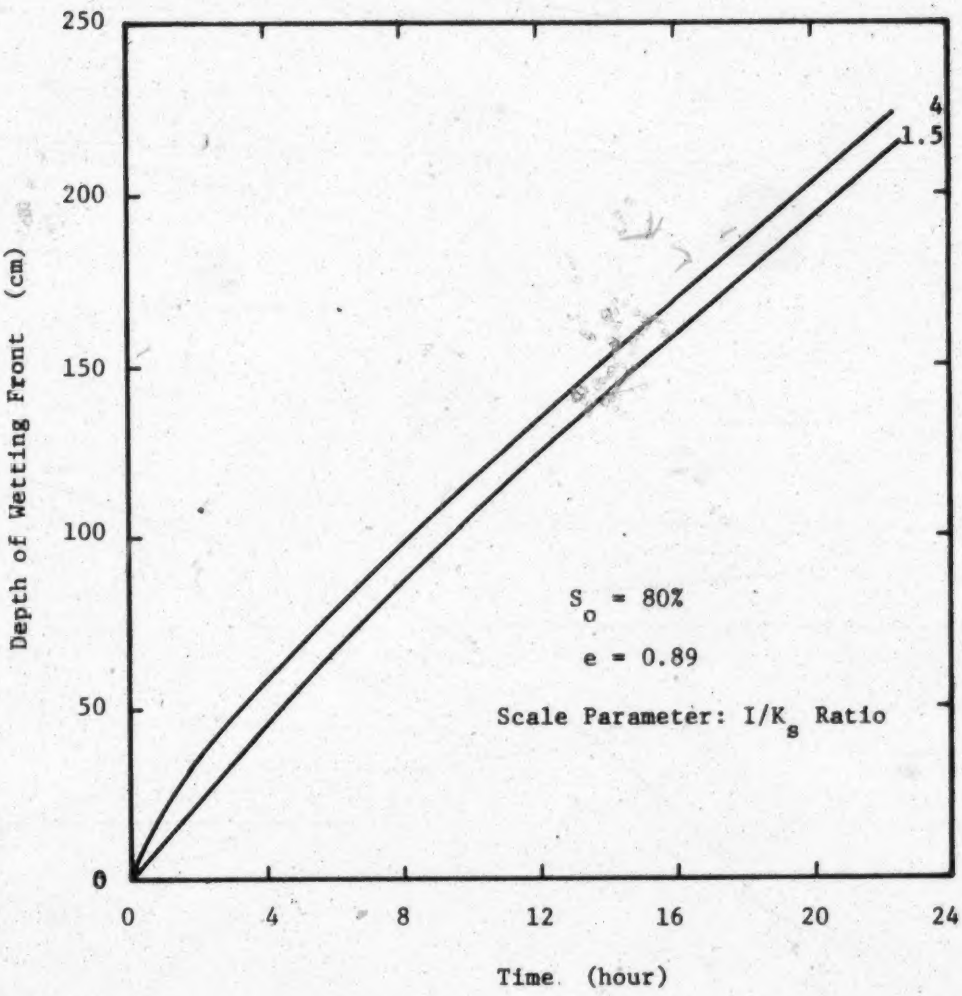

FIGURE 4.19 ADVANCE OF THE WETTING FRONT WITH TIME (S_o = 80%)

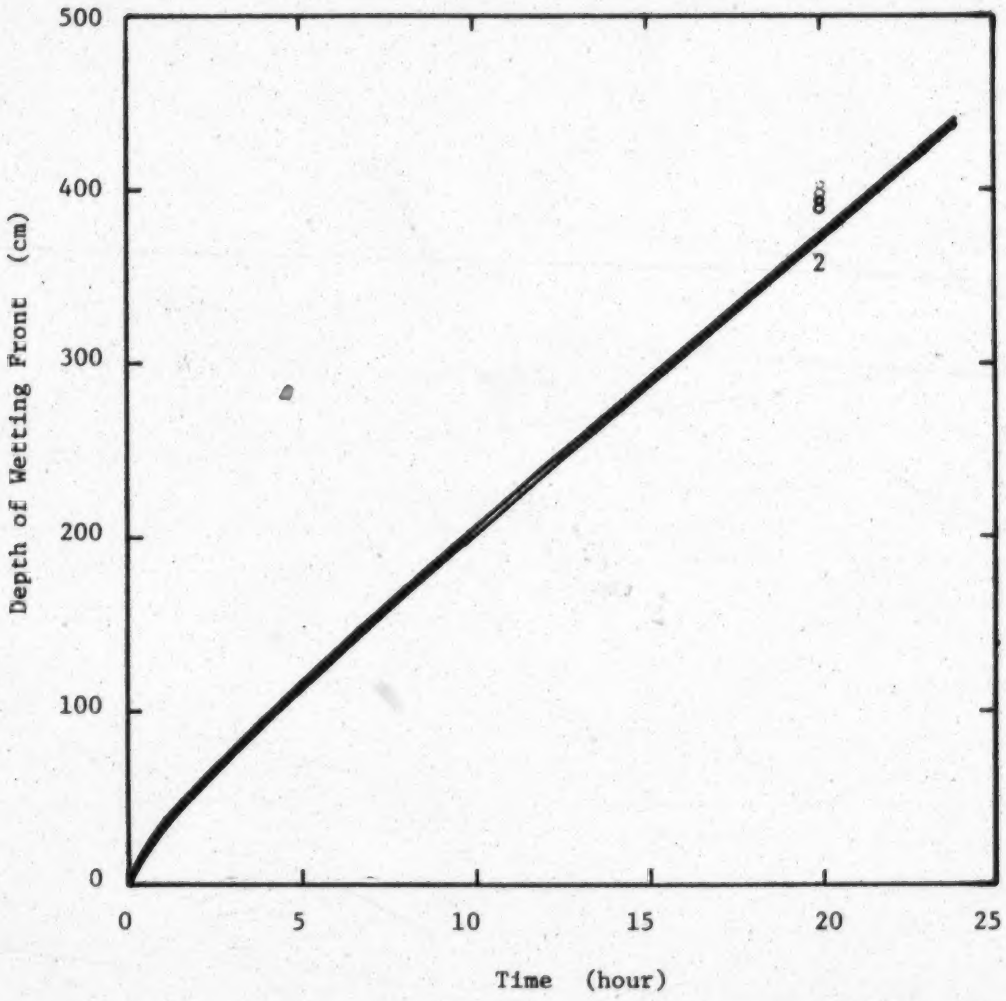

FIGURE 4.20 ADVANCE OF THE WETTING FRONT WITH TIME (S_o = 90%)

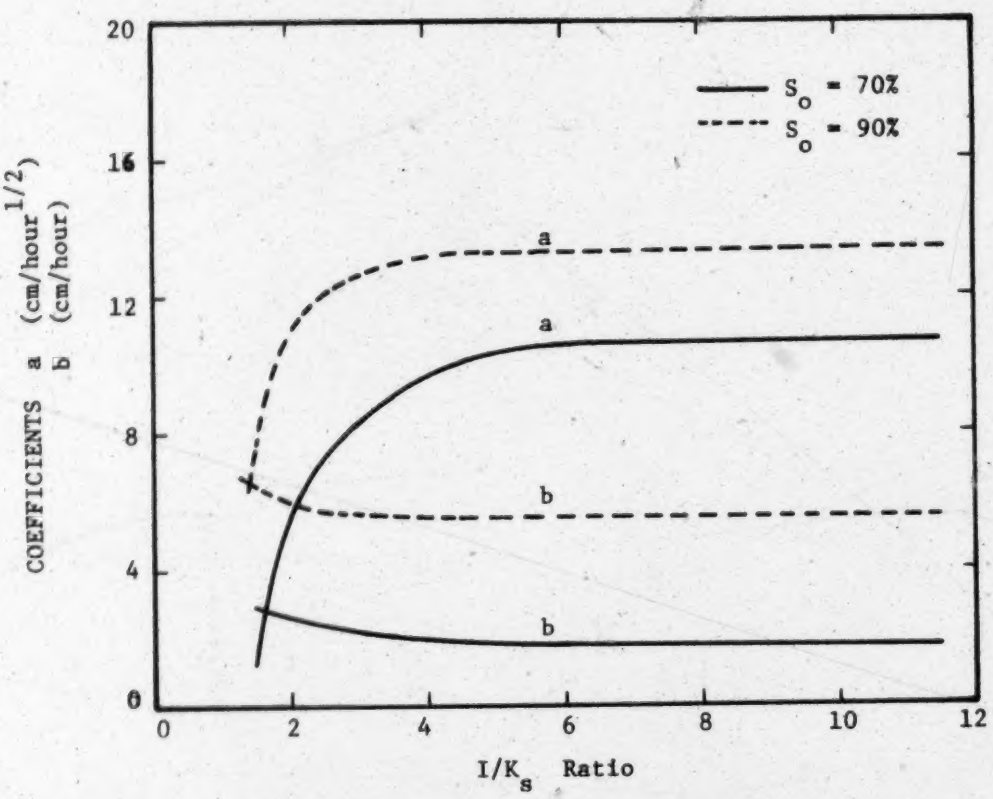

FIGURE 4.21 COEFFICIENTS a AND b VERSUS THE I/K_s RATIO FOR e = 0.75 AND $K_s = 8.0 \times 10^{-5}$ cm/sec

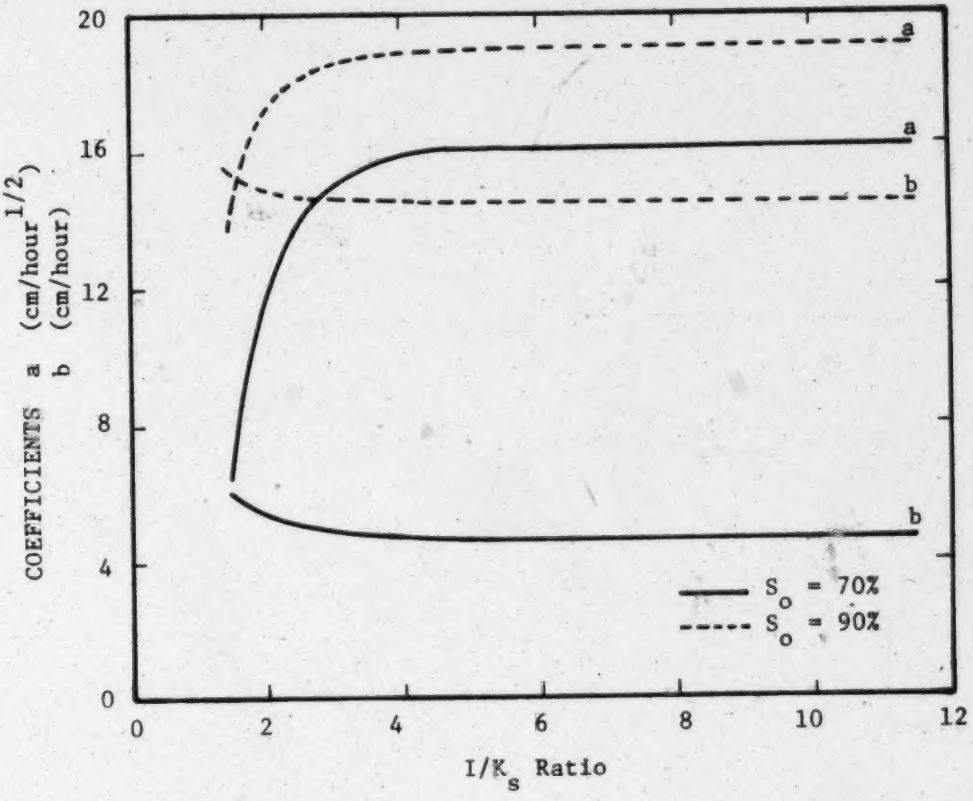

FIGURE 4.22 COEFFICIENTS a AND b VERSUS THE I/K_s RATIO FOR e = 0.75 AND $K_s = 2.0 \times 10^{-4}$ cm/sec

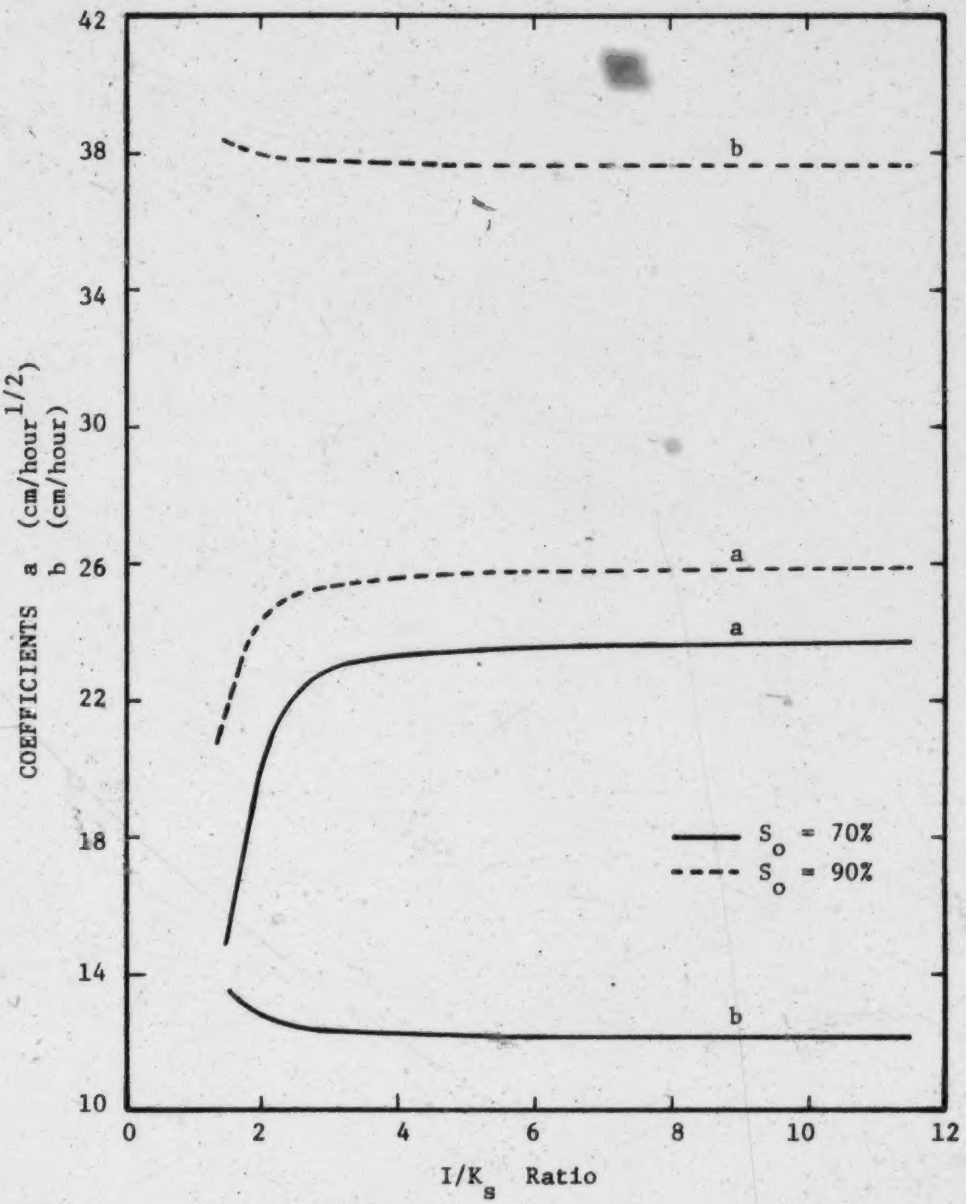

FIGURE 4.23 COEFFICIENTS a AND b VERSUS THE I/K_s RATIO FOR e = 0.75 AND $K_s = 5.0 \times 10^{-4}$ cm/sec

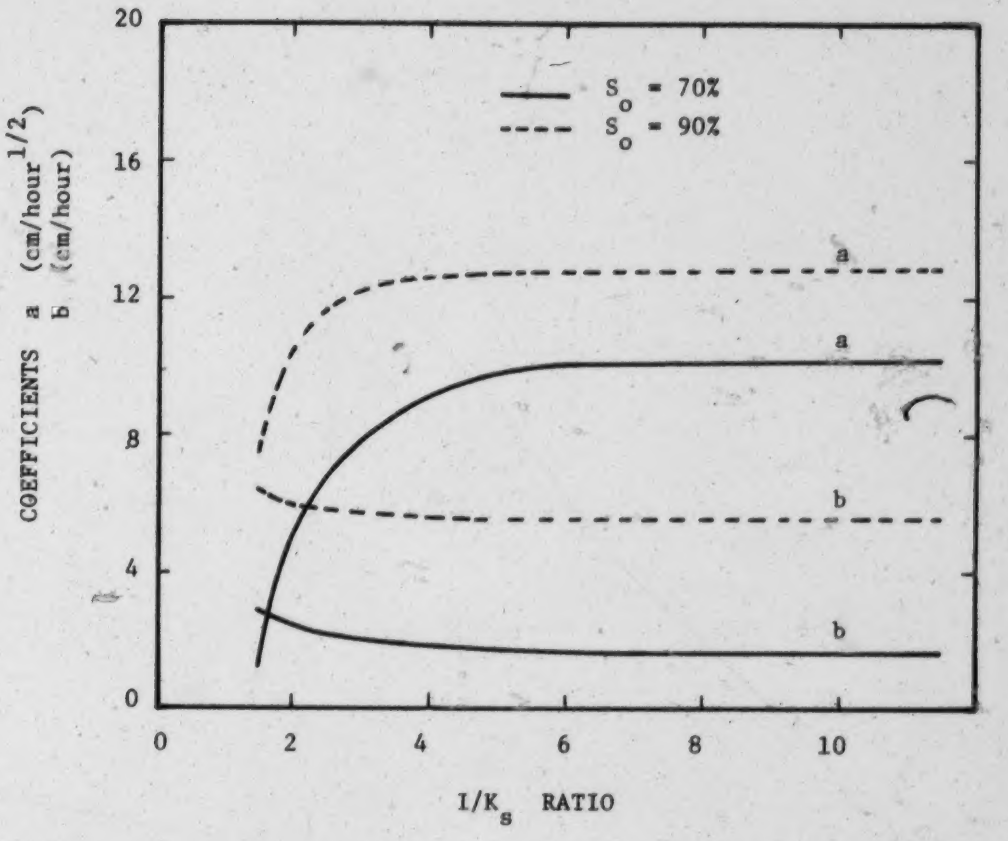

FIGURE 4.24 COEFFICIENTS a AND b VERSUS THE I/K_s RATIO FOR e = 0.89 AND $K_s = 8.0 \times 10^{-5}$ cm/sec

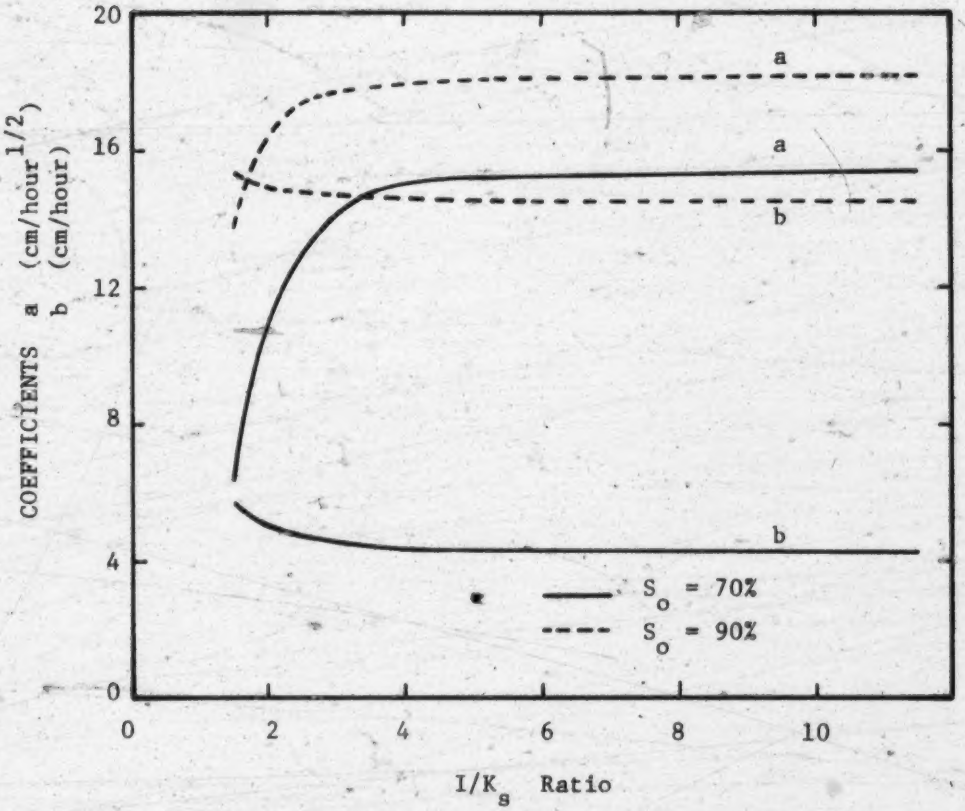

FIGURE 4.25 COEFFICIENTS a AND b VERSUS THE I/K_s RATIO FOR e = 0.89 AND $K_s = 2.0 \times 10^{-4}$ cm/sec

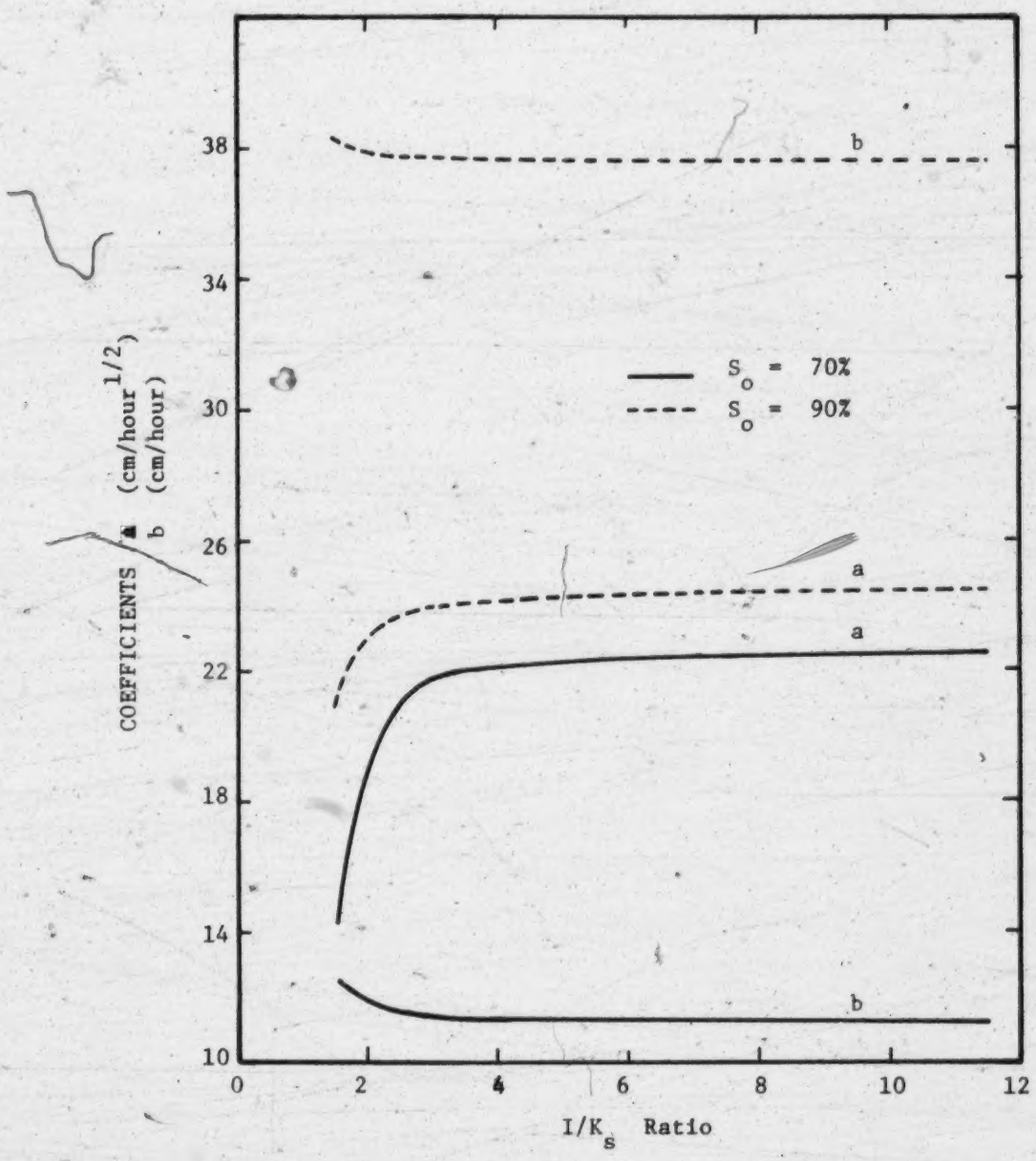

FIGURE 4.26 COEFFICIENTS a AND b VERSUS THE I/K_s RATIO FOR e = 0.89 AND $K_s = 5.0 \times 10^{-4}$ cm/sec

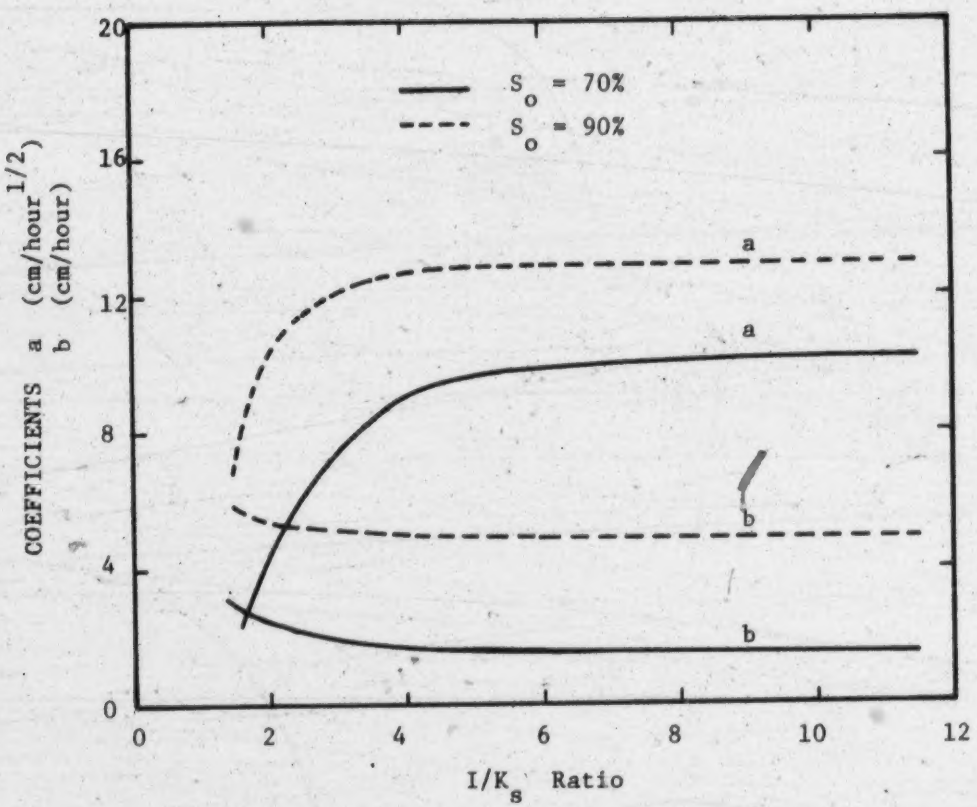

FIGURE 4.27 COEFFICIENTS a AND b VERSUS THE I/K_s RATIO FOR e = 1.00 AND $K_s = 8.0 \times 10^{-5}$ cm/sec

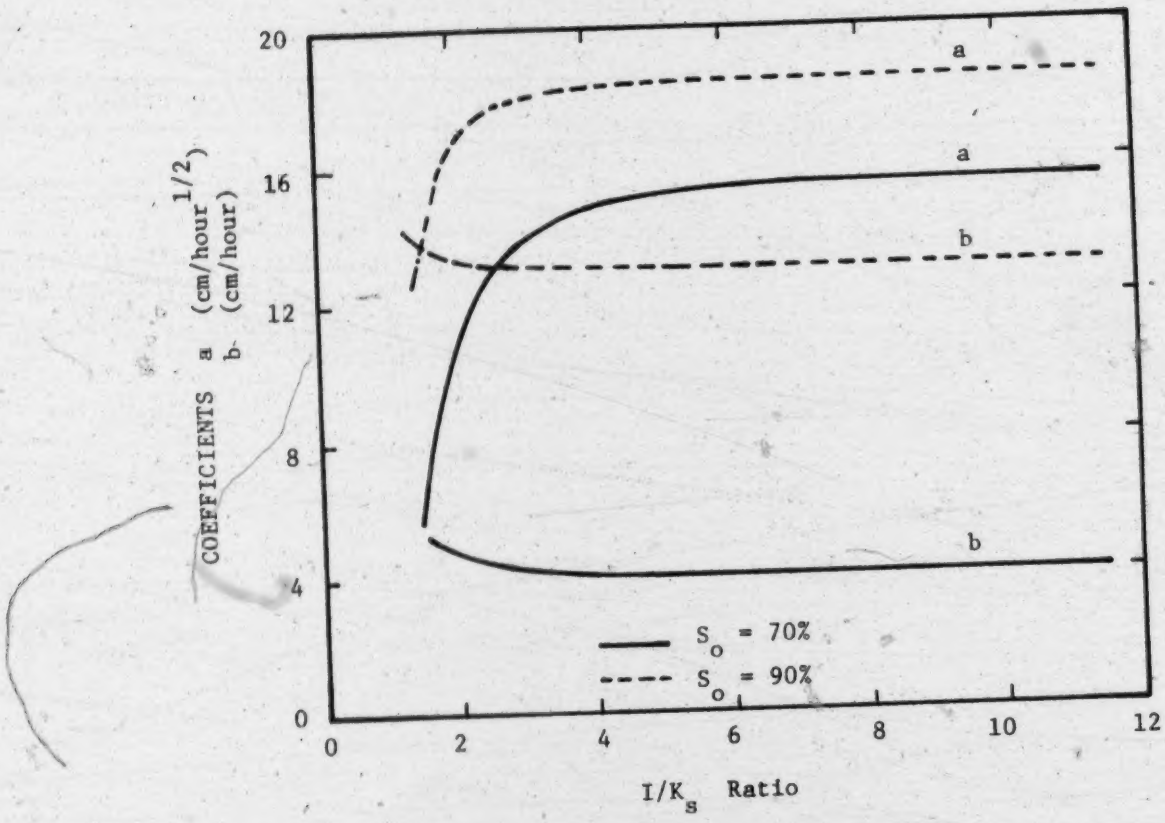

FIGURE 4.28 COEFFICIENTS a AND b VERSUS THE I/K_s RATIO FOR e = 1.00 AND $K_s = 2.0 \times 10^{-4}$ cm/sec

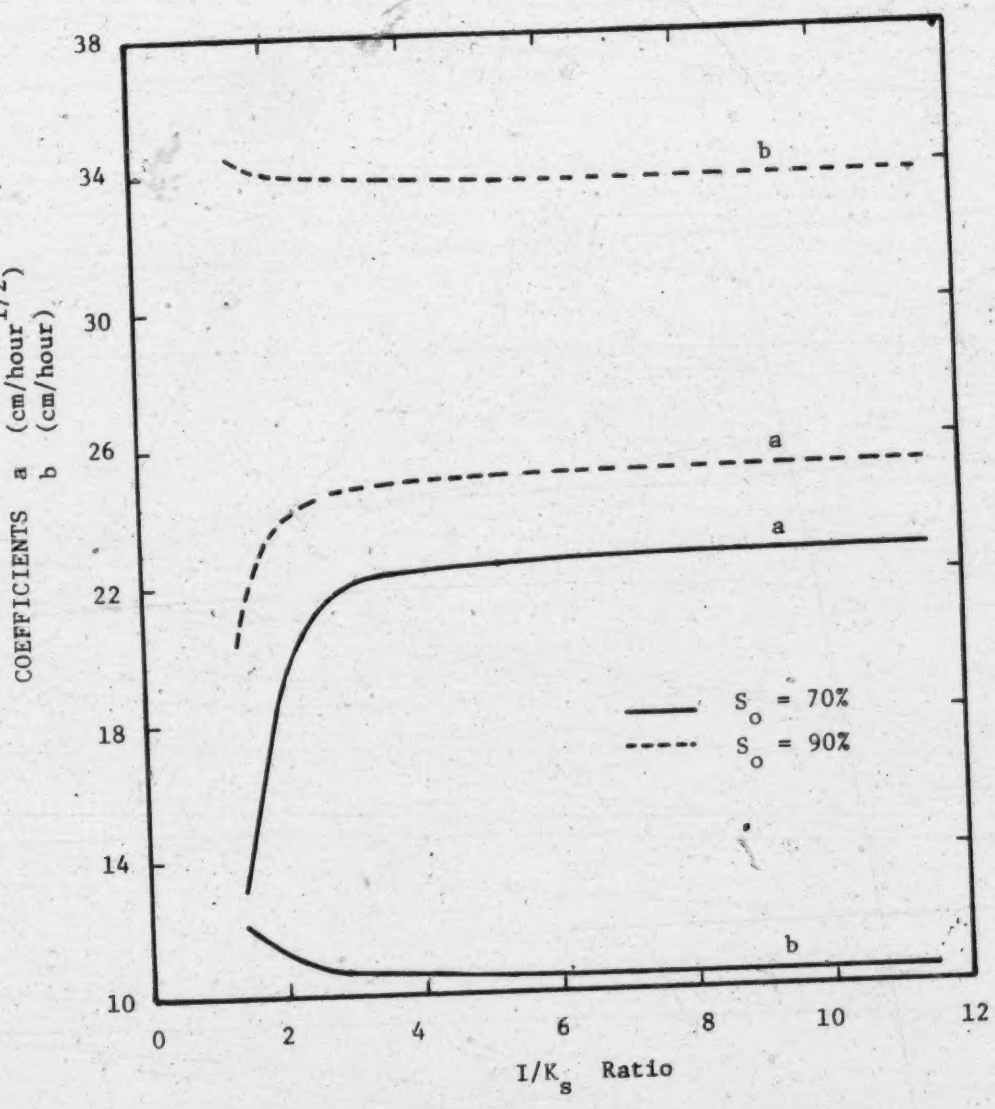

FIGURE 4.29 COEFFICIENTS a AND b VERSUS THE I/K_s RATIO FOR e = 1.00 AND $K_s = 5.0 \times 10^{-4}$ cm/sec

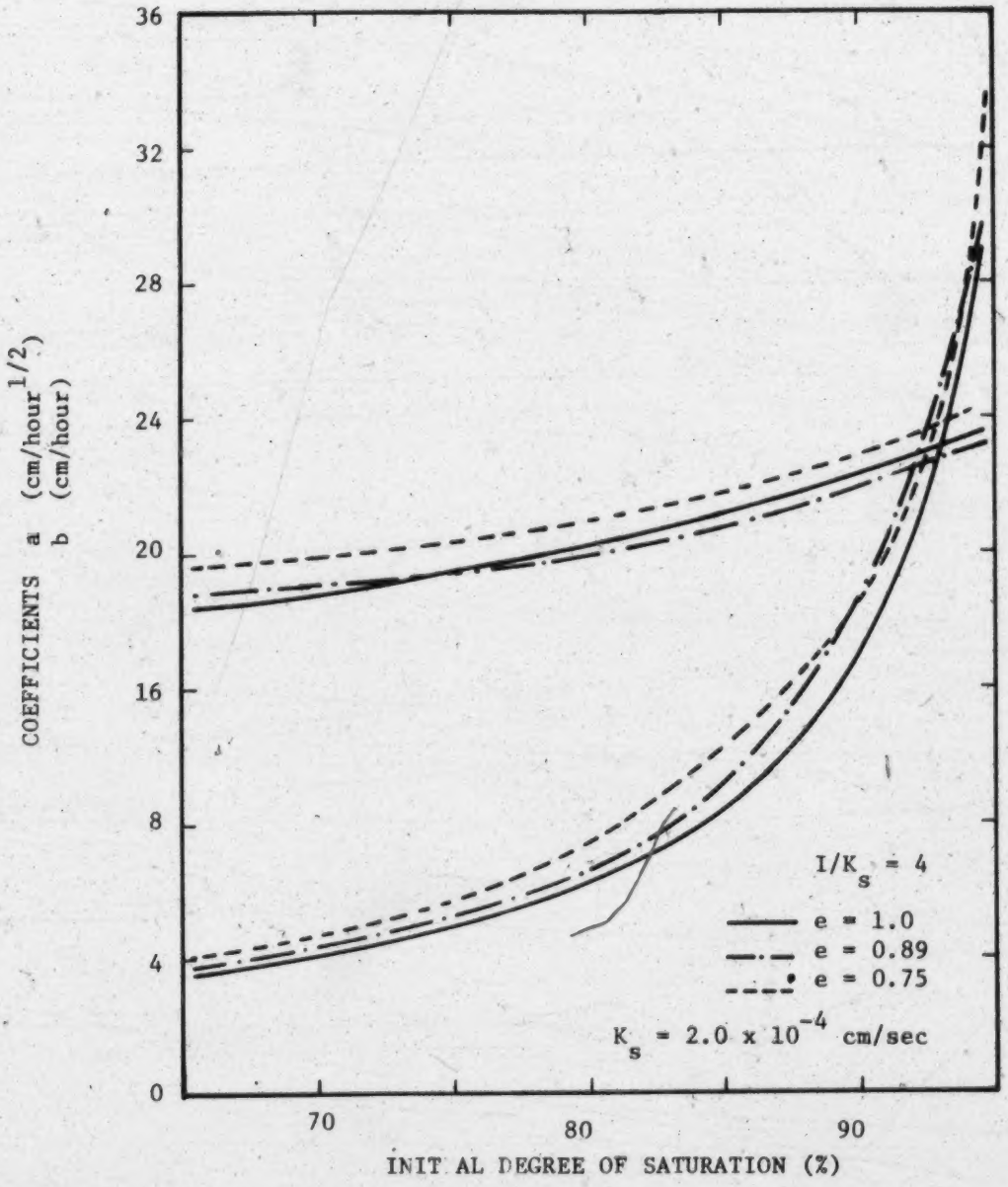

FIGURE 4.30 ANALYSIS OF SENSITIVITY OF VOID RATIO AND DEGREE OF SATURATION ON THE COEFFICIENTS a AND b

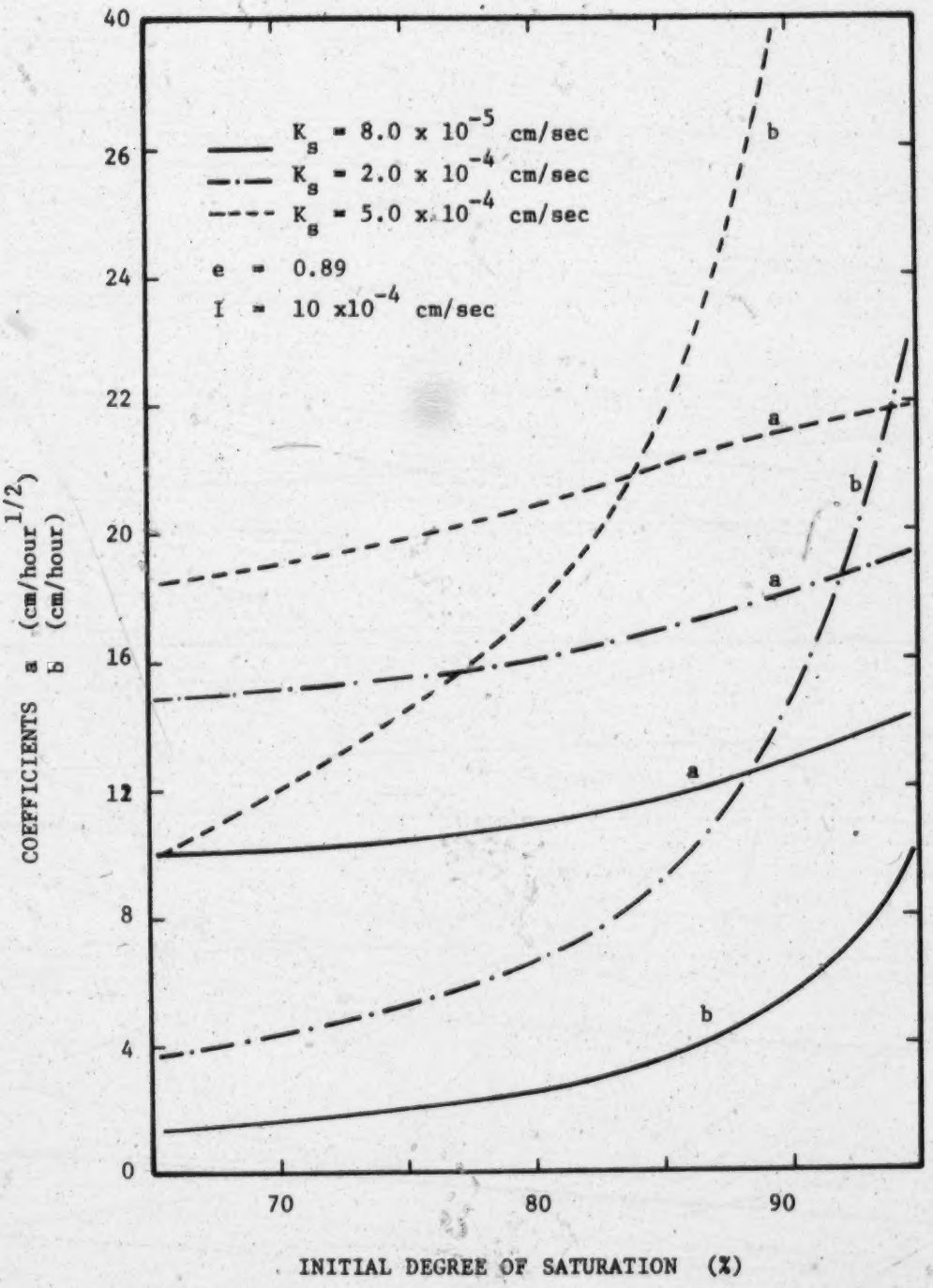

FIGURE 4.31 ANALYSIS OF SENSITIVITY OF HYDRAULIC CONDUCTIVITY AND DEGREE OF SATURATION ON THE COEFFICIENTS a AND b (FOR A PARTICULAR RAINFALL INTENSITY)

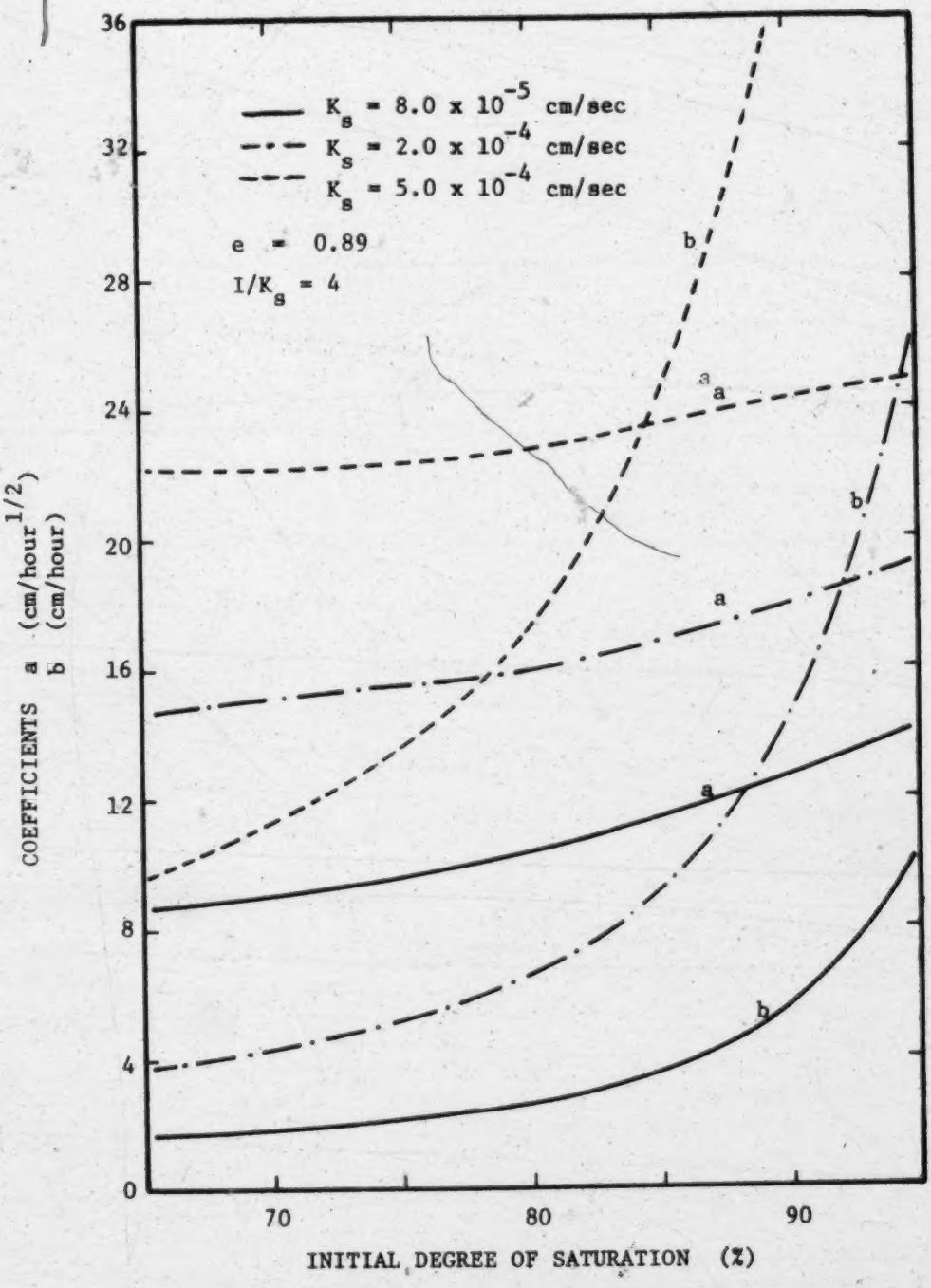

FIGURE 4.32 ANALYSIS OF SENSITIVITY OF HYDRAULIC CONDUCTIVITY AND DEGREE OF SATURATION ON THE COEFFICIENTS a AND b (FOR A PARTICULAR VALUE OF THE I/K_s RATIO)

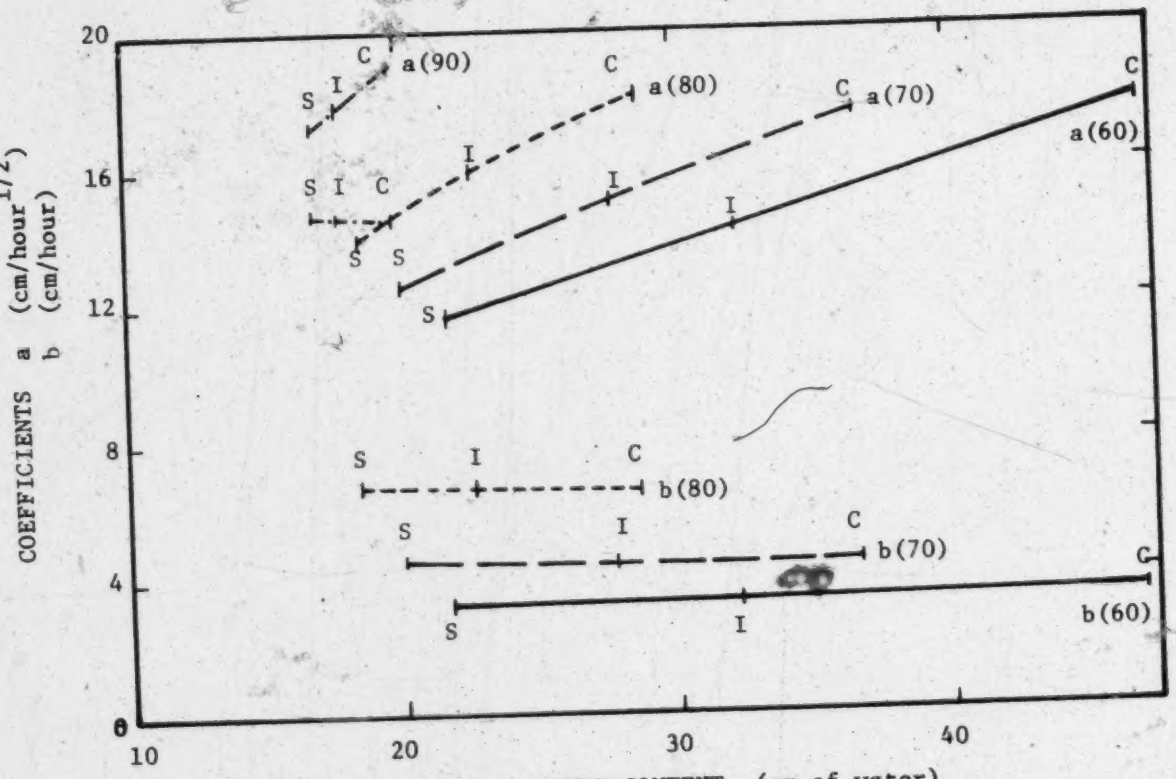

(60) Number in parenthesis refers to initial degree of saturation
S Assumed sandy soil
C Assumed clayey soil
I Intermediate soil

FIGURE 4.33 ANALYSIS OF SENSITIVITY OF CAPILLARY SUCTION AND DEGREE OF SATURATION ON THE COEFFICIENTS a AND b

CHAPTER V

DETERMINATION OF THE UNSATURATED FLOW PROPERTIES OF SOILS

5.1 Introduction

Many techniques are now available to determine the unsaturated flow properties of a soil, necessary to the solution of any problem of flow of water through unsaturated soils.

As noted in the previous chapters, the required parameters are the hydraulic conductivity, the capillary suction and the diffusivity, all functions of the moisture content.

Due to great numbers of reports that have been published on the techniques, they will not be discussed. Instead, we shall present a review of the reliability of these techniques with respect to macro-structural effects of the residual soils related to the flow of water.

References shall be provided on the pertinent techniques for field and laboratory determination of the relevant parameters.

5.2 Capillary Suction

The capillary suction is known to vary considerably with moisture content as noted in Chapter III. At saturation the suction is zero and as the moisture content decreases, the suction increases (numerically) at a rate that depends on the type of soil. For very fine soils (clayey soils) the increase in suction is very pronounced for even a small de-

crease in the degree of saturation of the soil, while for coarse soils (sandy soils) the increase in suction is characterized by a small rate of change for a large reduction of moisture content. However, as the soil becomes dryer, all types of materials will be subjected to large suctions. Many techniques are available for the determination of soil suction, each one related to a particular range of suctions, as shown in Figure 5.1 (Richards, 1974). The values of the suction we are concerned with are relatively small when compared to those corresponding to very low moisture contents, since we are particularly interested in values of degree of saturation over 60%.

Techniques have been discussed for field and laboratory determinations (Aitchison and Richards, 1965). Methods such as suction plate, pressure membrane, vacuum desiccator, centrifuge, are only applied for laboratory determinations. The porous blocks such as the gypsum block and the psychrometer techniques have been successfully applied to both laboratory and field determinations (Richards, 1974; Aitchison and Richards, 1965).

Adequate summaries of the techniques as well as specific references on the methods have been presented by Richards (1968, 1974) and Aitchison et al (1965).

5.3 Hydraulic Conductivity and Diffusivity

Techniques that permit the determination of the hydraulic conductivity are well known. Some of the methods also allow determination

of the diffusivity. We must note, however, that the diffusivity is not an independent parameter and once the hydraulic conductivity and the suction are known, the diffusivity is found by use of Equation 3.

An adequate summary of most of the available techniques has been given by Klute (1972).

A distinction must be made between the steady-state and the unsteady-state methods. The first methods are based on infiltration through either long columns (Childs and Collis-George, 1950; Youngs, 1964; Watson, 1967) or through short columns (Laliberte and Corey, 1967; Elrich and Bowman, 1964). The volumetric flux and hydraulic gradients are measured and the hydraulic conductivity calculated.

The unsteady-state methods make use of the time dependence of the outflow of water from a soil sample. They may be grouped into the outflow-inflow methods and the instantaneous profile methods, according to Tables 5.1, 5.2 and 5.3.

5.4 Comments on Reliability

The unsaturated flow properties of the soils are very dependent on the type of soil as sillustrated in Figures 4.1, 4.2 and 4.3, where the influence of both pore and grain size distribution are evident. Therefore, the presence of cracks and other relict structures in the residual soils affect considerably those parameters associated with a certain moisture content, and the flow of water is greatly influenced by the presence of these discontinuities.

Laboratory studies, due to the small size of the samples would not represent well the behaviour of soil in the field. Moreover, sampling techniques are associated with disturbance.

Therefore, field tests should provide better results in accordance with the characteristics of the natural materials.

However, with field tests it would be impractical to determine the properties of the materials as functions of the moisture content due to the impossibility of its control in the field, coupled with its variability.

Thus, although in favour of field tests for these determinations, both field and laboratory tests would be required for purposes of comparison, prediction of the behaviour and establishment of the curves $h_c(\theta)$, $K(\theta)$ and $D(\theta)$.

Method	Variations	References
Outflow-Inflow Methods	Short Column - Small Pressure Increment Method	Gardner (1956), Miller and Elrick (1958), Rijtema (1959) Peck (1966), Kunze and Kirkham (1962)
	Short Column - Large Pressure Increment Method	Gardner (1962) Doering (1965)
	Boltzman Transform Methods	Bruce and Klute (1956) Whisler et al (1968) Selim et al (1970)
	Vertical Infiltration Methods	Youngs (1974)
	Moment Methods	Zaslavsly and Ravina (1965) Youngs (1974), Bouma et al (1971)
Instantaneous Profile Methods	Table 5.2	

TABLE 5.1 METHODS FOR THE MEASUREMENT OF THE HYDRAULIC CONDUCTIVITY AND DIFFUSIVITY

Reference	Flow System	Water Content $\theta(z, t)$ from:	Pressure Head $h(z, t)$ from:	Known Flux from
Richards, S. J. and Weeks (46)	Drainage of a horizontal column of loam soil	Inferred from drainage $\theta(h)$ function	Tensiometers (mercury-water)	(1) One end of column closed (2) Measured drainage rate
Watson (56)	Drainage of a vertical column of initially saturated sand	Gamma attenuation	Tensiometers (Pressure transducers)	Top of column closed
Rogers and Klute (48)	Drainage and wetting of a vertical column of sand	Gamma attenuation	Tensiometers (Pressure transducers)	(1) Top of column closed (2) Measured drainage or inflow rate
Vachaud (53)	Horizontal infiltration into uniform column	Gamma attenuation	Inferred from $h(\theta)$ function for wetting	Measured infiltration rate
Weeks and Richards, S. J. (58)	Drainage of a horizontal soil column, both disturbed and undisturbed	Inferred from drainage $\theta(h)$ function	Tensiometers (mercury-water)	(1) Measured outflow rate (2) One end of column closed
Wind (60)	Evaporation of water from vertical columns of soil, undisturbed	Inferred from $\theta(h)$	(1) Tensiometers (2) Nylon resistance elements	(1) Measured evaporation rate (2) One end of column closed
Flocker et al. (15)	Evaporation of water from vertical columns. Disturbed structure	Gamma attenuation	Tensiometers (mercury-water)	(1) Measured evaporation rate (2) One end of column closed
Cassel et al. (7)	Redistribution of water in horizontal column. Diffusivity data only	Gamma attenuation	—	Closed ends of column
Vachaud and Thony (54)	Infiltration into air dry soil; drainage and redistribution	Gamma attenuation	Tensiometers (Pressure transducers)	(1) Position of zero hydraulic gradient (2) One end of column closed

TABLE 5.2 SUMMARY OF INSTANTANEOUS PROFILE METHODS FOR HYDRAULIC CONDUCTIVITY: LABORATORY MEASUREMENTS
(After Klute, 1972)

Reference	Flow System	Water Content $\theta(z, t)$ from:	Pressure Head $h(z, t)$ from:	Known Flux from:
Richards et al. (45)	Drainage and evaporation from a deeply wetted sandy loam	Gravimetric sampling	Tensiometers (mercury-water)	Depth at which hydraulic gradient was zero
Ogata and Richards (38)	Drainage of a deeply wetted sandy loam soil. Considered profile in three layers	Gravimetric sampling	Tensiometers (mercury-water)	Covered soil surface
Rose et al. (49)	Evaporation and drainage of a nonuniform soil	Neutron method	(1) Drainage $h(\theta)$ function (2) Direct measurement in wet soil	Estimated evaporation rate
Nielsen et al. (37)	Drainage of a deeply wetted nonuniform soil profile	(1) Neutron method (2) Drainage $\theta(h)$ function	Tensiometry	Covered surface
Renger et al. (41)	Evaporation and drainage from a nonuniform soil profile	Gamma attenuation 2-probe	Tensiometry	Depth at which hydraulic gradient was zero
van Bavel et al. (55)	Drainage of a wetted soil profile	Neutron method	Tensiometry	Covered surface

TABLE 5.3 SUMMARY OF INSTANTANEOUS PROFILE METHODS FOR HYDRAULIC CONDUCTIVITY: FIELD MEASUREMENTS
(After Klute, 1972)

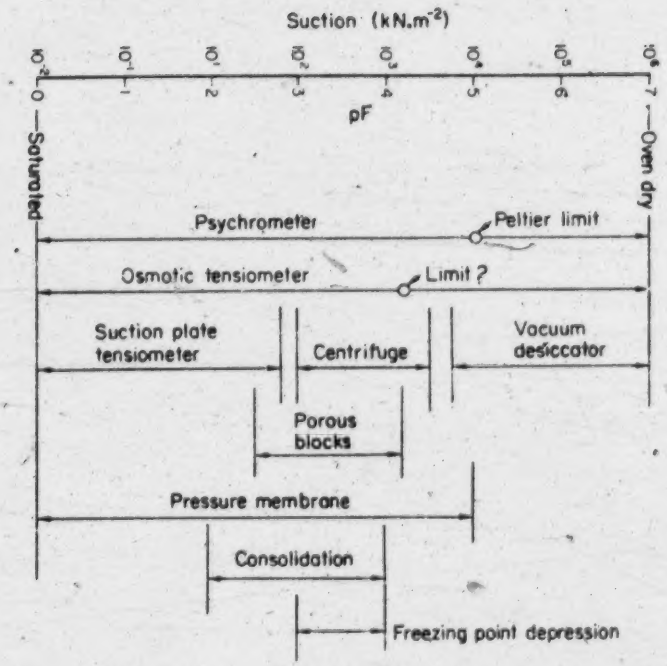

FIGURE 5.1 APPROXIMATE RANGE OF TECHNIQUES FOR MEASURING SUCTION (After Richards, 1974)

CHAPTER VI

MECHANISM OF LANDSLIDES

6.1 Introduction

This chapter presents an explanation of the phenomena related to landslides in areas where heavy rainfall occurs. Particular attention is paid to the subtropical areas of Rio de Janeiro and Serra do Mar in Brazil where slopes of residual soils exist.

Many studies have been carried out on landslides occurring in areas of high rainfall. All have noticed the great number of landslides which occur in these areas. Also, the high frequency of landslides has been noted to be associated with periods of rainfall of exceptionally high intensity and duration.

In Brazil, as reported by Deere and Patton (1971), we note the studies of Freise (1935, 1938) concerning observations in the coastal mountains of the country, who concluded that such moist tropical regions had cycles of recurrent avalanching that produce periodic deforestation.

Wentworth (1943) conducted studies on the island of Oahu, Hawaii and found that the mantle of weathered rock assumes slopes at the limit of stability for normal conditions and that most of the sliding was associated with periods of exceptional high rainfall, from 70 to 130 mm per hour to as much as 250 mm per hour (Deere and Patton, 1971).

Studies carried out by Vargas (1957, 1967a, 1967b) discussed the action of the water from the rains with the consequent saturation of the soil and development of pore water pressure either by the percolating groundwater or by shear deformations. However, tests on similar residual clays from the landslides he analysed, showed that the pore pressures due to shear may be rather small.

Barata (1969), analysing the causes of landslides in Rio de Janeiro, states that the main cause is the water action, by erosion, infiltration, increase of weight and pore pressure. Costa Nunes (1971) states that water leads to instability of slopes due to development of pore pressures, reduction of the shear strength parameters, principally the cohesion of the clayey-silty soils, increase of weight, and surface and subsurface erosion (piping).

Jones (1973) also called attention to the effects of water from rainfall, weight of the slope-forming material and gravity stresses and stated that the action of the rain would give rise to: raising the piezometric surface in the slope-forming material, seepage toward the slope, removal of soluble binders in joints, subsurface erosion, rearrangement of grains, chemical weathering and displacement of air in voids and joints. As a consequence of the combination of these factors, among others, pore water pressure would be increased and surface tension eliminated.

Vargas (1971) prescribed remedial measures for the slopes and recommended surface drainage to increase surface runoff, diminishing to

a minimum infiltration of water into the soil and also prevention of surface erosion.

All these studies contributed to a better understanding of the subject but it was felt that there was still a lack of detail concerning the phenomena involved.

Skempton and Hutchinson (1969) in their State of the Art report on stability of natural slopes were not able to draw any general conclusion regarding this class of problem. However, it appears that there is no doubt about influences of infiltration into the soil.

Lumb (1962) studying landslides in Hong Kong gives more insight into the problem and states that the stability of slopes is governed by the infiltration capacity of the soil and that the influence of a particular rainstorm depends on the intensity-duration curve of continuous rainfall during the storm and also on the amount of rainfall that has occurred previous to the storm.

Peck (1967) analysed some landslides produced by rainfall and found that "in connection with most slides, the variation in daily rainfall is too erratic to be correlated satisfactorily with the movements". He also concludes that "the rainfall that accumulates over a period of several days is more likely to be significant in affecting the movements of the mass. The larger the sliding mass and the lower its average permeability, the longer is the period of rainfall that is most likely to correlate well with the movement".

6.2 Mechanism of Landslides

As noted in Chapter II, the residual soil in its natural and stable condition is always unsaturated having a degree of saturation between 60 and 70% and sometimes even less, before the beginning of the rainy season. We have also seen that this soil has a relatively large void ratio, commonly with values as much as 1.0.

This soil of sandy-silty, silty-sandy or clayey-sandy nature normally contains a small percentage of clay, generally less than 30%. The clay fraction of the soil is responsible for the soil cohesion, acting as a cement linking the coarser grains of the soil, silt and sand.

The suction developed in the soil pore water increases the apparent cohesion of the soil which is greater for lower values of the moisture content. As the moisture content increases, the suction is decreased with a consequent reduction of apparent cohesion. The angle of internal friction may also reduce, although to a lesser degree due to some dilatancy effect. Therefore, soil particles supported by clay minerals may undergo collapse when saturated.

We have seen in Chapters III and IV that water from rainfall will infiltrate into the soil increasing its degree of saturation, characterized by the advance of a wetting front with time, provided there is water available at the surface.

To study infiltration of water into a soil slope, analyses

should be carried out two-dimensionally. However, for rainfalls of large intensity the depth of the wetting front could be considered relatively uniform throughout all the surfaces of the slope without much error (Figure 6.1)

Therefore, water will infiltrate into the slope increasing the moisture content of the slope-forming material and reducing the strength parameters for a particular period of time after rainfall has started. Of course, there will also be an increase of the weight of the slope-forming material but what appears to be more relevant is that seepage is not taking place in the common sense as it occurs for a saturated soil. However, after the wetting front reaches a certain depth, the upper part of the moisture profile will be saturated and the water subjected to a hydraulic gradient i parallel to the slope surface equal to:

$$i = \sin \alpha \tag{6.1}$$

where α is the slope angle and seepage would then take place generating pore pressures accordingly. The hydraulic gradient, however, due to gravitational and capillary potential will be much greater and therefore movement of moisture as already described will be dominant. As we shall also see in Chapter VII, slides may occur without the influence of the pore pressures generated by the percolating water.

If the strength of the soil s along a potential failure surface is expressed in terms of total stresses as:

$$s = c + \sigma \tan \phi \tag{6.2}$$

where c and ϕ are the shear strength parameters in terms of total stresses and σ denotes the total stress normal to the surface, we see that the shear strength will be reduced due to the reduction of shear strength parameters.

Thus, after infiltration, reduction of c and ϕ can lead to failure of the slope for a particular depth of the wetting front. This failure could take place without development of any positive water pressure and the shear strength parameters would be those corresponding to the saturated condition of the soil.

It is worthy of mention that failure would take place along the surface of the wetting front which represents an almost sharp boundary between the saturated upper part of the slope which slides and the lower portion still with the initial moisture content (Figure 6.2).

As we shall see in the subsequent section, the depth of wetting front at which failure takes place can be predicted for a factor of safety equal to 1 by making use of the shear strength parameters at saturation. This depth will be referred to as the critical depth h_{crit}.

Thus, knowing this depth h_{crit}, it is possible to predict the stability of a slope under a rainfall of known intensity and duration provided we know the equation of advance of the wetting front for the soil of concern. If the time for the critical depth to be reached by the wetting front is larger than the duration of rainfall,

the landslide would not take place.

We have to bear in mind, however, that the rate of advance of the wetting front depends on the initial degree of saturation, being larger for larger initial degrees of saturation, and if a rainfall does not lead to a landslide, after the rainfall there would be a redistribution of moisture content within the soil, thus increasing the degree of saturation prior to the next rainfall. The advance of the wetting front with time for a rainfall with the same intensity would be modified.

It is possible that during failure of the slope, pore pressures would build up due to the susceptibility of the residual soils to collapse with saturation. This may account for the extreme mobility of the sliding mass that is often observed.

It is also possible that a third factor related to infiltration, would play an important role in causing a landslide.

Theoretical and experimental studies made by Adrian (1970) have shown that infiltration into an unsaturated soil overlying an impermeable barrier displaces the air from the soil interstices. Unable to escape downward, the air may escape upward in bubbles travelling through large pores, or if the pores are small and the capillary forces are large, the air is compressed between the wetting front and the barrier. This reduces the infiltration rate and may result in an almost stable wetting front. Under certain calculable conditions, the air pressure build-up is sufficient to cause sudden localized horizontal

rupturing of the soil at the wetting front and to lift it along with the infiltrating water, forming a cavity. The air-filled cavity breaks the flow passages and percolation ceases through pores terminating in the cavity where pore water pressures will build up.

Let us examine the above features analytically. Consider first a column of soil of porosity n and length ℓ which is the distance from the soil surface to an impermeable barrier and let us assume that the air in the pores of the unsaturated soil is under atmospheric pressure (Figure 6.3). We will also assume that air will be compressed downward and that the soil down to a depth h of the wetting front is saturated. Thus, the total absolute downward pressure at the wetting front is given by:

$$p = p_o + \gamma_w h + \gamma_w h_c \tag{6.3}$$

where p_o denotes the atmospheric pressure

$\gamma_w h$ denotes the hydraulic pressure

$\gamma_w h_c$ denotes the capillary pressure at the interface, h_c being the capillary head or suction which is pulling the water downward

For the depth h of the wetting front, the pressure in the entrapped air p_1 can be calculated making use of Boyle's law for a perfect gas. Thus:

$$p_o V_o = p_1 V_1 \tag{6.4}$$

which yields:

$$p_1 = p_o \frac{\ell}{\ell - h} \tag{6.5}$$

If the pressure p_1 opposes the downward pressure p, then the wetting front reaches a stable condition at a depth h_o, obtained by equating Equations 6.3 and 6.5.

$$p_o \frac{\ell}{\ell - h_o} = p_o + \gamma_w h_o + \gamma_w h_c \tag{6.6}$$

Solving Equation 6.6 for h_o, we obtain:

$$h_o = \frac{1}{2}\left\{(\ell - \frac{p_o}{\gamma_w} - h_c) + \left[(\ell - \frac{p_o}{\gamma_w} - h_c)^2 + 4h_c\ell\right]^{1/2}\right\} \tag{6.7}$$

We can similarly obtain a depth h_s at which horizontal rupturing of the soil occurs. Assuming the wetting front to be at this depth h_s, the pressure exerted by the saturated soil above the wetting front is:

$$p_{soil} = \gamma_s h_s (1 - n) + \gamma_w h_s n \tag{6.8}$$

where γ_s is the specific weight of the soil particles.

The pressure in the entrapped air, according to Boyles' Law is as before (Equation 6.5):

$$p_1 = p_o \frac{\ell}{\ell - h_s} \tag{6.9}$$

For rupturing to occur, the pressure in the entrapped air must oppose the pressure exerted by the saturated soil above the wetting front plus the atmospheric pressure. Thus we have:

$$p_o \frac{\ell}{\ell - h_s} = \gamma_s h_s (1 - n) + \gamma_w h_s n + p_o \qquad (6.10)$$

which may be solved for h_s to give:

$$h_s = \ell - \frac{\frac{p_o}{\gamma_w}}{G(1 - n) + n} \qquad (6.11)$$

where the density of the solid particles is:

$$G = \frac{\gamma_s}{\gamma_w} \qquad (6.12)$$

Now, comparing h_o and h_s, if $h_o < h_s$ the wetting front would reach a stable condition at that depth h_o and, therefore, at an earlier stage than that required for the depth h_s to be reached. If, however, $h_s < h_o$, the depth h_s corresponding to the horizontal rupturing of the soil would be reached before the wetting front could reach the stable condition at depth h_o and thus instability would occur.

Figure 6.4 illustrates the values of the stable depth h_o plotted from Equation 6.6 as a function of the capillary head (suction) h_c and the depth ℓ to the barrier. Also plotted in this graph is a straight line $h_o = h_s$. If a point falls to the right of this straight line, then $h_s < h_o$ and a break or cavity formation is expected to occur thus contributing to landslide.

Experimental studies carried out by Adrian (1970) using columns of soil of different lengths ranging from 10 cm to 100 cm have

shown this phenomenon. We do not know yet whether the same thing would occur in the field, but it appears that for very intense rainfalls over an almost homogeneous soil without cracks, we should expect this factor to play an important role.

It is also important to note that these mechanisms do not imply that any intense rainfall will lead to instability. Previous rainfalls that have fallen in the area will also be important.

In other words, for a particular rainfall it takes a certain period of time for the wetting front to advance to a critical depth. As the initial moisture content of the soil in the beginning of the rainy season is rather low, then the critical depth would be reached only for a period of time larger than the duration of the rainfall. Thus, landslides would not occur. After this, however, redistribution of moisture content occurs, increasing the moisture content of the soil with respect to that prior to rainfall.

A second rainfall of the same intensity would produce a faster advance of the wetting front since the initial moisture content now would be larger.

Therefore, there is a sort of progressive increase of the moisture content of the soil through redistribution of moisture content after rainfall and during the final period of the rainy season, the moisture content of the soil would be large enough to lead to a fast advance of the wetting front. Consequently, a rainstorm of given intensity and duration will have more serious effects, the later in the

rainy season that it occurs, in agreement with the observation of Barata (1969), Vargas (1971) and CNP_q (1967) with respect to sliding taking place mostly at the end of the rainy season.

Rainfall to saturate the soil must have an intensity at least equal to the saturated hydraulic conductivity (permeability) of the soil. As we have seen in Chapter III, this is not restricted since these soils exhibit an average permeability of about 10^{-4} cm/sec or 3.6 mm/hour and rainfalls of intensity over 50 mm/hour have been observed.

Vargas (1971) mentions that rotational or planar slides mostly occur at the end of the rainy season during or after rainfalls of more than about 100 mm/day. This value is approximately the permeability of the residual soils.

Landslides thus produced in homogeneous soils due to rainfall would be planar ones by virtue of the advance of the wetting front as a surface parallel to the surface of the ground. However, residual soils are not exactly homogeneous and deviations from planar slides may obviously occur even if water does not infiltrate through cracks present in the soil.

Vargas (1971) has described the existence of planar slides that occurred in Santos and Barata (1969) describing landslides in Rio de Janeiro called attention to planar slides that occurred in natural slopes while rotational slides would occur in cut slopes.

6.3 Types of Slide

Many types of slide have been observed at Serra do Mar, Santos and Rio de Janeiro, all associated with the heterogeneity of the soil and with the intensity of rainfall. A classification of them should take into account both factors, and Table 6.1 illustrates an attempt to classify the slides. It is understood that slides being classified are those generated by rainfalls, although other types may occur by different causes such as creep, or failure of cut slopes.

In Table 6.1, reference is made to two types of slopes: homogeneous slopes which are those where only soil is present, although the soil is generally not homogeneous, and heterogeneous slopes, those where boulders also exist lying at the soil surface of the slopes.

6.3.1 Slides

Vargas (1971) described the rotational or planar slides that would occur for rainfall intensities of more than 100 mm/day. As noted before, such intensity corresponds approximately to the permeability of the soil which, as we have seen in Chapters III and IV, is enough to saturate the soil.

Slides occurring for such rainfalls are the most common and occur almost always at the end of the rainy season. Two types can be observed: rotational and planar slides.

Barata (1969) says that rotational slides occur only in the hill slopes of the thick mantle of residual soil, noting that they have

been in most cases caused by human interference such as cuts for highways.

It is possible that such a failure surface is caused mainly by the heterogeneities of the soil profile leading to an irregular wetting front surface of non-uniform depth, as well as due to the influence of a cut on the toe of the slope leading to a deeper landslide.

According to Barata (1969) the planar slides are typical of the hill slopes with shallow mantle, where the slide occurs along the contact of the soil with the bedrock. What is important is that these planar slides tend to occur in slopes not affected by human interference, but only by the rainfalls.

6.3.2 Avalanches

Another type of landslide, also conditioned by rainfall intensity and described by Vargas (1971), Barata (1969) and Costa Nunes (1969) is the avalanche or rapid flow.

Vargas (1971) says that they are caused by very intense and catastrophic rainstorms of more than 50 mm/hour, resulting from a hydraulic destruction of the residual soil mantle by erosional process. They start as a normal slide as explained, but due to the high intensity of rainfall which would cause a fast advance of the wetting front and saturation, collapse of the soil structure would occur and consequently they would slide like a flow. Erosion always takes place at the same time due to the high intensity of the rainfall that causes the runoff.

Avalanches occur in slopes of medium to steep inclination which are fairly long, allowing the development of the phenomenum without any obstacles (Barata, 1969).

6.3.3 Other Forms of Slides

When boulders are present at the surface of the soil slope, normally intense rainfalls would lead to erosional process beneath them and rolling would occur. For exceptionally intense rainfalls, the process is also associated with a deeper slide and in this case complex slides characterized by the association of rolling, slides and mud flows occur.

6.4 Analysis of Stability

Instability in a slope of homogeneous soil due to rainfall occurs along a planar surface if the slope is fairly long. If the slope is not long enough, the failure surface would deviate from the planar one but even here the controlling factor would be the depth of the wetting front in the slope-forming material.

Therefore, basically our analysis of stability of slopes is concerned with the depths of the advancing wetting front with time, for a particular rainfall intensity and a particular initial degree of saturation.

Such analyses may be performed either on homogeneous or heterogeneous slopes. For the former, analyses could be made by considering

vertical infiltration under the presence of a rainfall of reasonably large intensity and a knowledge of the parameters of unsaturated flow: hydraulic conductivity, suction and diffusivity, all functions of the moisture content of the soil would be required.

For the latter, where heterogeneous soils are assumed to exist, a vertical infiltration analysis is no longer satisfactory and a two-dimensional analysis should be performed. In this case, knowledge of the unsaturated flow characteristics for all the materials constituting the slope would be required. Also, here only numerical solutions by means of finite difference or finite element methods can be applied since there is no analytical procedure available at this moment to solve the infiltration equations for this complex case.

We shall concentrate our attention here on the analysis of slopes in homogeneous soil and give guide lines to analyse the more complex cases.

In the case of a planar slide occurring in an infinite slope, the factor of safety F can be calculated by Equation 6.13 referred to in Figure 6.5:

$$F = \frac{c'_{sat} + (\gamma_{sat} h \cos \beta - u) \tan \phi'_{sat}}{\gamma_{sat} h \sin \beta} \qquad (6.13)$$

where c'_{sat} and ϕ'_{sat} are the shear strength parameters in terms of effective stresses and are determined by tests on saturated samples; γ_{sat} is the saturated specific weight of the soil; β is the angle of the slope with respect to the horizontal and u is the pore water

pressure which will be considered zero in our analysis since the slide takes place with elimination of suction and before pore pressures build up. As we have seen earlier in this chapter, there is also the possibility of pore pressure build up which would occur after the slide commenced. This would be responsible for a further decrease of the factor of safety to a value less than one leading to slides of great mobility.

From Equation 6.13 we can determine the critical depth h_{crit} that corresponds to a factor of safety equal to one, as given by:

$$h_{crit} = \frac{c'_{sat}}{\gamma_{sat}(1 - \frac{\tan \phi'}{\tan \beta}) \sin \beta} \qquad (6.14)$$

We can now compare this depth with those of the wetting front with time for several rainfall intensities and for a particular value of the initial degree of saturation as shown in Figure 6.6.

On a basis of Figure 6.6, we can see that for rainfalls of relatively small intensity (region 1) the depth h_{crit} would be reached only for very large periods of time, while for more intense rainfalls (region 2) the depth h_{crit} would be reached much easier.

In both cases, for a particular rainfall of intensity I, the time t_{crit} for the depth h_{crit} to be reached should be compared to the duration of this rainfall (t_{dur}).

If $t_{dur} < t_{crit}$ that is if the duration of the rainfall is smaller than the time required for the wetting front to reach the

critical depth h_{crit} corresponding to a factor of safety equal to 1, instability would not occur since rainfall would stop before leading to a slide. Thus, there would be a redistribution of the moisture content as seen in Chapter III, only responsible for an increase in the initial degree of saturation. After this, another rainfall would lead to a faster advance of the wetting front due to the higher initial degree of saturation.

If $t_{dur} > t_{crit}$, that is, if the duration of the rainfall is larger than the time required for the wetting front to reach the depth h_{crit} then instability would occur.

As noted in Chapter IV, the depth of the advancing wetting front with time could be expressed, for a particular soil and for particular values of rainfall intensity and initial degree of saturation, through the equation:

$$z = at^{1/2} + bt \qquad (6.15)$$

If the rainfall duration t_{dur} is known, one can determine the corresponding depth z_d and compare it with the critical depth h_{crit}. If $z_d < h_{crit}$ then h_{crit} would not be reached and the slope would be stable. If $z_d \geq h_{crit}$ then slide would occur.

The design of a cut slope could be performed in the same way, for a particular rainfall of known intensity and duration. Thus, the advance of the wetting front with time could be predicted for this rainfall and the depth h_{crit} computed from Equation 6.14. This analy-

sis would be made for periods of time t smaller than or equal to the duration of the rainfall (see Figure 6.7).

To make $t_{crit} > t_{dur}$, h_{crit} can be increased by flattening of the slope and factor of safety would be computed from Equation 6.13, for a depth of the wetting front corresponding to $t = t_{dur}$.

For finite slopes, deviations from the planar slide occur due to effects of boundaries. Analyses can take into account the curvature in the toe of the slope as done by Lumb (1962). According to Figure 6.2 the factor of safety would be:

$$F = \frac{c}{\gamma h \sin \theta} \frac{1 + \frac{h}{H}\left\{\frac{\pi}{2} + \cot \theta - 1\right\} \sin \theta}{1 + \frac{h}{H}\left\{\frac{\pi}{8} + \frac{1}{2} \cot \theta - 1\right\} \sin \theta} \qquad (6.16)$$

and the analyses mentioned above may be applied in the same way here.

Analyses can also be made by using circular slip surfaces with respect to short slopes and here the depths of wetting front would be taken as an average depth to a surface parallel to the slope.

6.5 Methods of Treatment and Stabilization of Slopes

In the previous sections we saw that infiltration of water from rainfall into the slope is the dominant factor in reducing stability of both natural and man-made slopes in residual soils in Brazil.

Many special measures, isolated or combined, have been carried out to stabilize slopes or to prevent them from sliding. Here

we present and discuss the most common ones in use.

6.5.1 Flattening of Slope

As noted in the previous section, flattening of a slope would increase the required depth for a factor of safety equal to one. Consequently, the time for the wetting front to reach this critical depth and thus produce instability would be increased and could be made larger than the duration of the rainfall. Therefore, the slope would be safe for this particular rainfall since the wetting front would never reach the critical depth and there would be only redistribution of moisture content.

It was also pointed out that moisture content of the soil increases from the beginning of the rainy season to the end of the period and for a rainfall of the same intensity at the end of the season, the rate of advance of the wetting front would be increased by virtue of the larger initial moisture content as seen in Chapter IV. Therefore, analyses should also be made by taking into account this larger initial moisture content at the end of the rainy season.

This is the most critical case and according to Costa Nunes (1969), it would be suitable only for slopes of low height and for critical situations.

6.5.2 Slope Protection

Flattening of slopes could lead to uneconomical results and sometimes there is not available space to implement such a measure. Cut

slopes have been designed in Brazil with steeper angles (Vargas, 1967a and b) but additional measures must be undertaken to provide enough safety. These special measures to improve stability are basically related to the mechanism of the slide, say, the infiltration of water into the slope. Thus, a method that appears very convenient is slope protection.

This method consists of covering the slope surface by any means such as bitumen, asphalt, grass, soil cement, gunite, etc. They reduce or eliminate infiltration of water into the slope but attention has to be paid also to protection of the entire area so as to avoid infiltration into the upper surface of the slope.

Slope protection also eliminates erosion under normal intense rainfalls. This has an important role in generating shallow slides of the mud flow type. Costa Nunes (1969) and Vargas (1971a), however, point out that for abnormally intense rainfalls this method would be ineffective in eliminating erosion and avalanches that could occur.

With slope protection, surface runoff would be increased, thus reducing still more the possibility of infiltration. For a more successful treatment, slope protection must be combined with drainage.

6.5.3 Drainage

Drainage consists of interception of both surface and sub-surface water.

6.5.3.1 Surface Drainage: Surface drainage can be accomp-

lished by two systems of gutters to intercept surface water. One system is placed horizontally, roughly parallel to the contours to intercept any water moving through cracks in the slope. The second system of gutters to conduct water downward is placed on the surface of the slope, dipping in the same direction as the slope.

Water moving down through the system of gutters would have high velocity and thus special features to dissipate the water energy should be provided in order to avoid erosion.

In the case of a cut slope with berms, the horizontal gutters can be placed on the berms, at the toe of the adjacent slopes.

6.5.3.2 Underdrainage: Depending on the topography of the region and its extension, as well as on the behaviour of the groundwater in the region, percolating through relict cracks and fissures in the soil and rock masses, it is very difficult to ensure that infiltration will be completely avoided and eliminated. Thus a special drainage system should be provided so as to drain all water that has possibly entered into the slope by any means.

Underdrainage consisting of perforated pipes or drainage galleries driven almost horizontally with a small inclination toward the slope are useful. Galleries can be constructed to function as a drain, but they are expensive and their construction is difficult. Besides, due to the very erratic characteristic of the soil mass with respect to flow of water, a suitable large number of galleries would be prohibitive.

Perforated pipes furnish a better solution to the problem of deep drainage principally in erratic soils where a great number of them can be driven into drilled holes at a lower cost. They should also be surrounded by filter materials to prevent from their clogging.

These horizontal drains have proved to be very successful in stabilizing slopes principally of colluvial materials (Terzaghi, 1960; Teixeira and Kanji, 1970; Vargas, 1971a).

6.5.4 Filling of Cracks and Erosion Cavities

Rain water may open cavities at the slope surface due to its triggering action of erosion, that could also be very detrimental with respect to stability by allowing water to infiltrate into the slope. Similar to these cavities are the cracks opened during the dry season by shrinkage of the soil. All these cracks and cavities must be filled. Cement mortar or soil cement are often used. In the case of shrinkage cracks bitumen may also be used.

6.5.5 Other Methods

Other methods have been adopted to stabilize slopes as described by Costa Nunes (1971) but they have nothing to do with the infiltration of water. They are general methods that could be applied to any slope and thus they will be only briefly cited here.

Retaining walls could be used in cases where flattening of slope would not be possible and there is a need for a steep slope. An alternative is the use of anchored sheet piles.

Strengthening of the toe of the slope would increase the stability by improving the conditions of the foundation soil. This can be done by driving piles at the toe of the slope. This procedure would also transfer the loads to deeper strata.

In the case of the presence of loose large blocks of rock at the slope surface that could not be removed, methods of retaining them by the use of special retaining structures or anchor bolts would be suitable.

Grouting has also been used to improve the characteristic of the slope-forming materials. Cement grout or clay cement grout is used successfully according to Costa Nunes (1971) but chemicals can also be used to stabilize the slope.

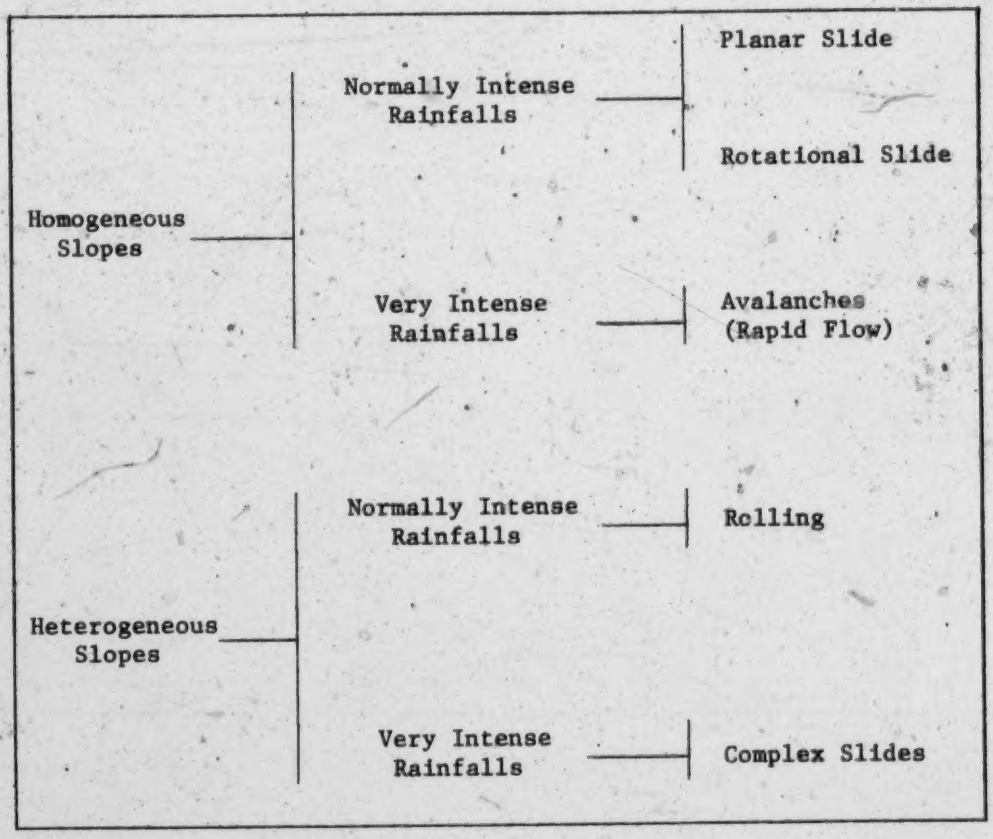

TABLE 6.1 CLASSIFICATION OF LANDSLIDES DUE TO RAINFALL

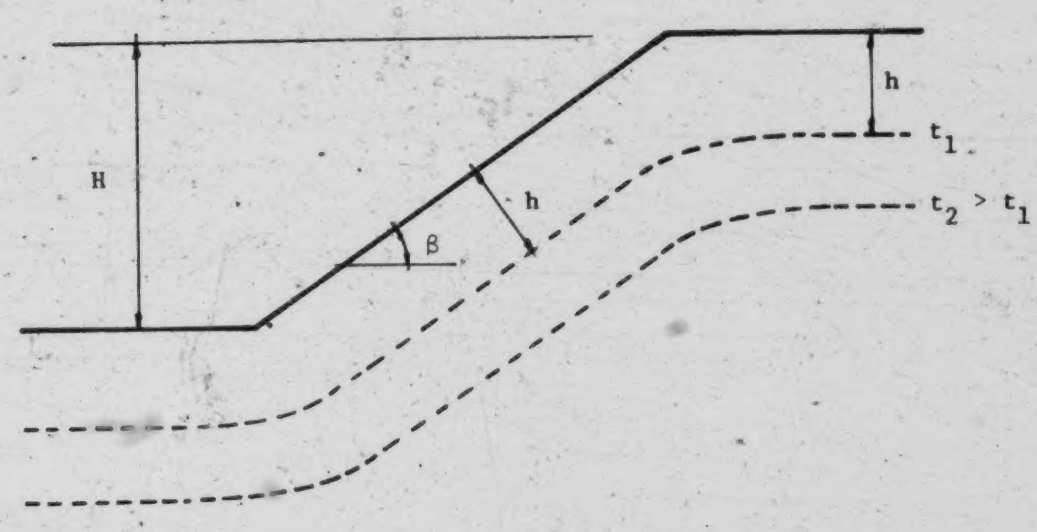

FIGURE 6.1 PATTERN OF WATER INFILTRATION INTO A SLOPE

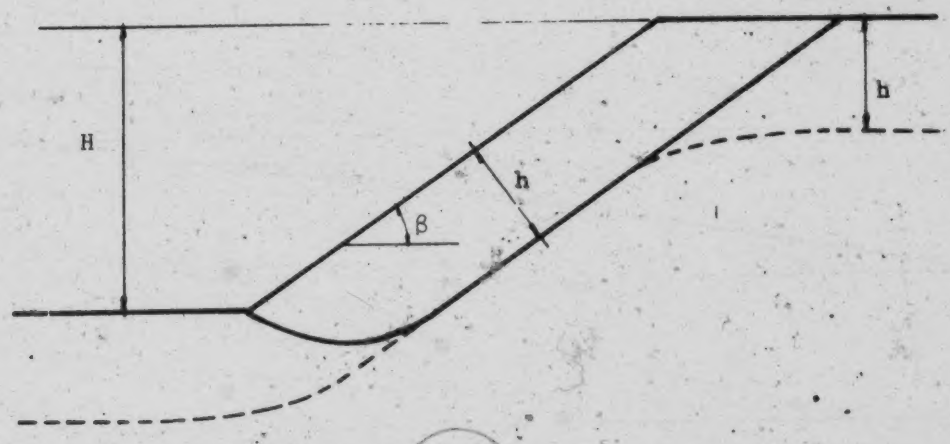

FIGURE 6.2 SLIP SURFACE ALONG THE WETTING FRONT SURFACE

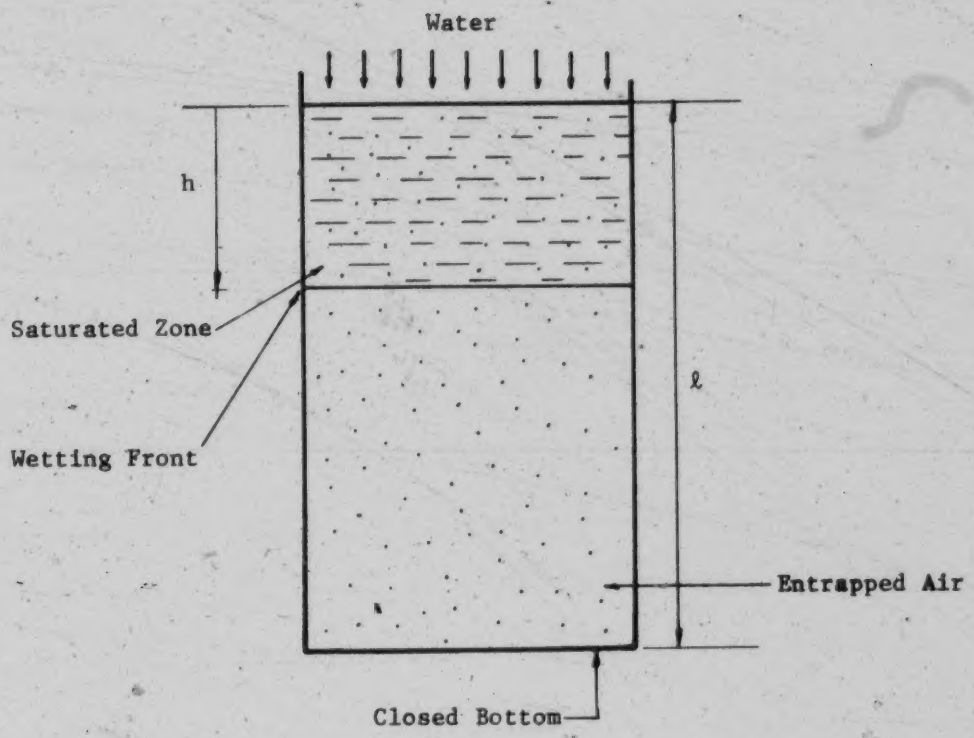

FIGURE 6.3 INFILTRATION OF WATER THROUGH A COLUMN OF SOIL

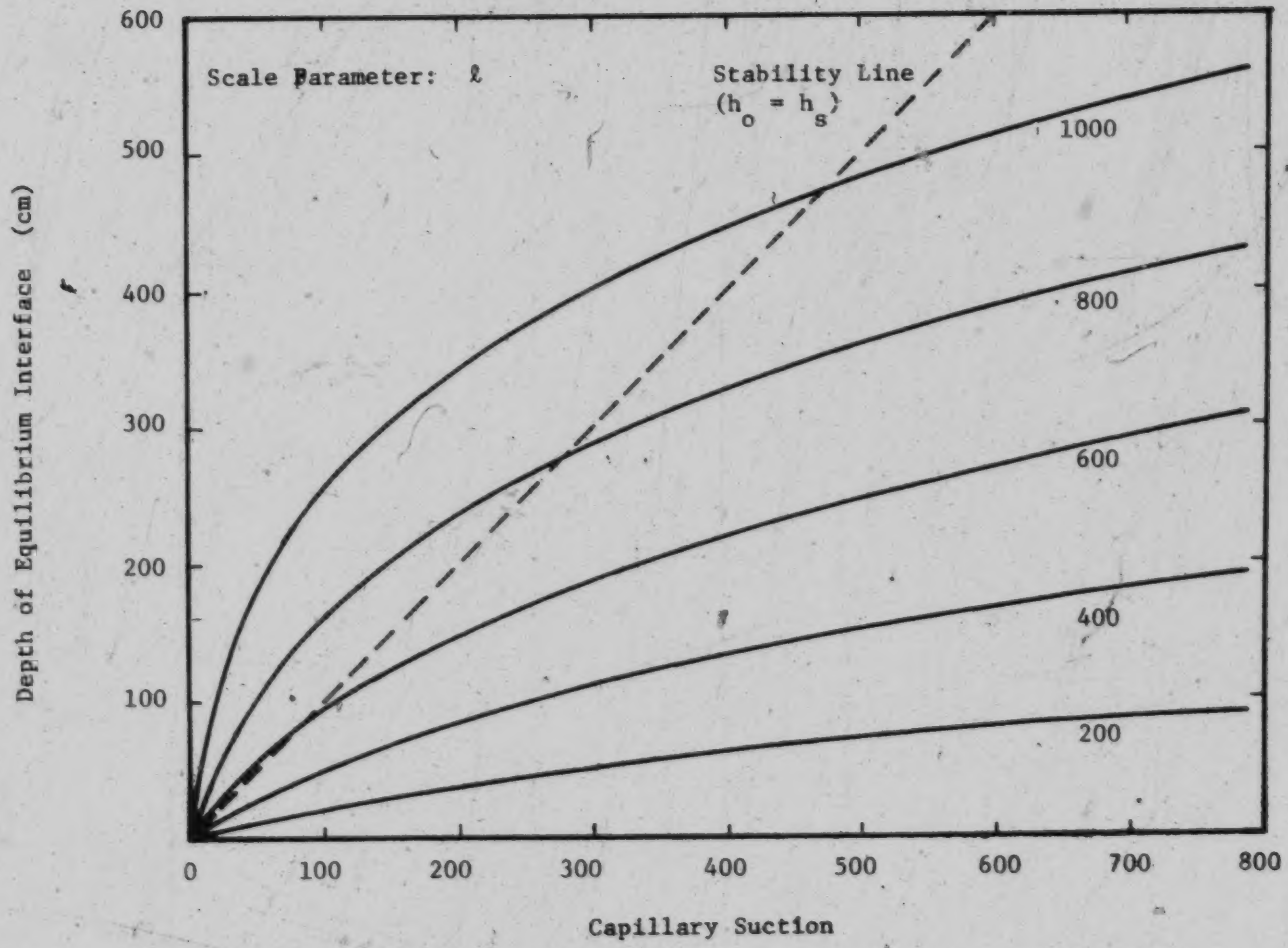

FIGURE 6.4 EQUILIBRIUM INTERFACE POSITION AND SOIL STABILITY
(After Adrian, 1970)

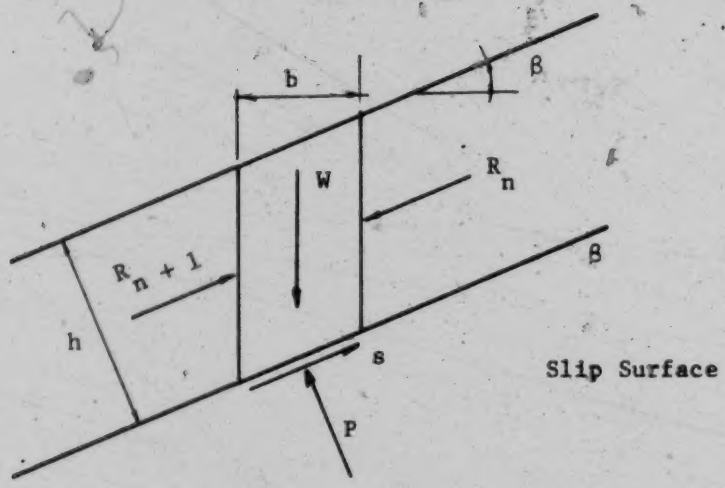

FIGURE 6.5 PLANAR SLIDE

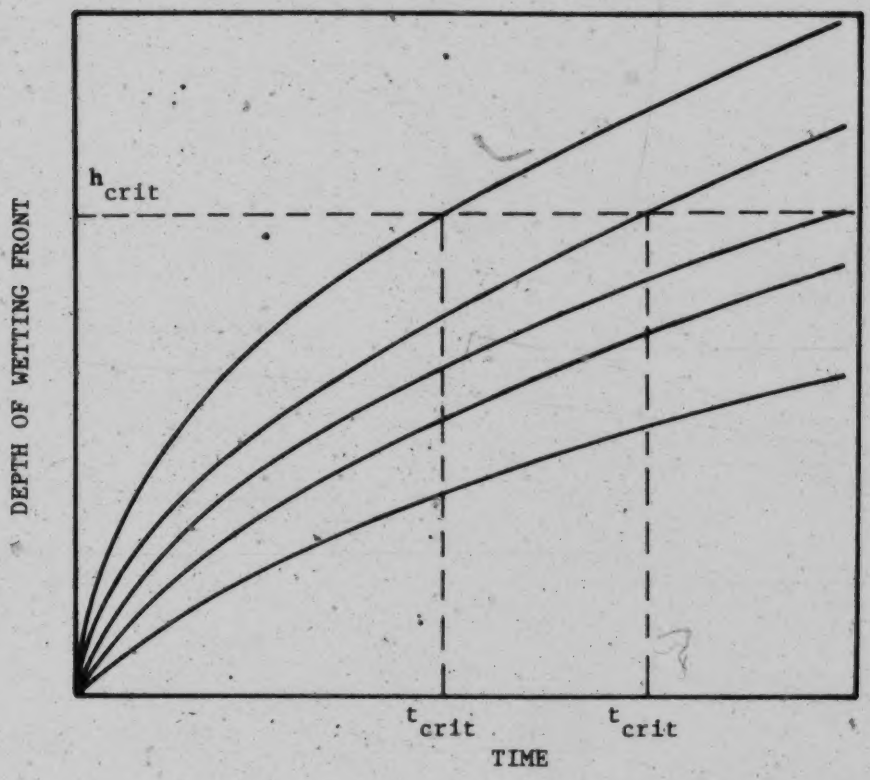

FIGURE 6.6 ANALYSIS OF OCCURRENCE OF A LANDSLIDE FOR CERTAIN RAINFALLS

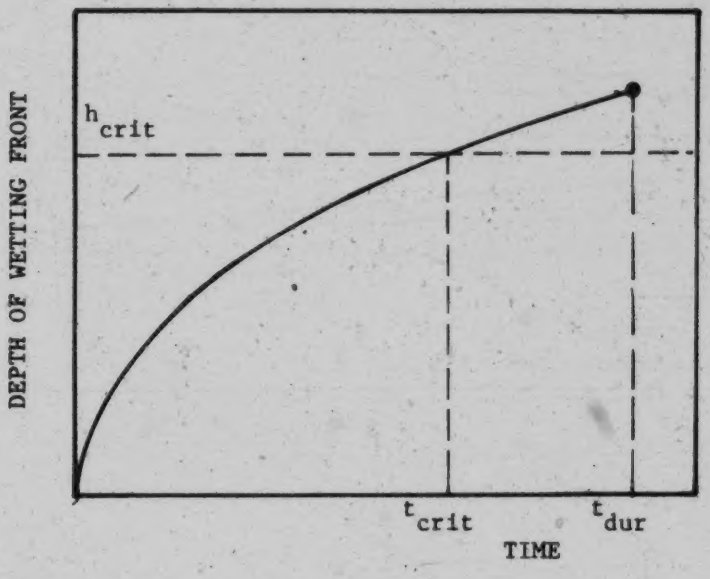

FIGURE 6.7 ANALYSIS OF OCCURRENCE OF A LANDSLIDE FOR A PARTICULAR RAINFALL

CHAPTER VII

CASE HISTORIES

7.1 Introduction

The previous chapters indicated the many parameters that must be taken into account to study the stability of slopes in residual soils and theoretical methods of analysis were also presented. However, to confidently incorporate these factors and analyses into a slope design, it is necessary to have case histories which indicate that the methods do work in practice. The case histories presented here are far from being complete with respect to the necessary data for their complete documentation but they are, nevertheless, worthy of discussion.

7.2 Estrada do Jequiá Slide

This slide took place close to Estrada do Jequiá at the Governador Island in Rio de Janeiro, as described by Geotécnica (1967).

A soil profile along the middle section of the landslide is illustrated in Figure 7.1, before the slide has occurred. The slope had an average angle of about 50° and was mainly composed of a silty-sandy residual soil, yellow and red in colour, as shown in Figure 7.1.

Figure 7.2 illustrates the topography after the landslide. The maximum height of the slope was about 37 m. The slide occupied an area of about 1200 m^2 having a width of about 40 m. A volume of 5000 m^3 slid.

Laboratory tests on these soils, down to a maximum depth of 23 m showed the following properties for the upper layer:

% of clay (< 2μ)	14 to 40
% of silt (2μ < ϕ < 0.06 mm) . .	36 to 50
% of sand (0.06 < ϕ < 2 mm) . .	24 to 45
Liquid Limit	26 to 49%
Plastic Limit	19 to 27%

Direct shear tests conducted slowly on cylindrical samples of 5" diameter and 2" height, saturated before shearing gave the following parameters in terms of effective stress:

Apparent cohesion	1.5 t/m^2
Angle of shearing resistance . . .	30°

The same type of tests conducted on samples at natural conditions gave the following parameters in terms of total stress:

Apparent cohesion	4.5 t/m^2
Angle of shearing resistance . . .	30°

As can be seen, there is an appreciable reduction of the apparent cohesion in terms of total stress upon saturation of the sample. Drained triaxial tests showed about the same reduction of the apparent cohesion. These tests conducted on samples at natural conditions gave:

Apparent cohesion	4.5 t/m^2
Angle of shearing resistance . . .	32.4°

and on samples saturated before shearing:

Apparent cohesion	1.0 t/m^2
Angle of shearing resistance . . .	32°

It is worth noting that the tests carried out on samples at

their natural moisture content, although performed slowly and thus with "possibility of drainage", have their results expressed in terms of total stress since a knowledge of pore air and pore water pressure would be implied for the perfect interpretation of the results in terms of effective stress. The tests on samples saturated before shearing, however, once carried out slowly, have their results expressed in terms of either effective stress or total stress, since the suction no longer exists and the possibility of drainage eliminates the pore pressure build up.

Slope stability analysis carried out with the use of Bishop's method on the circular slip surface indicated in Figure 7.2 have shown that assuming the shear strength parameters obtained from drained tests on saturated samples, and with no pore pressure build up, led to very good results. Indeed, for the parameters obtained from the direct shear tests, the factor of safety obtained was 0.925 and for the parameters from the drained triaxial tests, the factor of safety was 0.94.

These observations lead to consistent results as pointed out in the previous chapter that no pore pressure build up would be necessary to generate instability and only the elimination of suction upon saturation of the soil with the consequent reduction of the apparent cohesion appears to be the leading factor to instability.

Back analyses of the same slip surface assuming a factor of safety equal to 1.0 led to the required values below:

$$c' = 1.62\ t/m^2 \quad \text{and} \quad \phi' = 32°$$

or:

$$c' = 2.28\ t/m^2 \quad \text{and} \quad \phi' = 30°$$

These are in quite good agreement with the laboratory test results.

Figure 7.3 illustrates a summary of this analysis.

It must be emphasized, however, that, although practical, such analyses do not pertain to the actual critical slip surface. The reasons for this reside in the fact that:

1. There is not an uniform distribution of stresses along the slip surface.
2. The parameters assumed in the analysis are not necessarily valid along the whole slip surface.
3. The shear strength parameters in terms of effective stress do not predict the actual shear plane in the triaxial tests.
4. The shear strength parameters do not take into consideration rotation of direction of the principal stresses.
5. The shear strength parameters do not take into consideration the anysotropy of the whole mass.

The most critical slip surface that exists for the above parameters is indicated in Figure 7.2.

With respect to the depth of the landslide, by analysing the depths of infiltration with time shown in Appendix C, it is concluded that a permeability of 5.0×10^{-4} cm/sec would be required. The existence of cracks and other relict structures in the residual soils is necessary to account for this relatively large value, although for degrees of saturation over 90% the depths of infiltration would be much larger, as can be seen in Figures 4.30 and 4.31 where the values of the coefficients a and b are considerably large for the soil close to saturation and in this case a permeability of 2.0×10^{-4} cm/sec

would be sufficient.

7.3 Caneleira Slide

This slide occurred on the hillslope of Caneleira in the City of Santos in March 24th. 1956, at the end of the rainy season and after a very intense rainfall (Vargas, 1967a). As reported by Skempton and Hutchinson (1969) on the basis of a personal communication of Vargas, on the 19th. and 20th. of March, 268 mm of rain had fallen and in the night of 24th. to 25th. of March, 264 mm of rainfall were registered, causing another 60 slides simultaneously.

Figure 7.4 illustrates the landslide which as can be seen was shallow and planar, influenced by the bedrock at shallow depth. The average depth of the slide, measured perpendicular to the slope was about 5.2 m and the slope was fairly steep, i.e., 42° and high, i.e., of the order of 70 m.

The soil was a sandy clay of low plasticity, having the following characteristics:

Liquid Limit	20	to	48%
Plasticity Index	0	to	18%
Void Ratio	0.73	to	1.07

The natural moisture content of this soil was between 19 and 27% corresponding to a degree of saturation between 60 and 70%.

According to Vargas (op. cit.), direct shear tests carried

out slowly, gave the following values for the shear strength parameters for the samples under natural conditions:

Apparent cohesion . . . . . 4 t/m^2

Angle of shearing resistance . . . 40°

The same tests carried out on samples previously saturated gave:

Apparent cohesion . . . . . 4 t/m^2

Angle of shearing resistance . . . 39°

These values for the saturated samples are very high for this type of material. As noted, however, in Chapter II, according to Vargas (1974), the angle of shearing resistance of this material varies between 28 to 33° and the apparent cohesion for the saturated condition is, indeed, very low and sometimes even zero, which makes this soil compatible with the residual soils of Rio de Janeiro.

Analysis of the landslide by application of Equation 6.13 and assuming a factor of safety equal to unity, gives the values:

Apparent cohesion . . . . . 2.0 t/m^2

Angle of shearing resistance . . 32°

Other pairs of values c' and ϕ' would also give a factor of safety equal to unity, but the above pair of values was selected since they also lead to a critical depth obtained through Equation 6.14 comparable to the actual depth of the landslide.

On the basis of the rainfall intensity previous to the landslide and of the curves for the depth of infiltration with time presen-

ted in Appendix C, it is concluded that, for this case, a permeability value between 2.0×10^{-4} and 5.0×10^{-4} cm/sec would also be required, taking into consideration the final degree of saturation at the end of the rainy season. For this, it is assumed a degree of saturation equal to 90%, although it can be expected even a larger value and therefore, a value of 2.0×10^{-4} cm/sec would be sufficient according to Figure 4.30 where it is indicated the large values of the coefficients a and b for degrees of saturation over 90%.

7.4 Monte Serrate Slides

Two slides have been reported by Vargas (1967a) that occurred on the same site. The first slide took place on the 10th. of March of 1928 and the second on the 24th. of March of 1956, simultaneously with the Caneleira Slide. Both were at the end of the rainy season and after a very intense rainfall.

The two slides are shown in Figure 7.5. Their maximum depths were 15 m and 8 m respectively. Although both were very high, about 55 m, the slope was not very steep, of the order of 30 to 35°.

The slope-forming soil was very sandy, with a percentage of clay (< 2μ) less than 5% and of low plasticity. Classification tests gave the following results:

Liquid Limit	20 to 40%
Plasticity Index	13 to 20%
Void Ratio	0.87 to 1.02

Natural moisture content . . . . . 20 to 25%

Direct shear tests carried out slowly on samples under natural conditions gave:

Apparent cohesion . . . . . 4 t/m^2

Angle of shearing resistance . . . 42°

On samples saturated before shearing the same test gave:

Apparent cohesion . . . . . 3 t/m^2

Angle of shearing resistance . . . 31°

The above results are also very high and back-analyses of the first and second landslides showed that the necessary parameters for a factor of safety equal to unity are:

For the first slide:

$c' = 0.0\ t/m^2$ and $\phi' = 28°$

or: $c' = 0.2\ t/m^2$ and $\phi' = 27°$

For the second slide:

$c' = 0.2\ t/m^2$ and $\phi' = 29°$

or: $c' = 0.5\ t/m^2$ and $\phi' = 27°$

These results are, however, in perfect agreement with the real values for these soils presented by Vargas (1974) and discussed in Chapter II. A summary of the above analyses is indicated in Figure 7.6.

Again here for the Monte Serrate slides, a permeability larger than 2.0×10^{-4} cm/sec would be required to account for the infiltration.

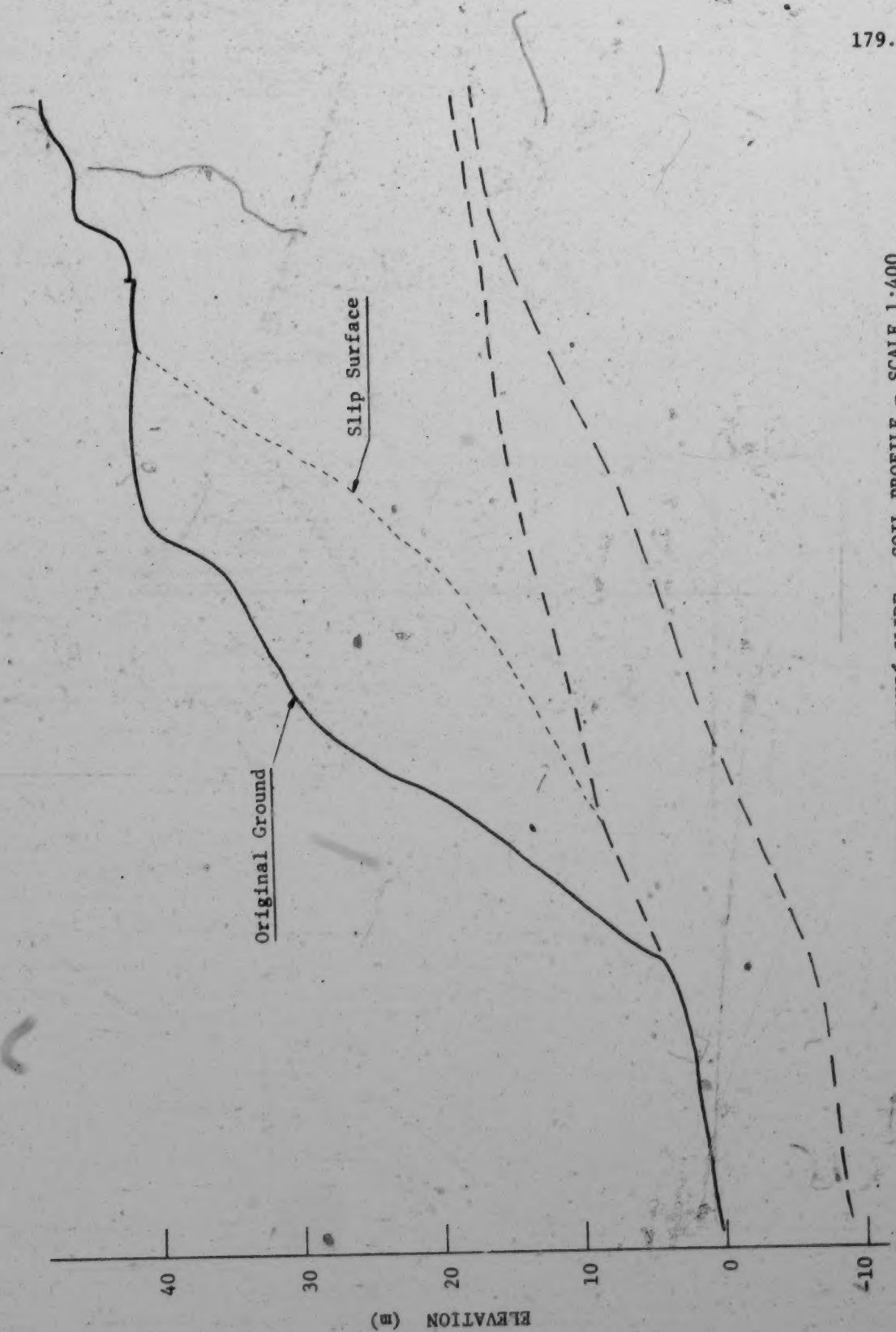

FIGURE 7.1 ESTRADA DO JEQUIÁ SLIDE. SOIL PROFILE - SCALE 1:400

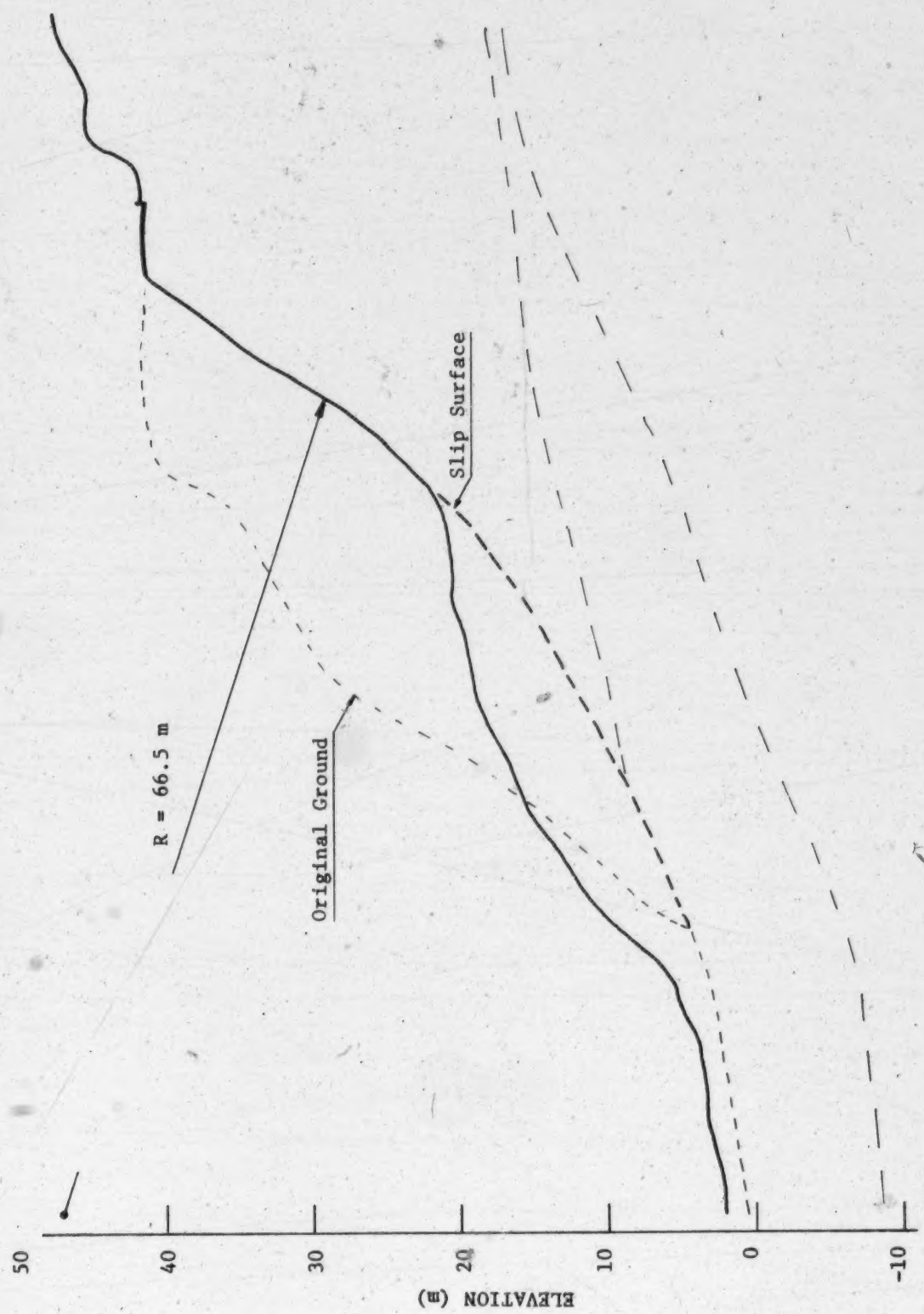

FIGURE 7.2 ESTRADA DO JEQUIÁ SLIDE. SITUATION AFTER SLIDE

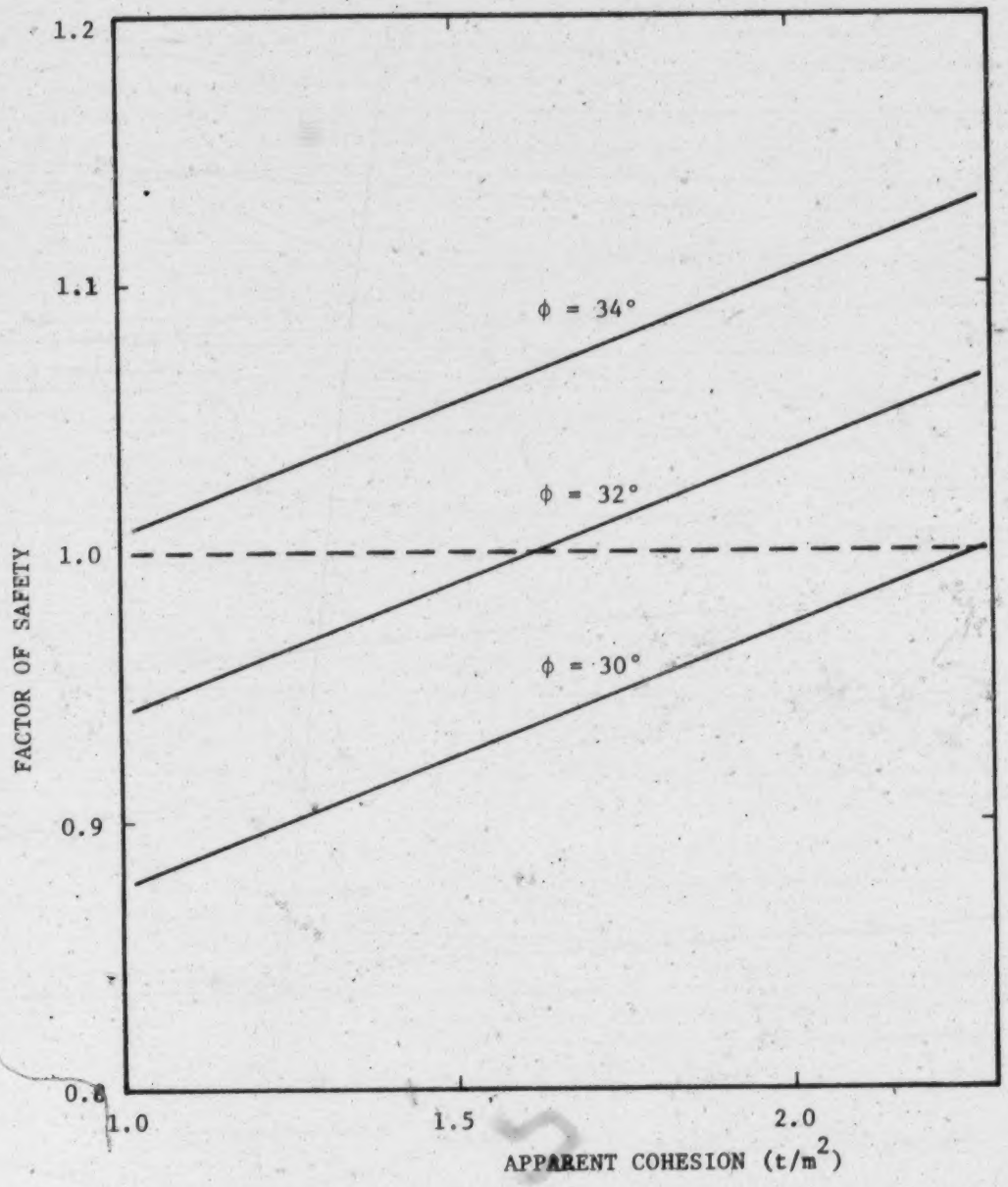

FIGURE 7.3 ANALYSIS OF STABILITY FOR THE ESTRADA DO JEQUIÁ SLIDE

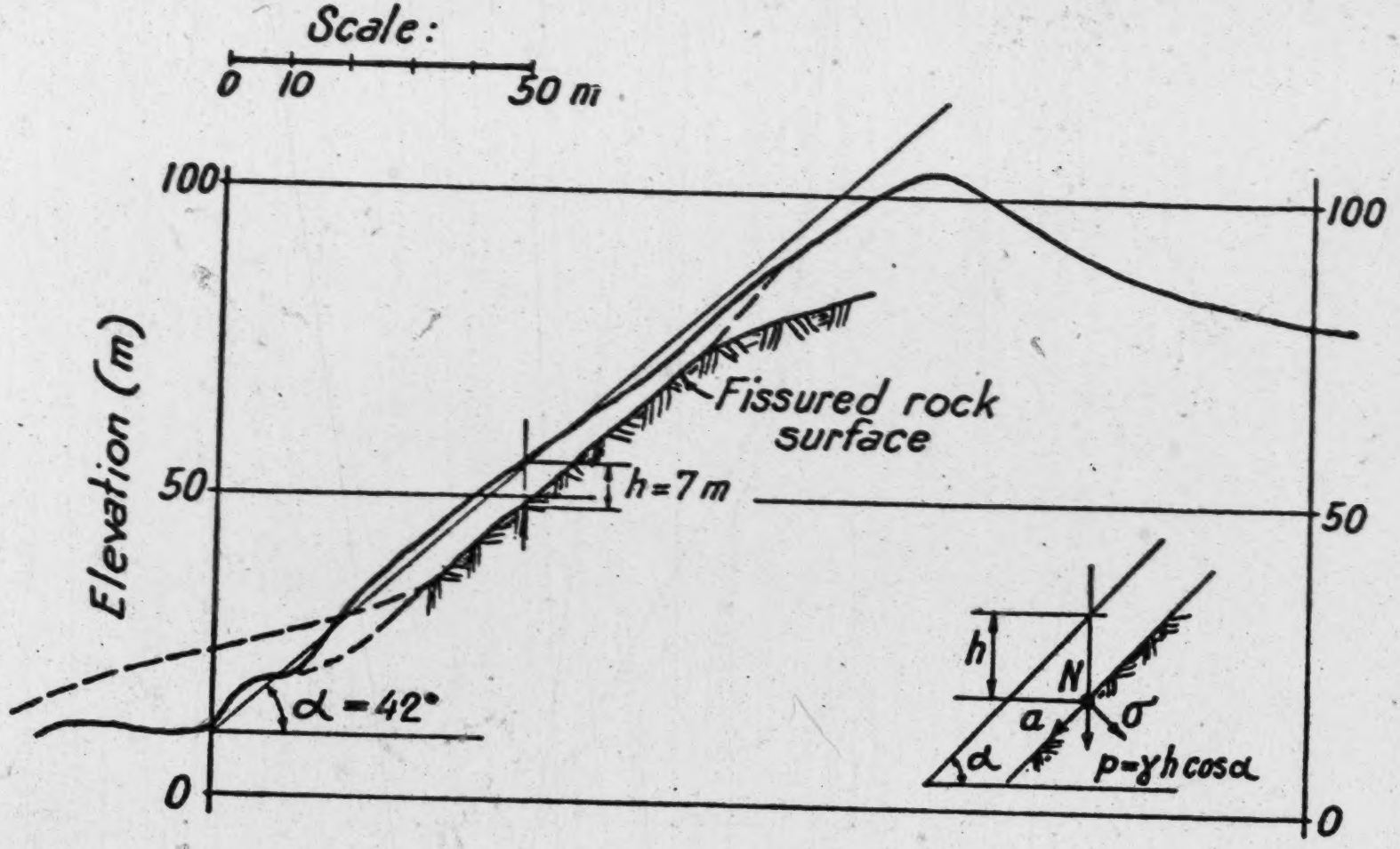

FIGURE 7.4 CANELEIRA SLIDE
(After Vargas, 1967a)

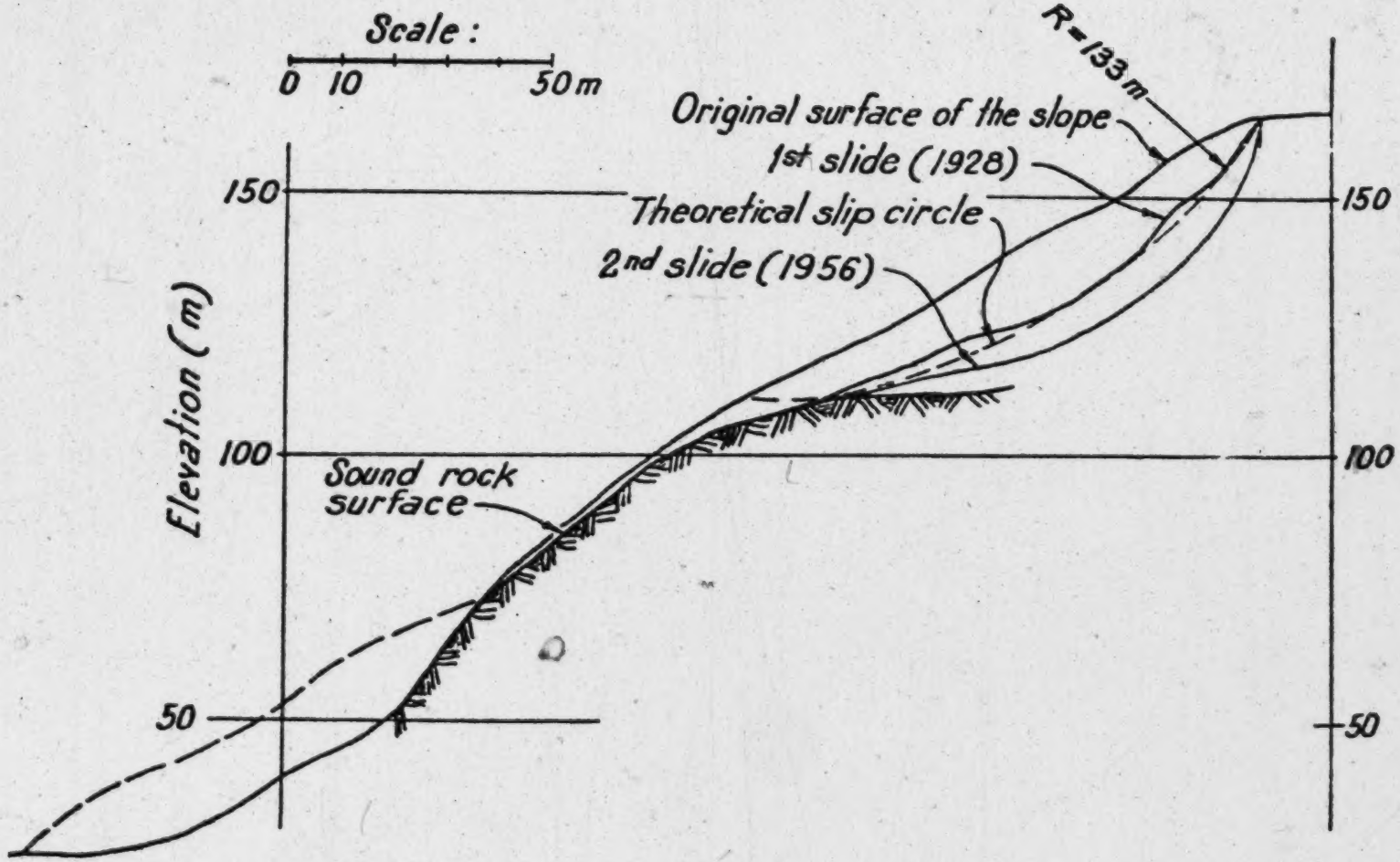

FIGURE 7.5 MONTE SERRATE SLIDES

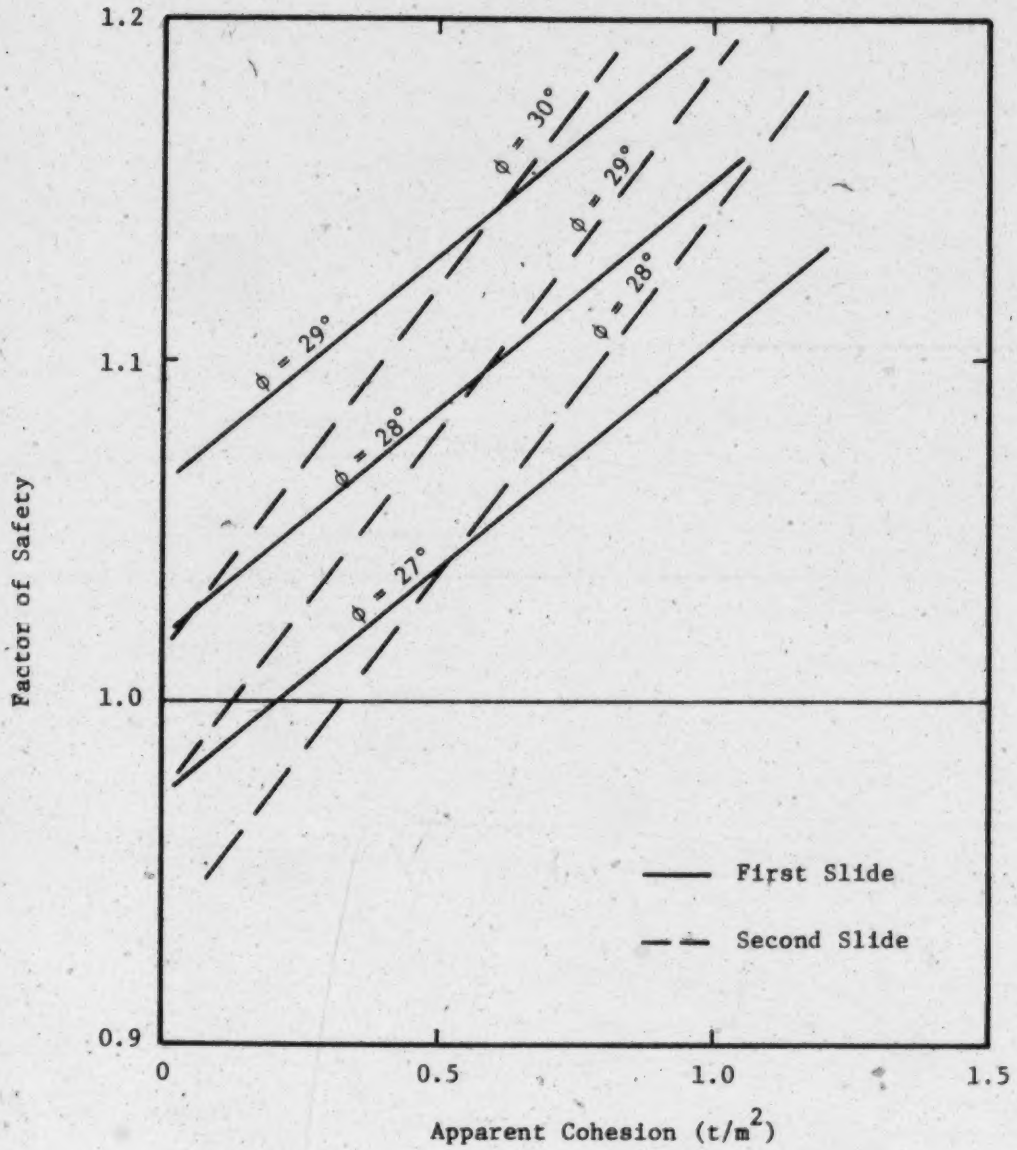

FIGURE 7.6 ANALYSIS OF STABILITY FOR MONTE SERRATE SLIDES

CHAPTER VIII

CONCLUDING REMARKS AND SUGGESTIONS FOR FURTHER RESEARCH

In this thesis, an examination was made of the sliding process that takes place in hot and humid areas characterized by intense rainfalls. Particular attention was given to the subtropical areas of Brazil. The residual soils in these areas are normally unsaturated and therefore the soil water is under a suction.

A mechanism of slope failure was formulated and it was concluded that:

1. Slope failure occurs due to the reduction of the apparent cohesion by virtue of the elimination of the suction due to infiltration of water from rainfalls.
2. Positive pore pressure, if generated, is not the dominant factor causing sliding, since flow of water is not occurring in the common sense as for saturated soils.
3. Analyses of slope stability can be made by use of the parameters c' and ϕ' obtained from triaxial or direct shear drained tests on samples saturated before shearing.
4. The mechanism formulated is more gneral in the way that it also applies to areas other than tropical or subtropical ones. Therefore, in cold regions, availability of water due to snow melt could produce slides as well provided that the apparent cohesion of the soil is reduced upon saturation.

5. Prolonged rainfalls or rainfalls at the end of the rainy season are more likely to produce a slide than an intense rainfall of low duration falling early in the rainy season. An intense rainfall, however, could cause detrimental effects such as surface erosion.

In view of these results, an effective treatment of the slope to impede water infiltration into the slope, associated with complementary measures such as drainage should provide adequate means for slope safety.

Certain basic assumptions have been made in this study, particularly those related to the infiltration of water through unsaturated soils. The vertical infiltration problem was studied and it was assumed that for the case of a slope the advance of the wetting front would take a uniform pattern parallel to the slope surface. It was pointed out, however, that the non-homogeneity of the soils could lead to an irregular distribution of the advancing wetting front, thus producing irregular saturation. Therefore, a two-dimensional analysis of infiltration should give a better approximation for the advancing wetting front surface. As an example, a report by Neuman (1972) describes the two-dimensional solution for the unsaturated flow problem making use of the Finite Element Method by application of Galerkin's method of weithted residuals.

The curves K, h_c and D, respectively the hydraulic conductivity, suction and diffusivity, as functions of the moisture content, have been adopted as variables over a wide range consistent with known

curves for other soils published in the literature, and a parametric sensitivity study was performed.

The determination of the above parameters either in the laboratory or in the field and their application in conjunction with other case histories would be very useful.

In relation to the analyses presented in this thesis, certain questions could be formulated:

1. What is the significance of a factor of safety equal to unity in relation to the mechanism of failure presented?

There is a certain depth corresponding to which a factor of safety equal to unity occurs. If this critical depth, as it was referred to, is sufficienty large that it would not be reached for a particular rainfall intensity and duration, then instability would not occur. Conversely, a landslide would occur when this depth would be reached.

2. Can this critical depth be predicted?

For infinite slopes in homogeneous soils, the depth of the wetting front is more likely to be uniform and the slide planar. Thus, as we have seen in conjunction with the Caneleira Slide, the approximate depth at which sliding occurs can be predicted through Equation 6.14. In cases where the slip surfaces deviate from the planar ones, Equation 6.14 would give a depth more related to the critical slip surface that only fortuitously would correspond to the actual slip surface. For non-

homogeneous soils, an irregular shape for the advancing wetting front occurs and if these surfaces are predicted as a function of time, a factor of safety also as a function of time could be determined by means of the Morgenstern and Price method of slope stability. This should also be investigated.

3. Can the critical depth be increased?

As noted in Chapter VI, a flattening of the slope would lead to a larger value of the critical depth, thus the likelihood of a slope failure occurrence would be decreased.

4. Finally, can a slope be designed with a factor of safety equal to unity?

Since the shear strength parameters for the soils in a natural state are significantly larger than the parameters corresponding to the saturated state, a slope designed on the basis of the shear strength parameters corresponding to the natural moisture content would be safe as well, provided that an effective measure prevents from water infiltrating into the soil slope. This is basically a problem of "calculated risk".

Finally, it must be noted that permeability values must be determined in situ so as to reproduce the influence of the macrostructure of the residual soils, related to the presence of cracks and other relict structures that dominate the behaviour of the soil with respect to infiltration of water. In conjunction with this, a comparison of the unsaturated flow parameters determined in the laboratory and in the

field should also be obtained, since, irrespective of the technique used, these results are expected to be considerably different due to disturbance, stress removal, and so forth, in the specimen.

It is also important that tests must be carried out on the natural materials just after a landslide has occurred, so as to determine their moisture content and the shear strength parameters, believed to be those prevailing at the time of the landslide.

Field tests to determine the variation of the soil moisture content with time after rainfalls and moisture redistribution, would be important in the analysis of the aspects of the infiltration as occurring in natural soils.

Publication of more case histories are needed and it is hoped that analyses following this approach be undertaken.

REFERENCES

Adrian, D.D. (1970) "Infiltration Induced Soil Instabilities", Ground Water, Vol. 8, No.1, pp. 29-36.

Aitchison, G.D. and B.G. Richards (1965) "A Broad Scale Study of Moisture Conditions in Pavement Subgrades throughout Australis", Moisture Equilibria and Moisture Change in Soils Beneath Covered Areas, Butterworths, Australia, pp. 184-282.

Aichison, G.D., K. Russam and B.G. Richards (1965) "Engineering Concepts of Moisture Equilibria and Moisture Changes in Soils", Moisture Equilibria and Moisture Change in Soils Beneath Covered Areas, Butterworths, Australia, pp. 7-21.

Barata, F.E. (1969) "Landslides in the Tropical Region of Rio de Janeiro", Procs. 7th International Conference on Soil Mechanics and Found. Engrg., Vol 2, pp. 507-516, Mexico.

Bodman, G.B. and E.A. Coleman (1944) "Moisture and Energy Conditions During Downward Entry of Water into Soils", Soil Sci. Soc. Am. Proc., 8:116-122.

Bouma, J., D.I. Hillel, F.D. Hale and C.R. Amerman (1971) "Field Measurement of Unsaturated Hydraulic Conductivity by Infiltration through Artificial Crusts", Soil Sci. Soc. Amer. Proc. 35:362-364.

Braester, C. (1973) "Moisture Variation at the Soil Surface and the Advance of the Wetting Front during Infiltration at Constant Flux", Water Resources Research, Vol. 9, No.3:687-694.

Bruce, R.R. and A. Klute (1956) "The Measurement of Soil Moisture Diffusivity", Soil Sci. Soc. Amer. Proc. 20:458-462.

Carslaw, H.S. and J.C. Jaeger (1959) "Conduction of Heat in Solids", Oxford, Clarendon Press, 2nd. Edition.

Childs, E.C. (1967) "Soil Moisture Theory", Advances in Hydroscience, 4:73-117.

Childs, E.C. (1969) "An Introduction to the Physical Basis of Soil Water Phenomena", John Wiley and Sons Ltd., London

Childs, E,C. and N. Collis-George (1950) "The Permeability of Porous Materials", Proc. Roy. Soc. 201A:392-405.

CNP_q (1967) "Os Movimentos de Encosta no Estado da Guanabara e Regiões Circunvizinhas", pp. 13-15, CNP_q, Brazil.

Costa Nunes, A.J. (1969) "Landslides in Soils of Decomposed Rock Due to Intense Rainstorms", Procs. 7th International Conference on Soil Fechanics and Foundation Engineering, Volume 2, pp. 547 -554.

Costa Nunes, A.J. (1971) "Fatores Geomorfológicos e Climáticos na Estabilidade de Taludes de Estradas", Revista Latinoamericana de Geotecnia, Volume 1, No. 3.

Dantas, M.E.R. (1966) "Tectonismo", in Atlas Nacional do Brasil, IBGE - Conselho Nacional de Geografia, Brazil.

Dapples, E.C. (1959) "Basic Geology for Science and Engineering", John Wiley and Sons, Inc., New York.

Deere, D.V. and F.D. Patton (1971) "Slope Stability in Residual Soils", State of the Art Report, 4th Panamerican Conference on Soil Mechanics and Foundation Engineering, Volume 1, pp. 87-170, Puerto Rico.

Doering, E.J. (1965) "Soil Water Diffusivity by the One-Step Method", Soil Science, 99:322-326.

Domingues, A.J.P. and M.H. Whately (1966) "Geomorfologia", in Atlas Nacional do Brasil, IBGE - Conselho Nacional de Geografia, Brazil.

Elrick, D.E. and D.H. Bowman (1964) "Improved Apparatus for Soil Moisture Flow Measurements", Soil Sci. Soc. Amer. Proc., 28:450-453.

Fereira, M.S. (1967) "Estudo Comparativo dos Resultados de Ensaios em Solos Provenientes de Diferentes Rochas", Appendix No. 8 in "Os Movimentos de Encosta no Estado da Guanabara e Regiões Circunvizinhas", CNP_q, Brazil.

Fortes, A.B., L.M. Prunes, M.I.B. Castro and S.R. Piva (1966) "Dicionário Geográfico Brasileiro", Editora Globo, Brazil.

Freise, F.W. (1935) "Erscheinungen des Erdfliessens im Tropen Urwalde, Beobachtungen aus Brasilianischen Küstenwäldern", Zeisch f. Geomorph., Volume 9, pp. 88-98, cited in Deere and Patton (1971).

Gardner, W.R. (1956) "Calculation of Capillary Conductivity from Pressure Plate Outflow Data", Soil Sci. Soc. Amer. Proc., 20:317-320.

Gardner, W.R. (1962) "Note on the Separation and Solution of Diffusion Type Equations", Soil Sci. Soc. Amer. Proc., 26:404-405.

Geotecnica (1967) "Estabilização de Talude - Estrada do Jequiá", Report GB-224/67 from Geotecnica SA to Sursan-Guanabara, Brazil.

Haberlehner, H. (1967) "O Mapa Geotécnico do Estado da Guanabara", Appendix No. 6 in "Os Movimentos de Encosta no Estado da Guanabara e Regiões Circunvizinhas", CNP_q, Brazil.

Haines, W.B. (1930) "Studies in the Physical Properties of Soil: V. The Hysteresis Effect in Capillary Properties and the Modes of Moisture Associated Therewith", J. Agr. Sci., 20:97-116.

Hembold, R. (1967) "Resumo da Geologia do Estado da Guanabara", Appendix No. 5 in "Os Movimentos de Encosta no Estado da Guanabara e Regiões Circunvizinhas", CNP_q, Brazil.

Hessing, J.M. (1969) "Solos da Encosta da Serra do Mar na Região de Cubatão", Anais da 1a Semana Paulista de Geologia Aplicada, Vol.3, pp. VIII-1 - VIII-8, São Paulo, Brazil.

Jones, F.O. (1973) "Landslides of Rio de Janeiro and the Serra das das Araras Escarpment, Brazil", Geological Survey Professional Paper 697, U.S. Department of the Interior.

Kirkham, D. and W.L. Powers (1972) "Advanced Soil Physics", John Wiley and Sons, Inc., New York.

Klute, A. (1972) "The Determination of the Hydraulic Conductivity and Diffusivity of Unsaturated Soils", Soil Sci., 113:264-276.

Kunze, R.J. and D. Kirkham (1962) "Simplified Accounting for Membrane Impedance in Capillary Conductivity Determinations", Soil Sci. Soc. Amer. Proc., 26:421-426.

Laliberte, G.E. and A.T. Corey (1967) "Hydraulic Properties of Disturbed and Undisturbed Samples", In Permeability and Capillarity of Soils, ASTM STP 417, pp. 56-71.

Leinz, V. and S.E. do Amaral (1962) "Geologia Geral", Companhia Editora Nacional, Brazil.

de Lima, G.R. and M.R.M. de Meis (1966) "Hipsometria", In Atlas Nacional do Brasil, IBGE, Conselho Nacional de Geografia, Brazil.

Lumb, P. (1962) "Effect of Rain Storms on Slope Stability", Symposium on Hong Kong Soils, Paper No. 7, pp. 73-87.

Mein, R.G. and C.L. Larson (1973) "Modelling Infiltration During a Steady Rain", Water Resources Research, Vol. 9, No.2, pp. 384-394.

de Mello, V.F.B. and E.B.S. Silveira (1965) "Estrutura das Argilas", Notes of Lectures, University of São Paulo, Brazil.

Miller, E.E. and D.E. Elrich (1958) "Dynamic Determination of Capillary Conductivity Extended for Non-negligible Membrane Impedance", Soil Sci. Soc. Amer. Proc., 22:483-486.

Miller, E.E. and A. Klute (1967) "The Dynamics of Soil Water - Part I Mechanical Forces", in Irrigation of Agricultural Lands, Hagan, R.M. et al., editors, American Society of Agronomy.

Morgenstern, N.R. (1974) "Personal Communication"

Neuman, S.P. (1972) "Finite Element Computer Programs for Flow in Saturated-Unsaturated Porous Media", Second Annual Report (Part 3), Technion, Israel Institute of Technology.

Peck, A.J. (1966) "Diffusivity Determination by a New Outflow Method", in Water in the Unsaturated Zone, Vol. I:191-202, Publ. No. 82, International Assoc. Sci. Hydrol.

Peck, R.B. (1967) "Stability of Natural Slopes", Journal of the Soil Mechanics and Foundations Division, ASCE, SM4, pp. 403-418.

Philip, J.R. (1955) "Numerical Solution of Equations of the Diffusion Type with Diffusivity Concentration-Dependent", Trans. Faraday Society, 51:885-892.

Philip, J.R. (1957a) "The Theory of Infiltration: I The Infiltration Equation and its Solution", Soil Sci., 83:345-357.

Philip, J.R. (1957b) "Numerical Solution of Equations of the Diffusion Type with Diffusivity Concentration-Dependent: II", Austr. Journal of Physics, 10:29-42.

Philip, J.R. (1969) "Theory of Infiltration", Advances in Hydroscience, 5:215-296.

Pichler, E. (1957) "Aspectos Geológicos dos Escorregamentos de Santos", Bulletin, Sociedade Brasileira de Geologia, Volume 6, No. 2, pp. 69-77.

Poulovassilis, A. (1969) "The Effect of Hysteresis of Pore Water on the Hydraulic Conductivity", J. of Soil Sci., 20.

Richards, L.A. (1931) "Capillary Conduction of Liquids through Porous Mediums", Physics, L:318-333.

Richards, B.G. (1968) "Review of Measurement of Soil Water Variables and Flow Parameters", Proc. 4th. Conference, ARRB, 4, No.2, 1843-1861.

Richards, B.G. (1974) "Behaviour of Unsaturated Soils", in Soil Mechanics - New Horizons, edited by I.K. Lee, pp. 112-157, American Elsevier Publishing Co., Inc., New York.

Rijtema, P.E. (1959) "Calculation of Capillary Conductivity from Pressure Plate Outflow Data with Non-Negligible Membrane Impedance", Netherlands, J. Agric. Sci., 7:209-215.

Sandroni, S.S. (1973) "Resistência ao Cisalhamento dos Solos Residuais das Encostas da Guanabara", Série Pesquisa - 01, Grupo de Solos da PUC, Rio de Janeiro, Brazil.

Selim, H.M., D. Kirkham and M. Amemiya (1970) "A Comparison of Two Methods for Determining Soil Water Diffusivity", Soil Sci. Soc. Amer. Proc., 34:14-18.

Skempton, A.W. and J. Hutchinson (1969) "Stability of Natural Slopes and Embankment Foundations", State of the Art Volume, 7th. International Conf. on Soil Mechanics and Foundation Engineering, pp. 291-340.

Teixeira, A.H. and M.A. Kanji (1970) "Estabilização do Escorregamento da Encosta da Serra do Mar na Area da Cota 500 da Via Anchieta", 4th Brazilian Congress on Soil Mechanics.

Terzaghi, K. (1960) "Memorandum Concerning Landslide on Slope Adjacent to Power Plant, South America", in From Theory to Practice in Soil Mechanics, Terzaghi Volume, pp. 410-415, John Wiley and Sons, Inc., New York.

Vargas, M. (1953a) "Some Engineering Properties of Residual Clay Soils Occurring in Southern Brazil", Procs. 3rd International Conf. on Soil Mechanics and Foundation Engineering, Volume 1, pp. 67-71, Zurich.

Vargas, M. (1967a) "Estabilizacão de Taludes em Encostas de Gneisses Decompostos", 3rd Congresso Brasileiro de Mecânica dos Solos, Brazil.

Vargas, M. (1967b) "Design and Construction of Large Cuttings in Residual Soils", Proc. 3rd Panamerican Conference on Soil Mechanics and Foundation Engineering - Vol. II, pp. 243-254, Venezuela.

Vargas, M. (1971a) "Geotécnica dos Solos Residuais", Revista Latino-americana de Geotecnia, Volume 1, No.1:20-41.

Vargas, M. (1971b) "Discussion on Stability of Slopes in Residual Soils", 4th Panamerican Conference on Soil Mechanics and Foundation Engineering - Vol. III, pp. 135-143, Puerto Rico.

Vargas, M. (1973) "Structurally Unstable Soils in Southern Brazil", Proc. 8th International Conf. on Soil Mechanics and Foundation Engineering, Volume 2.2, pp. 239-246, Moscow.

Vargas, M. (1974) "Personal Communication".

Vargas, M. and E. Pichler (1957) "Residual Soil and Rock Slides in Santos (Brazil)", 4th International Conf. on Soil Mechanics and Foundation Engineering, Volume II, pp. 394-398.

Watson, K.K. (1967) "The Measurement of the Hydraulic Conductivity of Unsaturated Porous Materials Using a Zone of Entrapped Air", Soil Sci. Soc. Amer. Proc., 31:71 -721.

Wentworth, C.K. (1943) "Soil Avalanches on Oahu, Hawaii", Bulletin, Geol. Soc. Am., Volume 54, January, pp. 53-64. Cited in Deere and Patton (1971).

Whisler, F.D., A. Klute and D.B. Peters (1968) "Soil Water Diffusivity from Horizontal Infiltration", Soil Sci. Soc. Amer. Proc., 32:6-11.

Youngs, E.G. (1957) "Moisture Profiles During Vertical Infiltration", Soil Sci., 84:283-290.

Youngs, E.G. (1958) "Redistribution of Moisture in Porous Materials After Infiltration", Soil Sci., 86:117-125; 202-207.

Youngs, E.G. (1964) "An Infiltration Method of Measuring the Hydraulic Conductivity of Unsaturated Porous Materials", Soil Sci., 97:307-311.

Youngs, E.G. (1968) "An Estimation of Sorptivity for Infiltration Studies from Moisture Moment Considerations", Soil Sci., 106:157-163.

Zaslavsky, D. and I. Ravina (1965) "Measurement and Evaluation of Hydraulic Conductivity Through the Moisture Moment Method", Soil Sci., 100:104-108.

APPENDIX A

VERTICAL INFILTRATION SOLUTION BY PHILIP'S METHOD

This Appendix presents the computer program for the solution of the vertical infiltration problem, following the method proposed by Philip (1955, 1957a, 1957b).

As noted in Chapter IV for this analysis, the soil parameters needed are the porosity and the hydraulic conductivity and diffusivity, both functions of the volumetric moisture content.

This program computes the first 4 coefficients of the series of Equation 4 as functions of the volumetric moisture content, thus predicting the moisture profile and the rate of infiltration, both as functions of time. Two infiltration rates are presented: the one making use of the 4 coefficients of Philip (Equation 4) and the modified infiltration rate (Equation 4) as proposed by Miller and Klute (1967).

The solution presented here follows the method as presented in Kirkham and Powers (1972) for the first coefficient and as presented in Philip (1957b) for the subsequent coefficients. The input information required for the program is:

1. N: Number of moisture content intervals within the range $\theta_{in} - \theta_{sat}$.
2. DELTET: Value of each moisture content interval.

3. TET(I), HK(I), D(I): Values of the moisture content and of the corresponding hydraulic conductivity and diffusivity.
4. TIME: Values of the times at which the advancing moisture profile and the infiltration rate are to be computed.

```
C     VERTICAL INFILTRATION PROBLEM
C     SOLUTION BY PHILIP'S METHOD
C     THIS PROGRAM COMPUTES THE ADVANCING MOISTURE PROFILE AND THE RATE
C     OF INFILTRATION WITH TIME
C
      DOUBLE PRECISION SUM1,SUM2
      DOUBLE PRECISION RINDPR,RIND2P
      DOUBLE PRECISION RATE4,RATE2A,RATE2B,AR,A,C,E,F
      DOUBLE PRECISION SUMTET,DPRIM,AJ,RISTAR,ADEX,TA(10),SUMA,R2STAR,DE
     1LTA,X1,AX1,AX2
      DOUBLE PRECISION X12
      DOUBLE PRECISION DELTET,TET(50),HK(50),D(50),DM(50),HKM(50),ALFA(5
     10),BETA(50),       FC(50),XAUX,AX,T(6),SUM,BX,X,CHI(50),ANUM,AUX,D
     2EN,PSI(50),DERIV,AUX1,AUX2,OMEG(50),FP(50),RIP(40),F2P(50),RI2P(50
     3),RICOR,F(50),RI(50),TEST
      DOUBLE PRECISION TIME,DEPTH(50)
      DIMENSION NA(50)
      COMMON NMA1,FI(50),DELTET
C
C     READ NUMBER OF MOISTURE INTERVALS AND INTERVAL VALUE
      READ(5,800)N,DELTET
      NME1=N-1
      NMAI=N+1
      NMA1=N+1
C
C     READ MOISTURE CONTENT,HYDRAULIC CONDUCTIVITY AND DIFFUSIVITY
      READ(5,801) (TET(I),HK(I),D(I),I=1,NMAI)
      WRITE(6,805)
  805 FORMAT(1H1,10X,2H N,18X,8HMOISTURE,19X,12HCONDUCTIVITY,16X,11HDIFF
     1USIVITY)
      WRITE(6,806)
  806 FORMAT(33X,3H(%),29X,8H(CM/SEC),22X,9H(CM2/SEC))
      DO 1100 I=1,NMA1
 1100 NA(I)=I
      DO 20 K=1,N
      DM(K)=(D(K)+D(K+1))/2.D0
   20 HKM(K)=(HK(K)+HK(K+1))/2.D0
      WRITE(6,807)
  807 FORMAT(//)
      WRITE(6,810) (NA(I),TET(I),HK(I),D(I),I=1,NMA1)
  810 FORMAT(8X,I5,15X,D12.4,15X,D12.4,15X,D12.4)
C
C     SOLUTION FOR FUNCTION FI(THETA)
C
      SUMTET=0.D0
      DO 2033 I=1,N
 2033 SUMTET=SUMTET+(TET(I)-TET(NMA1))*D(I)
      DPRIM=2.D0*DELTET*SUMTET/(TET(1)-TET(NMA1))**2
      AN=N
      AJ=DBLE(AN)
      RIP(1)=2.D0*AJ*DSQRT(DPRIM/3.141592654D0)
      FI(1)=0.D0
      DO 2047 L=1,10
      DO 2049 I=1,NME1
      FI(I+1)=FI(I)+2.D0*DM(I)/RIP(I)
 2049 RIP(I+1)=RIP(I)-FI(I+1)
      RISTAR=RIP(N)
```

```
      X1=0.5D0*FI(N)/DSQRT(DM(N))
      IF(X1-5.D0) 3050,3050,3080
 3050 ADEX=2.D0*X1*DEXP(-1.D0*X1**2)/(DSQRT(3.141592654D0)*(1.D0-DERF(X1
     1)))-2.DC*X1**2
      GO TO 3200
 3080 X2=2.D0*X1**2
      TA(1)=1.D0
      TA(2)=-2.D0/X2
      TA(3)=10.D0/X2**2
      TA(4)=-74.D0/X2**3
      TA(5)=706.D0/X2**4
      TA(6)=-8162.D0/X2**5
      TA(7)=108830.D0/X2**6
      SUMA=0.D0
      DO 3100 I=1,7
 3100 SUMA=SUMA+TA(I)
      ADEX=SUMA
 3200 R2STAR=0.5D0*FI(N)+2.D0*DM(N)*ADEX/FI(N)
      DELTA=RISTAR-R2STAR
      RIP(1)=RIP(1)-DELTA/2.D0
 2047 CONTINUE
      FI(NMA1)=FI(N)+2.D0*DM(N)/RIP(N)
      WRITE(6,820)
      WRITE(6,825)
      WRITE(6,826)
      WRITE(6,830) (TET(K),FI(K),K=1,NMA1)
      CALL INTEG
      WRITE(6,3572)AR
 3572 FORMAT(//,20X,12HINTEGRAL A =,D12.6)
C
C     GENERATION OF PARAMETERS ALFA AND BETA FOR FUNCTION CHI
C
      DO 60 K=1,N
   60 BETA(K)=HK(N+1)-HKM(K)
      DO 70 K=1,N
   70 ALFA(K)=DM(K)*DELTET**2/((FI(K+1)-FI(K))**2)
      WRITE(6,71)
   71 FORMAT(//,25X,8HMOISTURE,10X,7HALFA(I))
      WRITE(6,72) (TET(I),ALFA(I),I=1,N)
   72 FORMAT(20X,D12.4,10X,D15.6)
C
C     SOLUTION OF FUNCTION CHI
C
      FP(1)=0.D0
      RIP(1)=C.D0
      DO 300 J=1,N
      FP(J+1)=FP(J)-(BETA(J)/DELTET+RIP(J))/(ALFA(J)/(DELTET**2)-1.D0/8.
     2D0)
  300 RIP(J+1)=RIP(J)-FP(J+1)
      RINDPR=RIP(N)-0.5DC*FP(NMA1)
      F2P(1)=0.D0
      RI2P(1)=-1.D0
      DO 340 J=1,N
      F2P(J+1)=F2P(J)-RI2P(J)/(ALFA(J)/(DELTET**2)-1.D0/8.D0)
  340 RI2P(J+1)=RI2P(J)-F2P(J+1)
      RIND2P=RI2P(N)-0.5DC*F2P(NMA1)
      RICOR=RINDPR/RIND2P
      DO 360 J=1,NMA1
  360 FC(J)=FP(J)-RICOR*F2P(J)
      DO 98 I=1,NMA1
```

```
      98 CHI(I)=FC(I)
         WRITE(6,850)
         WRITE(6,855)
         WRITE(6,856)
  856 FORMAT(//)
         WRITE(6,860) (TET(K),CHI(K),K=1,NMA1)
         DO 6001 I=1,NMA1
 6001 FI(I)=CHI(I)
         CALL INTEG
         WRITE(6,3574)AR
 3574 FORMAT(//,20X,12HINTEGRAL C =,D12.6)
C
C     GENERATION OF PARAMETERS ALFA AND BETA FOR FUNCTION PSI
C
         DO 110 K=1,N
  110 ALFA(K)=2.D0*ALFA(K)/3.D0
         DO 120 K=1,N
  120 BETA(K)=2.D0*DM(K)*(DELTET/(FI(K)-FI(K+1)))**3*((CHI(K)-CHI(K+1))/
     1DELTET)**2/3.D0
         WRITE(6,121)
  121 FORMAT(//,30X,29HFUNCAO BETA * PARA FUNCAO PSI)
         WRITE(6,122) (TET(I),BETA(I),I=1,N)
  122 FORMAT(40X,D12.4,10X,D15.6)
C
C     SOLUTION OF FUNCTION PSI
C
         FP(1)=0.D0
         RIP(1)=0.D0
         DO 400 J=1,N
         FP(J+1)=FP(J)-(BETA(J)/DELTET+RIP(J))/(ALFA(J)/(DELTET**2)-1.D0/8.
     2D0)
  400 RIP(J+1)=RIP(J)-FP(J+1)
         RINDPR=RIP(N)-0.5D0*FP(NMA1)
         F2P(1)=0.D0
         RI2P(1)=-1.D0
         DO 440 J=1,N
         F2P(J+1)=F2P(J)-RI2P(J)/(ALFA(J)/(DELTET**2)-1.D0/8.D0)
  440 RI2P(J+1)=RI2P(J)-F2P(J+1)
         RIND2P=RI2P(N)-0.5D0*F2P(NMA1)
         RICOR=RINDPR/RIND2P
         DO 460 J=1,NMA1
  460 FC(J)=FP(J)-RICOR*F2P(J)
         DO 160 K=1,NMAI
  160 PSI(K)=FC(K)
         WRITE(6,870)
         WRITE(6,875)
         WRITE(6,876)
  876 FORMAT(//)
         WRITE(6,880) (TET(K),PSI(K),K=1,NMA1)
         DO 6002 I=1,NMA1
 6002 FI(I)=PSI(I)
         CALL INTEG
         WRITE(6,3576)AR
 3576 FORMAT(//,20X,12HINTEGRAL E =,D12.6)
C
C     GENERATION OF PARAMETERS ALFA AND BETA FOR FUNCTION OMEGA
C
         DO 170 K=1,N
  170 ALFA(K)=3.D0*ALFA(K)/4.D0
         DO 180 K=1,N
```

```
182           DO 180 K=1,N
183           AUX1=0.5D0*DM(K)*(DELTET/(FI(K)-FI(K+1)))**3*((CHI(K)-CHI(K+1))/DE
184          1LTET)
185           AUX2=2.D0*((PSI(K)-PSI(K+1))/DELTET)-((CHI(K)-CHI(K+1))/DELTET)**2
186          1*(DELTET/(FI(K)-FI(K+1)))
187       180 BETA(K)=AUX1*AUX2
188           WRITE(6,181)
189       181 FORMAT(//,30X,30HFUNCAO BETA * PARA FUNCAO OMEG)
190           WRITE(6,182) (TET(I),BETA(I),I=1,N)
191       182 FORMAT(40X,D12.4,10X,D15.6)
192     C
193     C     SOLUTION OF FUNCTION OMEGA
194     C
195           FP(1)=0.D0
196           RIP(1)=0.D0
197           DO 500 J=1,N
198           FP(J+1)=FP(J)-(BETA(J)/DELTET+RIP(J))/(ALFA(J)/(DELTET**2)-1.D0/8.
199          2D0)
200       500 RIP(J+1)=RIP(J)-FP(J+1)
201           RINDPR=RIP(N)-0.5D0*FP(NMA1)
202           F2P(1)=0.D0
203           RI2P(1)=-1.D0
204           DO 540 J=1,N
205           F2P(J+1)=F2P(J)-RI2P(J)/(ALFA(J)/(DELTET**2)-1.D0/8.D0)
206       540 RI2P(J+1)=RI2P(J)-F2P(J+1)
207           RIND2P=RI2P(N)-0.5D0*F2P(NMA1)
208           RICOR=RINDPR/RIND2P
209           DO 560 J=1,NMA1
210       560 FC(J)=FP(J)-RICOR*F2P(J)
211           DO 190 I=1,NMA1
212       190 OMEG(I)=FC(I)
213           WRITE(6,900)
214           WRITE(6,905)
215           WRITE(6,906)
216       906 FORMAT(//)
217           WRITE(6,910) (TET(K),OMEG(K),K=1,NMA1)
218           DO 6003 I=1,NMA1
219      6003 FI(I)=OMEG(I)
220           CALL INTEG
221           WRITE(6,3578)AR
222      3578 FORMAT(//,20X,12HINTEGRAL F =,D12.6)
223     C
224     C     READ THE VALUES OF TIME
225     C
226      1400 READ(5,1500)TIME
227      1500 FORMAT(D10.2)
228           DO 2000 I=1,NMA1
229      2000 DEPTH(I)=FI(I)*DSQRT(TIME)+CHI(I)*TIME+PSI(I)*(DSQRT(TIME))**3+OME
230          1G(I)*TIME**2
231           WRITE(6,6003)
232      6003 FORMAT(//,20X,22HDEPTH USING FOUR TERMS)
233      5071 WRITE(6,2010)TIME
234      2010 FORMAT(///,20X,6HTIME =,D10.2,2X,3HSEC)
235           WRITE(6,2020)
236      2020 FORMAT(//,40X,8HMOISTURE,20X,5HDEPTH)
237           WRITE(6,2030)
238      2030 FORMAT(43X,3H(%),23X,4H(CM))
239           WRITE(6,2039)
240      2039 FORMAT(//)
241           WRITE(6,2040) (TET(I),DEPTH(I),I=1,NMA1)
```

```
      2040 FORMAT(37X,D12.4,16X,D12.4)
      5081 RATE4=0.5D0*A/DSQRT(TIME)+HK(NMA1)+C+1.5D0*E*DSQRT(TIME)+2.D0*AF*T
     1IME
           RATE2B=0.5D0*A/DSQRT(TIME)+HK(1)
           WRITE(6,5083)RATE4,RATE2B
      5083 FORMAT(//,5X,15HRATE(4 TERMS) =,D15.6,5X,19HRATE(I TERMS*SAT) =,D1
     15.6)
           GO TO 1400
       800 FORMAT(I5,D12.4)
       801 FORMAT(3D12.4)
       820 FORMAT(///,37X,27HVALORES DA FUNCAO FI(THETA))
       825 FORMAT(//,35X,8HMOISTURE,15X,9HFI(THETA))
       826 FORMAT(//)
       830 FORMAT(32X,D12.4,9X,D15.6)
       850 FORMAT(///,37X,28HVALORES DA FUNCAO CHI(THETA))
       855 FORMAT(//,35X,8HMOISTURE,14X,10HCHI(THETA))
       860 FORMAT(32X,D12.4,9X,D15.6)
       870 FORMAT(///,37X,28HVALORES DA FUNCAO PSI(THETA))
       875 FORMAT(//,35X,8HMOISTURE,14X,10HPSI(THETA))
       880 FORMAT(32X,D12.4,9X,D15.6)
       900 FORMAT(///,37X,29HVALORES DA FUNCAO OMEG(THETA))
       905 FOPMAT(//,35X,8HMOISTURE,13X,11HOMEG(THETA))
       910 FORMAT(32X,D12.4,9X,D15.6)
           END
           SUBROUTINE INTEG
           COMMON NMA1,FI(50),DELTET
           NM1=N-1
           IM=NMA1/2
           IL=2*IM
           IF(IL-IM)4100,4101,4100
      4101 AR=FI(1)+FI(NMA1)
           SUM1=0.D0
           SUM2=0.D0
           DO 4110 I=2,N,2
           SUM1=SUM1+2.D0*FI(I)
      4110 SUM2=SUM2+4.D0*FI(I+1)
           AR=DELTET*(AR+SUM1+SUM2)/3.D0
           GO TO 5000
      4100 IM=N/3
           IL=3*IM
           IF(IL-N)4120,4121,4120
      4121 AR=FI(1)+FI(NMA1)
           SUM1=0.D0
           SUM2=0.D0
           DO 4130 I=2,NM1,3
           SUM1=SUM1+3.D0*(FI(I)+FI(I+1))
      4130 SUM2=SUM2+2.D0*FI(I+2)
           SUM2=SUM2-2.D0*FI(NMA1)
           AR=3.D0*(AR+SUM1+SUM2)*DELTET/8.D0
           GO TO 5000
      4120 AR=0.D0
           DO 5010 I=1,N
      5010 AR=AR+0.5D0*(FI(I)+FI(I+1))*DELTET
      5000 A=AR
           RETURN
           END
END OF FILE
```

APPENDIX B

VERTICAL INFILTRATION SOLUTION BY MEIN AND LARSON'S METHOD

The computer program for the solution of the vertical infiltration problem according to the method proposed by Mein and Larson (1973) is presented in this Appendix.

The basic soil data required for this analysis are the porosity of the soil, the hydraulic conductivity and the capillary suction, both functions of the moisture content and the initial degree of saturation.

The program computes for each rainfall intensity, the depth of the wetting front and the infiltration rate, both functions of the time and the coefficients a and b of Equation 4 by means of regression analysis. Details of the method are presented in Chapter IV.

The input information required for the program is:

1. TITLG: General title.
2. NSOILS: Number of soils to be analysed.
3. NDS: Number of degrees of saturation to be considered in the analyses.
4. DEG(I): Values of the degrees of saturation.
5. NR: Number of rainfall intensities.
6. RAINRT(I): Values of the rainfall intensities.
7. NT: Number of times considered.

8. TIME(I): Values of the times.

9. MREG: Maximum number of terms of the series of Equation 4 to be considered for the regression analysis plus one.

10. TITLS: Title for each soil.

11. MGIV: Number of moisture content values given.

12. TET(I), HK(I), SUC(I): Values of the moisture content and of the corresponding hydraulic conductivity and suction for each soil.

13. DELTET: Value of each moisture content interval.

```
      C     VERTICAL INFILTRATION PROBLEM
      C     SOLUTION BY REIN AND LARSON'S METHOD
            DIMENSION NA(60)
            DIMENSION X(50),Y(50),ALPHA(20)
            DIMENSION TET(60),RELHK(60),SUC(60),HK(60),D(60)
            DIMENSION XSQR(200),YS(200)
            DIMENSION TITLG(20),DEG(10),TITLS(20)
            DIMENSION TIME(40),RAINRT(40)
            COMMON XSQR,YS
            COMMON NOBS,MREG
      C
      C     READ GENERAL TITLE OF THE PROBLEM
      C
            READ(5,502) (TITLG(I),I=1,20)
            WRITE(6,809)
        809 FORMAT(1H1)
            WRITE(6,502) (TITLG(I),I=1,20)
      C
      C     READ NUMBER OF SOILS CONSIDERED
      C
            READ(5,601)NSOILS
      C
      C     READ NUMBER OF INITIAL DEGREES OF SATURATION
      C
            READ(5,601)NDS
      C
      C     READ INITIAL DEGREES OF SATURATION
      C
            READ(5,602) (DEG(IDS),IDS=1,NDS)
        602 FORMAT(F6.2)
      C
      C     READ NUMBER OF RAINFALL INTENSITIES
      C
            READ(5,601)NR
      C
      C     READ RAINFALL INTENSITIES
      C
            READ(5,821) (RAINRT(IR),IR=1,NR)
      C
      C     READ NUMBER OF TIMES
      C
            READ(5,601)NT
      C
      C     READ TIMES
      C
            READ(5,821) (TIME(IT),IT=1,NT)
        821 FORMAT(E12.4)
      C
      C     READ NUMBER OF TERMS CONSIDERED FOR THE DEPTH OF INFILTRATION
      C
            READ(6,822)MREG
        822 FORMAT(I5)
            DO 4000 ISOIL=1,NSOILS
      C
      C     READ NAME OF SOIL TO BE ANALYSED
      C
            READ(5,502) (TITLS(I),I=1,20)
```

```
      C
      C     READ NUMBER OF MOISTURE INTERVALS
      C
            READ(5,601)NGIV
          601 FORMAT(I5)
      C
      C     READ MOITURE CONTENT,CONDUCTIVITY AND SUCTION
      C
            READ(5,800) (TET(I),HK(I),SUC(I),I=1,NGIV)
          800 FORMAT(3E12.4)
      C
      C     READ MOISTURE INTERVAL
            READ(5,820)DELTET
          820 FORMAT(E12.4)
            DO 4000 IDS=1,NDS
            TETSIN=TET(1)*DEG(IDS)/100.
            I=1
          456 IF(TETSIN-TET(I))451,452,453
          451 I=I+1
            GO TO 456
          452 M=I
            GO TO 455
          453 DIF1=TETSIN-TET(I)
            DIF2=TET(I-1)-TETSIN
            M=I
            IF(DIF1.GE.DIF2)M=M-1
          455 HKSAT=HK(1)
            TETIN=TET(M)*100.
            TETFIN=TET(1)*100.
            SATIN=TETIN/TET(1)
            SATFN=TETFIN/TET(1)
            WRITE(6,807)
            WRITE(6,502) (TITLS(I),I=1,20)
          502 FORMAT(20A4)
            WRITE(6,805)
          805 FORMAT(///,20X,2H N,18X,8HMOISTURE,17X,12HCONDUCTIVITY,17X,7HSUCTI
           1ON)
            WRITE(6,804)
          804 FORMAT(44X,3H(%),21X,8H(CM/SEC),21X,4H(CM))
            WRITE(6,807)
          807 FORMAT(//)
            DO 808 I=1,M
          808 NA(I)=I
            WRITE(6,826) (NA(I),TET(I),          HK(I),SUC(I),I=1,M)
          826 FORMAT(18X,I5,15X,E12.4,15X,          E12.4,15X,E12.4)
            MM1=M-1
            MM2=M-2
            ND=NT
            DO 4000 IR=1,NR
            NF=IR
            RAIN=RAINRT(IR)
            IF(RAIN.LE.HKSAT)GO TO 4000
            RATIO=RAIN/HK(1)
            IF(RAINRT(IR)-HK(1))401,402,400
          402 TETU=TET(1)
            GO TO 907
          401 I=2
          702 IF(RAINRT(IR).GE.HK(I))GO TO 905
          900 I=I+1
            GO TO 702
```

```
      905 TETU=TET(I)+(RAINRT(IR)-HK(I))*(TET(I)-TET(I-1))/(HK(I-1)-HK(I))
      907 DEFMOS=TETU-TET(M)
          RATE=RAINRT(IR)
          TETU=TETU*100.
          WRITE(6,3001)RAIN
          WRITE(6,3002)RATIO
          WRITE(6,3006)TETIN
          WRITE(6,3015)SATIN
          WRITE(6,3007)TETU
          SATFN=TETU/TET(1)
          WRITE(6,3016)SATFN
          WRITE(6,1000)
     1000 FORMAT(//,24X,63HRAINFALL INTENSITY IS LESS THAN KSAT*SATURATION I
         1S NOT ACHIEVED)
          WRITE(6,3008)
          GO TO 2999
C
C         SAV COMPUTATION
C
      400 TETU=TET(1)
          IM=M/2
          IL=2*IM
          IF(IL.NE.IM)GO TO 200
      201 AREA=SUC(1)+SUC(M)
          SUM1=0.
          SUM2=0.
          DO 210 I=2,MM1,2
          SUM1=SUM1+2.*SUC(I)
      210 SUM2=SUM2+4.*SUC(I+1)
          SAV=DELTET*(AREA+SUM1+SUM2)/3.
          SAV=SAV/(TET(1)-TET(M))
          GO TO 300
      200 IM=(M-1)/3
          IL=3*IM
          IF(IL.NE.MM1)GO TO 220
      221 AREA=SUC(1)+SUC(M)
          SUM1=0.
          SUM2=0.
          MM2=M-2
          DO 230 I=2,MM2,3
          SUM1=SUM1+3.*(SUC(I)+SUC(I+1))
      230 SUM2=SUM2+2.*SUC(I+2)
          SUM2=SUM2-2.*SUC(M)
          SAV=3.*(AREA+SUM1+SUM2)*DELTET/8.
          SAV=SAV/(TET(1)-TET(M))
          GO TO 300
      220 SAV=0.
          DO 20 I=1,MM1
       20 SAV=SAV+0.5*(SUC(I)+SUC(I+1))*DELTET
          SAV=SAV/(TET(1)-TET(M))
      300 DEFMOS=TET(1)-TET(M)
          FS=SAV*DEFMOS/(RAINRT(IR)/HK(1)-1.)
          TSAT=FS/RAINRT(IR)
          ZSAT=FS/DEFMOS
          TSH=TSAT/3600.
          WRITE(6,3001)RAIN
     3001 FORMAT(//,30X,30HRAINFALL INTENSITY          = ,E10.4,2X,6HCM/SEC)
          WRITE(6,3002)RATIO
     3002 FORMAT(30X,30HI/KSAT RATIO                   = ,E10.4)
          WRITE(6,3003)TSH
```

```
182      3003 FORMAT(30X,30HTIME FOR SURFACE SATURATION = ,E10.4,2X,4HHOUR)
183           WRITE(6,3004)ZSAT
184      3004 FORMAT(30X,30HDEPTH OF SURFACE SATURATION = ,E10.4,2X,2HCM)
185           WRITE(6,3005)SAV
186      3005 FORMAT(30X,30HAVERAGE SUCTION             = ,E10.4,2X,11HCM OF WAT
187          1ER)
188           WRITE(6,3006)TETIN
189      3006 FORMAT(30X,30HINITIAL MOISTURE CONTENT    = ,E10.4,2X,2H% )
190           WRITE(6,3015)SATIN
191      3015 FORMAT(30X,30HINITIAL DEGREE OF SATURATION= ,E10.4,2X,2H% )
192           WRITE(6,3007)TETFIN
193      3007 FORMAT(30X,30HFINAL MOISTURE CONTENT      = ,E10.4,2X,2H% )
194           WRITE(6,3016)SATFN
195      3016 FORMAT(30X,30HFINAL DEGREE OF SATURATION  = ,E10.4,2X,2H% )
196           WRITE(6,3008)
197      3008 FORMAT(//)
198      2999 MM1=M-1
199           DO 3000 IT=1,NT
200           TIM=TIME(IT)
201           THOUR=TIM/3600.
202           IF(RAINRT(IR).GT.HK(1))GO TO 322
203       321 FCUM=RATE*TIME(IT)
204           ZFRONT=FCUM/DEFMOS
205           IF(IT-1)3014,3013,3014
206       322 A=HKSAT*SAV*DEFMOS
207     C
208     C     SOLUTION FOR ACCUMULATED INFILTRATION * FCUM
209     C
210           IF(TIME(IT).GE.TSAT)GO TO 505
211       500 RATE=RAINRT(IR)
212           FCUM=RATE*TIME(IT)
213           ZFRONT=FCUM/DEFMOS
214           IF(IT-1)3014,3013,3014
215       505 AF=FS
216           IA=0
217           PEXP=HK(1)*(TIME(IT)-TSAT)+FS
218       699 SEXP=AF-A/HKSAT*ALOG((A+HKSAT*AF)/(A+HKSAT*FS))
219           IA=IA+1
220           DELTA=PEXP-SEXP
221           IF(ABS(DELTA).LE.0.001)GO TO 700
222       705 AF=AF+DELTA/2
223           GO TO 699
224       700 FCUM=AF
225           ZFRONT=FCUM/DEFMOS
226           RATE=HKSAT+A/FCUM
227           IF(IT.NE.1)GO TO 3014
228      3013 WRITE(6,3009)
229      3009 FORMAT(19X,4HTIME,17X,20HRATE OF INFILTRATION,10X,22HDEPTH OF WETT
230          1ING FRONT)
231           WRITE(6,3010)
232      3010 FORMAT(12X,6H(HOUR),6X,5H(SEC),17X,8H(CM/SEC),25X,4H(CM))
233           WRITE(6,3011)
234      3011 FORMAT(//)
235      3014 X(IT)=THOUR
236           Y(IT)=ZFRONT
237           WRITE(6,3012)THOUR,TIM,RATE,ZFRONT
238      3012 FORMAT(10X,E10.4,2X,E10.4,13X,E10.4,21X,E10.4)
239      3000 CONTINUE
240           XSQR(1)=0.0
241           YS(1)=0.0
```

```
      IC=1
  265 IF(X(IC).GT.TSH)GO TO 270
      IF(IC.EQ.NT)GO TO 290
      IC=IC+1
      GO TO 265
  270 NOBS=NT-IC+2
      DO 280 II=IC,NT
      JX=II-IC+2
      XSQR(JX)=SQRT(X(II))
  280 YS(JX)=Y(II)
      IF(NOBS.GT.MREG)GO TO 287
  285 WRITE(6,286)
  286 FORMAT(//,5X,'NUMBER OF POINTS INSUFFICIENT FOR REGRESSION')
      GO TO 4000
  287 CALL GENAR
      GO TO 4000
  290 WRITE(6,291)
  291 FORMAT(//,5X,'LAST VALUE OF TIME GIVEN IS LESS THAN TSAT')
 4000 CONTINUE
      END
C     REGRESSION ANALYSIS FOR THE DEPTH VS TIME FUNCTION
      SUBROUTINE GENAR
      DIMENSION X(200),DI(25),D(20)
      DIMENSION B(10),E(10),SB(10),T(10)
      DIMENSION XBAR(11),STD(11),COE(11),SUMSQ(11),ISAVE(11)
      DIMENSION ANS(10),P(300)
      DIMENSION XSQR(200),YS(200)
      COMMON XSQR,YS
      COMMON NOBS,MREG
      N=NOBS
      M=MREG
      WRITE(6,3)
      WRITE(6,4)N
      L=N*M
      DO 110 I=1,N
      J=L+I
      X(I)=XSQR(I)
  110 X(J)=YS(I)
      CALL GDATA(N,M,X,XBAR,STD,D,SUMSQ)
      MM=M+1
      SUM=0.0
      NT=N-1
      DO 200 I=1,M
      ISAVE(I)=I
      CALL ORDER(MM,D,MM,I,ISAVE,DI,E)
      CALL MINV(DI,I,DET,B,T)
      CALL MULTR(N,I,XBAR,STD,SUMSQ,DI,E,ISAVE,B,SB,T,ANS)
      WRITE(6,5)I
      IF(ANS(7))140,130,130
  130 SUMIP=ANS(4)-SUM
      IF(SUMIP)140,140,150
  140 WRITE(6,13)
      GO TO 4007
  150 WRITE(6,6)ANS(1),(B(J),J=1,I)
      SUM=ANS(4)
      WRITE(6,10)SUMIP
      NI=ANS(8)
      COE(I)=ANS(1)
      DO 160 J=1,I
  160 COE(J+1)=B(J)
```

```
      LA=I
  200 CONTINUE
    3 FORMAT(///,'POLYNOMIAL REGRESSION')
    4 FORMAT(23HONUMBER OF OBSERVATIONS,I6)
    5 FORMAT(12X,32H POLYNOMIAL REGRESSION OF DEGREE,I3)
    6 FORMAT(15X,'REGRESSION COEFFICIENTS IN INCREASING ORDER',6E20.7)
   10 FORMAT(15X,'IMPROVEMENT IN TERMS OF SUM OF SQUARES',F20.5)
   13 FORMAT(15X,'NO IMPROVEMENT')
 4007 M=MREG
      RETURN
      END
END OF FILE
```

APPENDIX C

RESULTS OF MEIN AND LARSON'S SOLUTION FOR RESIDUAL SOILS

Figures A.1 to A.9 summarise part of the results obtained for the 9 assumed residual soils by application of Mein and Larson's solution to the vertical infiltration problem.

Only the curves for the depth of infiltration with time are presented. Here, times up to 24 hours have been considered since they are the practical period in which slides would occur. Rainfall durations larger than this value have occurred, as noted by Barata (1969) but they correspond to rainfalls of periods of return that are excessively high. Larger times could also be considered but it is expected that 24 hours is a reasonable value for purposes of presentation of the results and carrying out the analyses.

In these figures, only the curves corresponding to rainfall intensities 2, 4 and 8 or 10 times the permeability are presented. It is observed that these curves practically coincide as noted before.

Although the initial degree of saturation of the residual soils starts at a value about 60%, it is felt on the basis of the analyses presented in this thesis, that critical situations arise when the initial degree of saturation is about 90% due to the moisture redistribution during the rainy season. Therefore, the curves presented here correspond to this value of the initial degree of saturation only.

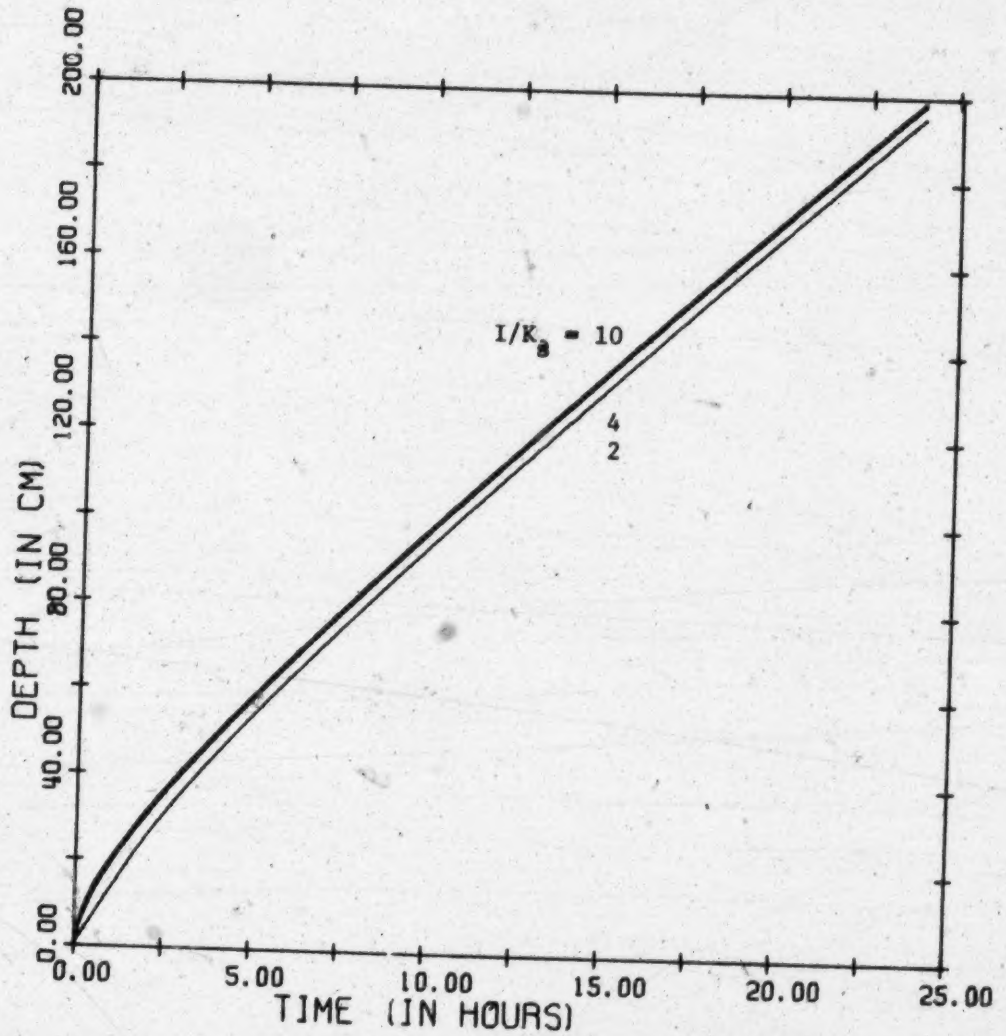

FIGURE C1 VOID RATIO=0.75 KSAT=8.0E-5 SAT=90%

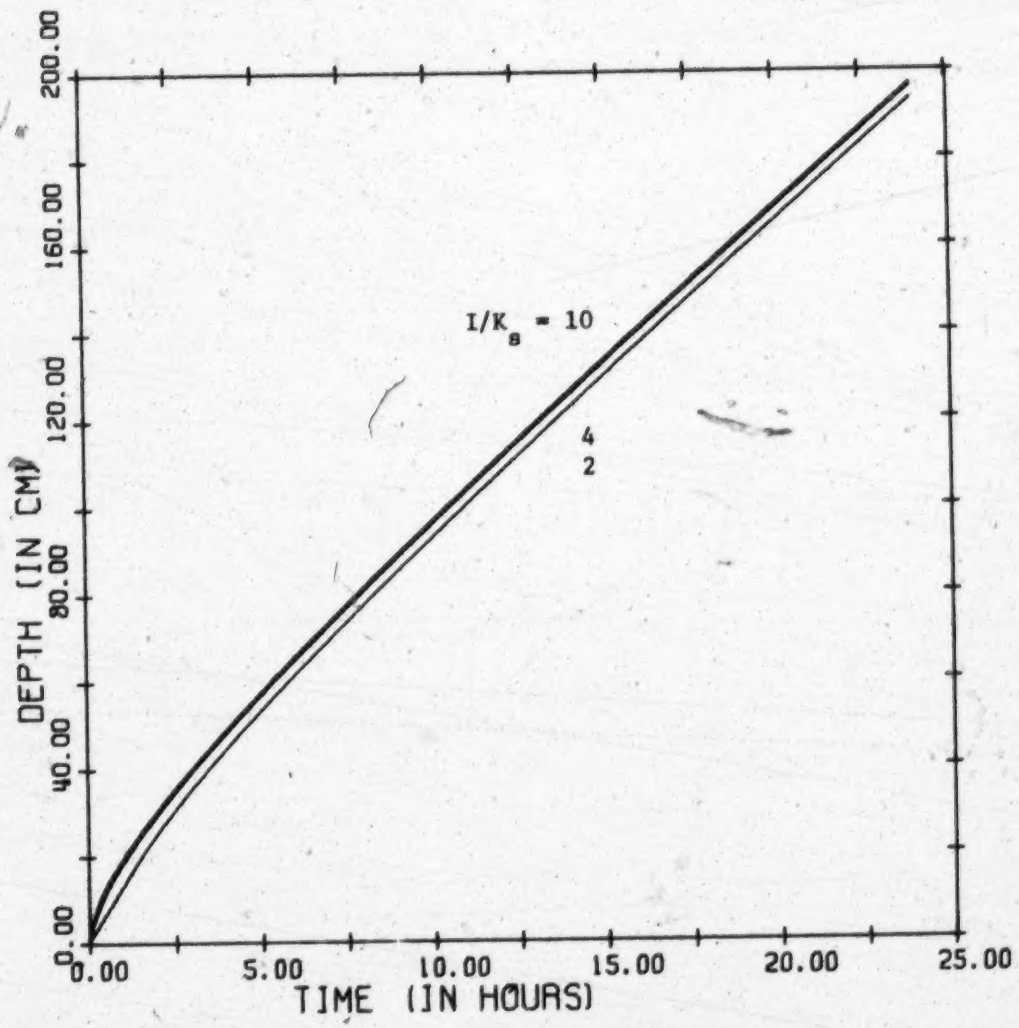

FIGURE C2 VOID RATIO=0.89 KSAT=8.0E-5 SAT=90%

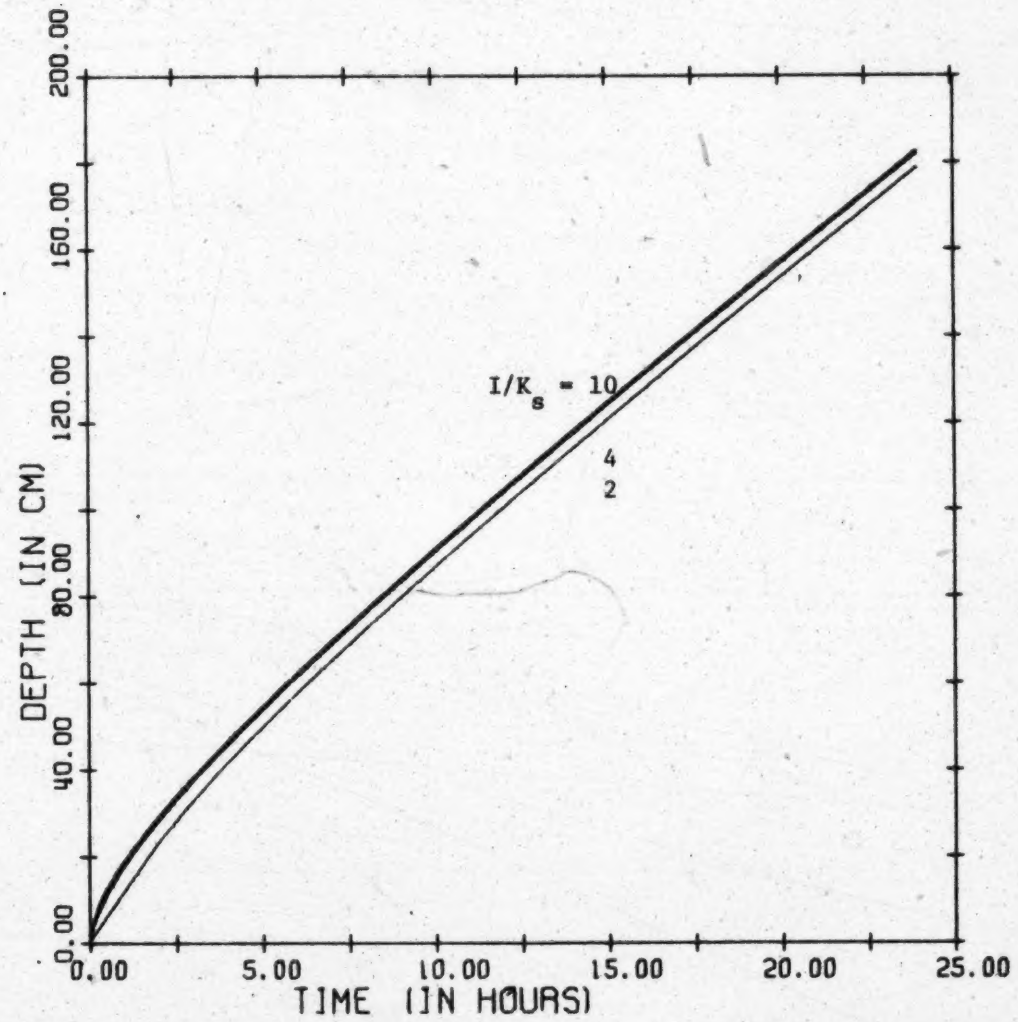

FIGURE C3 VOID RATIO=1.00 KSAT=8.0E-5 SAT=90%

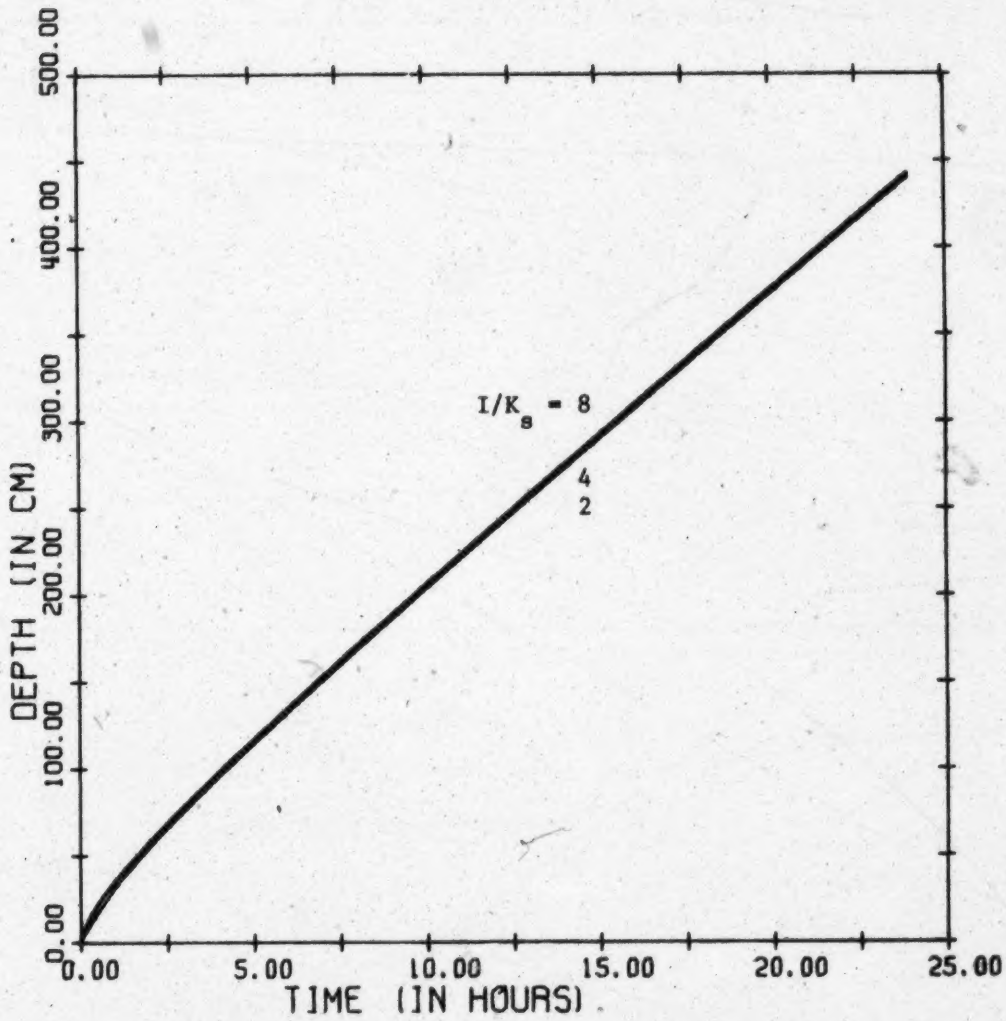

FIGURE C4 VOID RATIO=0.75 KSAT=2.0E-4 SAT=90%

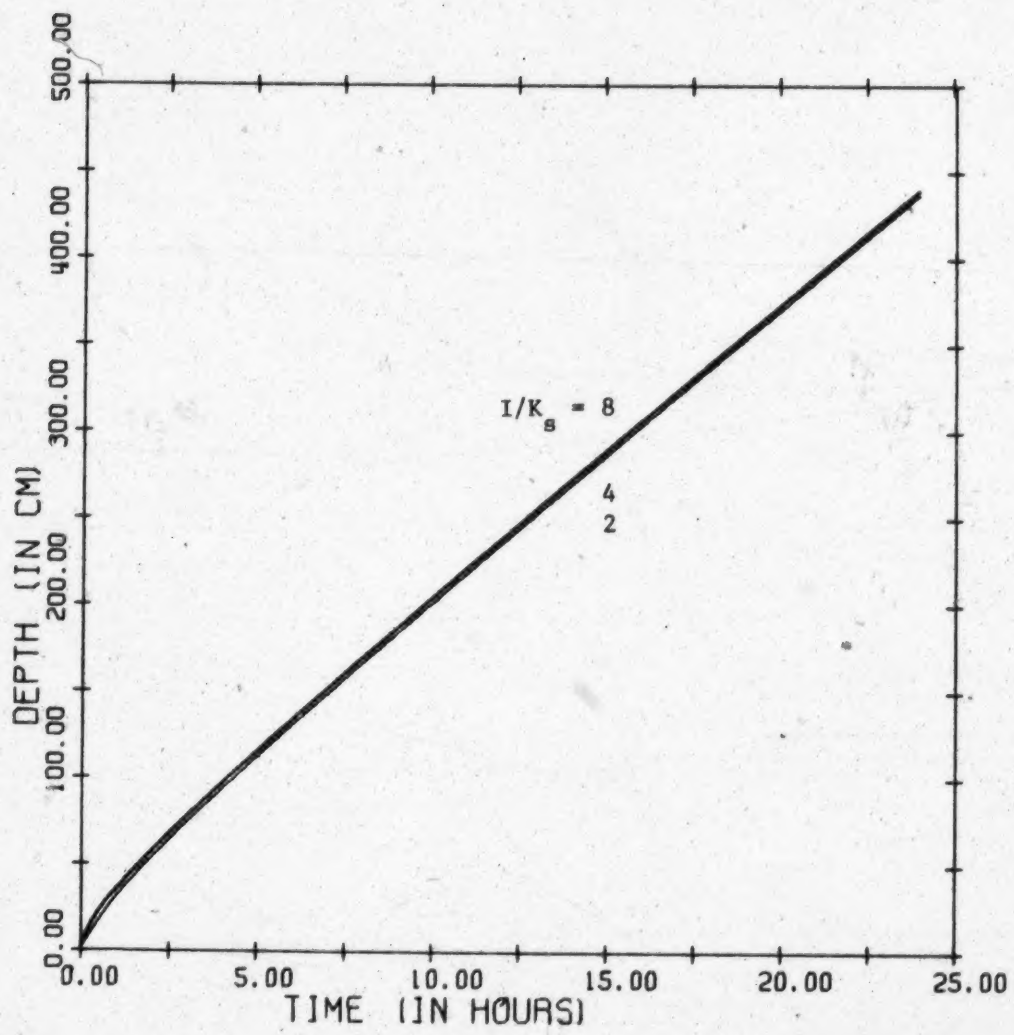

FIGURE C5 VOID RATIO=0.89 KSAT=2.0E-4 SAT=90%

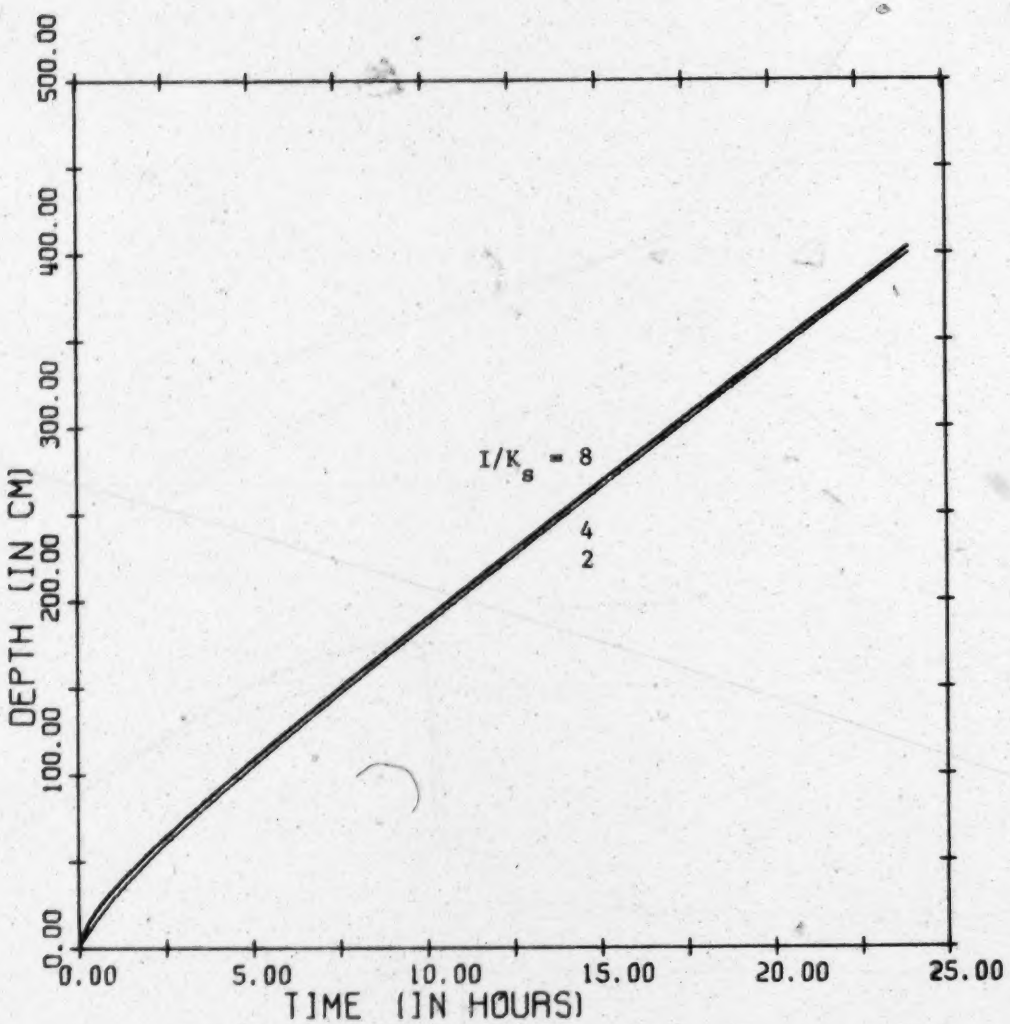

FIGURE C6 VOID RATIO=1.00 KSAT=2.0E-4 SAT=90%

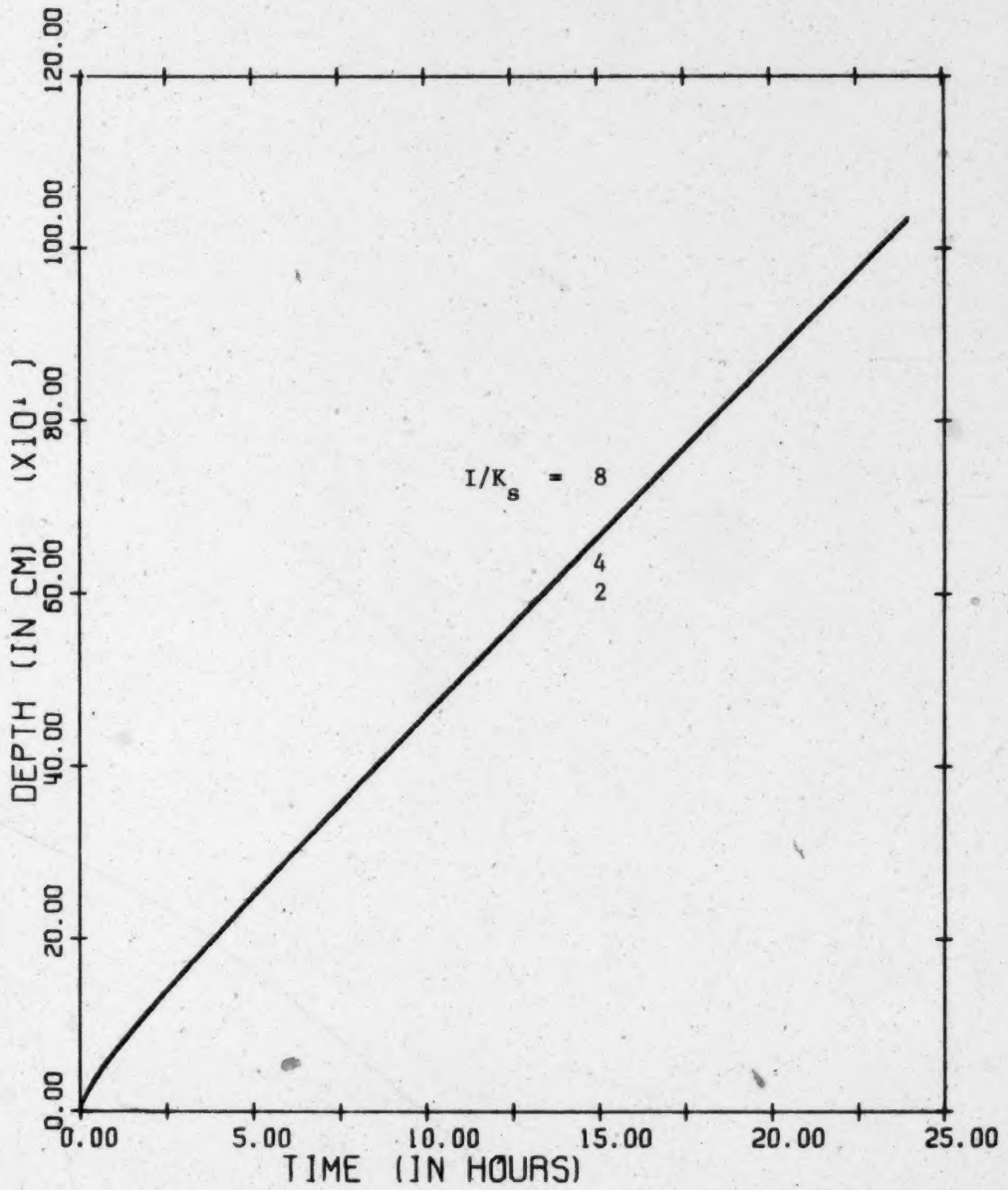

FIGURE C7 VOID RATIO=0.75 KSAT=5.0E-4 SAT=90%

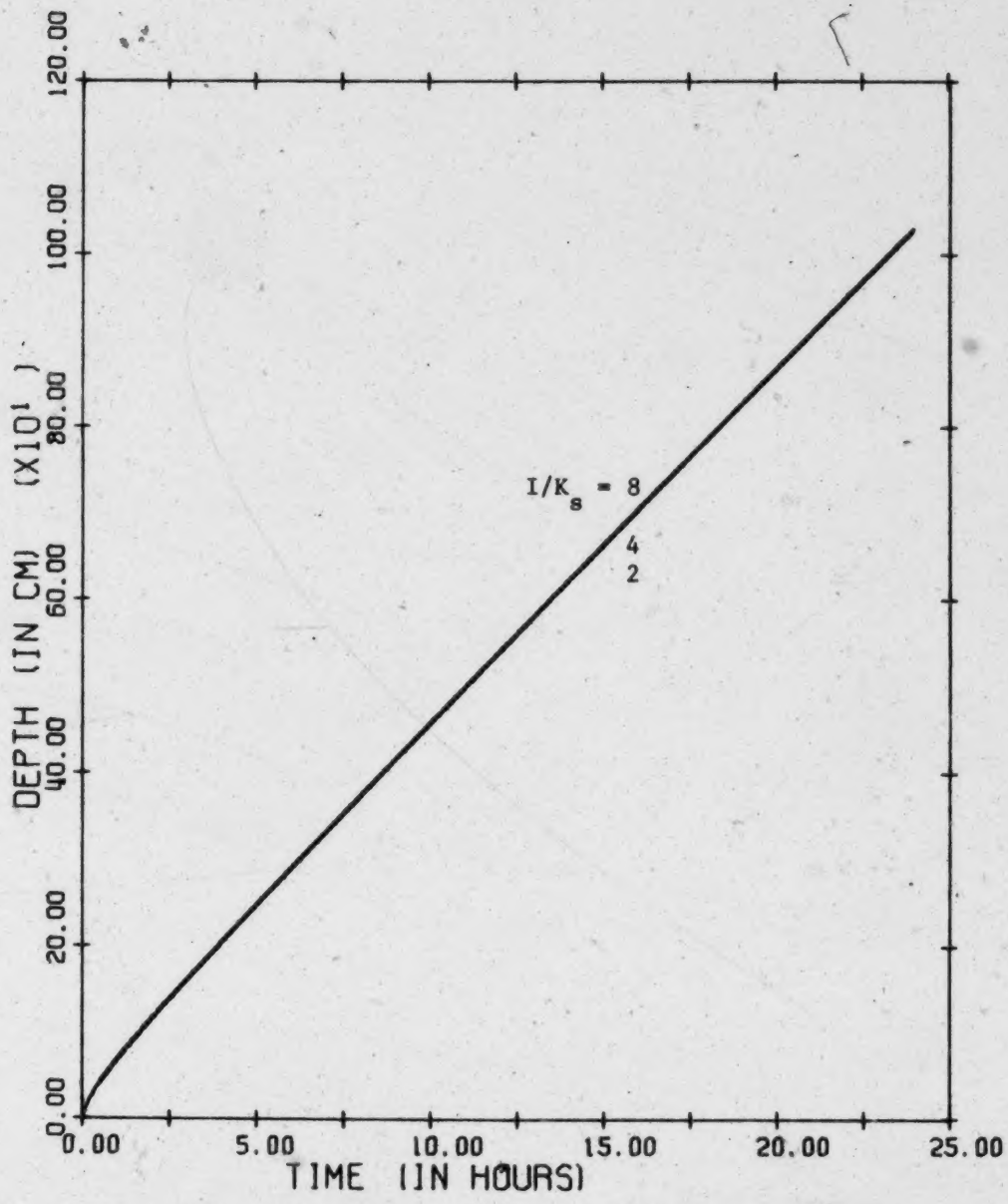

FIGURE C8 VOID RATIO=0.89 KSAT=5.0E-4 SAT=90%

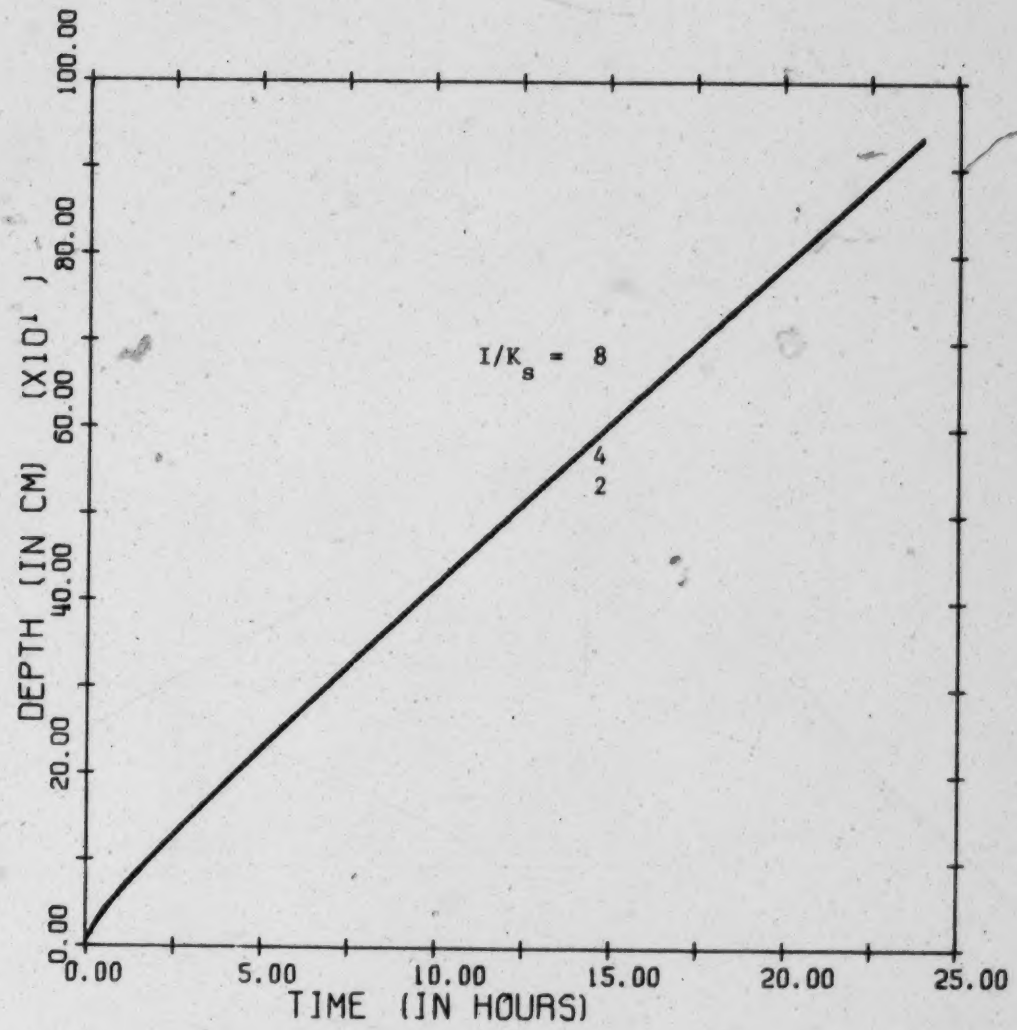

FIGURE C9 VOID RATIO=1.00 KSAT=5.0E-4 SAT=90%